POLITECNICO DI MILANO
Scuola di Ingegneria Industriale e dell'Informazione
Laurea magistrale in Ingegneria Matematica

Pedestrian dynamics: modelling and calibration of a 2-dimensional cellular automata model

Relatore: Prof. Roberto LUCCHETTI
Correlatore: Prof. Santo FORTUNATO

Tesi di Laurea di:
Andrea RIBOLDI
Matr. n. 782642

Anno Accademico 2013–2014

Contents

List of Figures

List of Tables

Sommario

Lo studio delle dinamiche pedonali è un passo fondamentale nella progettazione di strutture pedonali più sicure ed efficienti. Per questo motivo negli ultimi decenni diversi fisici hanno iniziato a sviluppare modelli in grado di riprodurre queste dinamiche in modo realistico.

In particolare in questo lavoro abbiamo deciso di usare il modello ad automi cellulari bidimensionale con *campi di forza*. L'introduzione di questi campi rende il modello in grado di replicare situazioni complesse senza perdere la sua semplicità.

Lo scopo di questo lavoro è in primo luogo di dare una visione generale delle valutazioni sperimentali già presenti in letteratura, fondamentali per la comprensione della materia, e dei vari modelli matematici usati per la simulazione delle dinamiche. La seconda parte invece si concentrerà sulle simulazioni fatte con il modello appena menzionato.

La parte originale del lavoro è lo studio eseguito sul *campo di forze dinamico* e la conseguente calibrazione del modello, fatta grazie al contributo di questo studio. L'analisi accurata delle diverse simulazioni ha reso possibile la comprensione dell'influenza che ha ogni parametro del modello sulle dinamiche dei pedoni. Questo ci ha portato a capire anche quali sono i vantaggi e gli svantaggi del modello CA. Infine abbiamo trovato un'unica combinazione di parameteri, che ha reso il modello in grado di replicare soddisfacentemente diversi dati sperimentali.

Abstract

The study of pedestrian dynamics is an important task in the planning of efficient and safe pedestrian facilities. For this reason physicists began to develop models in order to reproduce these dynamics in a realistic way.

In particular the model used in this work is the 2-dimensional Cellular Automata model with *floor fields*. The introduction of these fields allows us to reproduce even complex situations without loosing the advantage of the simplicity of the model.

The aim of this work is firstly to give an extensive summary of existent experimental observations, fundamental for a deep understanding of the subject, and to introduce different type of modelling of pedestrian dynamics. The second part has as its goal the reproduction of the evacuation dynamics by computational simulations with the model mentioned before.

The original part of the work is the study of the *dynamic floor field* and the consequent calibration of the model developed thanks to this study. This accurate analysis of the model made us understand firstly the influences of the different parameters on the dynamics of the simulated particles and secondly the benefits and disadvantages of the use of this model. Eventually an unique combination of values of the different parameters of the model has been found, so that the model is able to reproduce different experimental data satisfactorily.

Estratto della tesi

Negli ultimi decenni molti fisici si sono interessati allo studio delle dinamichi pedonali, in modo da trovare soluzioni più sicure ed efficienti. Lo studio di queste dinamiche è molto complesso e va analizzato sotto diversi punti vista: fisico, psicologico e sociale.

In questo lavoro abbiamo analizzato i diversi tipi di comportamenti dei pedoni, i vari modelli con cui simularli e infine ci siamo concentrati sul modello ad automi cellulari per simulare queste dinamiche.

La parte originale del lavoro è lo studio eseguito sul *campo di forze dinamico* del modello appena menzionato e la conseguente calibrazione, fatta grazie al contributo di questo studio. L'analisi accurata delle diverse simulazioni ha reso possibile la comprensione dell'influenza che ha ogni parametro del modello sulle dinamiche dei pedoni. Questo ci ha portato a capire anche quali sono i vantaggi e gli svantaggi del modello CA. Infine abbiamo trovato un'unica combinazione di parameteri, che ha reso il modello in grado di replicare soddisfacentemente diversi dati sperimentali.

L'elaborato è suddiviso nel seguente modo:

- **Capitolo 1** — riassumiamo in modo accurato tutti gli studi riguardanti le dinamiche pedonali. In particolare vengono analizzate le osservazioni sperimentali presenti nella letteratura e le diverse grandezze fisiche utili per questo studio.

- **Capitolo 2** — questo capitolo è diviso in due sezioni. Nella prima parte ci occupiamo di descrivere le caratteristiche dei vari modelli utilizzati per la simulazione delle dinamiche pedonali. Nella seconda parte invece vengono descritti i primi modelli sviluppati dai fisici per la simulazione di queste dinamiche: i modelli ispirati dalla fluidodinamica e dalla cinetica dei gas, il modello "Social force" e il modello "Optimal velocity".

- **Capitolo 3** — questo capitolo contiene la descrizione del modello ad automi cellulari con campi di forza utilizzato in questo lavoro per la

simulazione dei pedoni. La parte finale del capitolo riguarda lo studio del *campo di forze dinamico*, utile al fine di ottenere successivamente una calibrazione più accurata del modello.

- **Capitolo 4** — descriviamo i risultati della calibrazione del modello CA. Lo scopo di questo capitolo è di ottenere una combinazione di parameteri del modello, al fine di renderlo capace di riprodurre in modo realisto diversi esperimenti presenti in letteratura. Nella parte finale viene descritta la validazione dei parameteri ottenuti nella calibrazione, confrontando i risultati delle simulazioni con quelli di due diversi esperimenti.

- **Capitolo 5** — contiene una sintesi delle tematiche e dei metodi proposti ed impiegati nella tesi, e affronta alcuni punti aperti che saranno oggetto della futura ricerca in questo ambito.

Chapter 1

Introduction

In the last 30 years the interest of physicists in pedestrian dynamics has grown a lot, in order to find solutions for better and safer evacuations. Nowadays in many occasions a large number of people gathers in small areas. On regular basis large events related to sport, religion and entertainment are organized all over the world. Office buildings and apartments are becoming larger and more complex. These situations cause serious safety issues for the organizers and participants of the event that have to be ready for any emergency and critical situations. For example, crowds stampede, are still a problem nowadays. Even if the safety standards are better today, the total number of victims per panic events increases with the frequency of mass events. Since 1995 [4],[5],[37] more than 40 large crowd panics have occurred, in which more than 2000 people were killed and at least 5000 were seriously injured. Before 1995 one of the most famous disaster was "The Who concert disaster", which took place in Riverfront Coliseum in Cincinnati in 1979. In 1994 and 2006, 270 and 345 people respectively were killed at Jamarat Bridge in Mecca during the stoning of the Devil. In 1996 in Guatemala City there were 82 fatalities and 147 injuries during a World Cup qualifying match. Another example is of course the terrorist attacks of 9/11, in which more than 2500 people died. In 2001 over 160 people were killed in two major crowd stampede in football stadiums in South Africa and Ghana. It is possible to find examples also in the United States, where in 2003 over 120 people died in Rhode Island and Chicago due to crowd panics in night clubs. The first one is known as the Station nightclub fire. In 2005 one of the deadliest stampede happened in Baghdad on the Al-Aaimmah bridge, where 953 people died. More recently 21 people were killed and more than 500 were injured during the mass panic at the Love Parade in Duisburg.

During these situations the people have to be guided out of the building or the dangerous area as soon as possible. That is why it is so important

(a) Love Parade disaster (2010)

(b) Station Nightclub fire (2003)

(c) Disaster at the Jamarat Bridge (1994)

(d) Al-Aaimmah bridge stampede (2005)

Figure 1.1: Pictures of famous crowds stampede

to understand the dynamics of a large group of people. The study of these situations is really complex due to large number of people and their interactions, external factors like fire etc., complex buildings geometries and the panic behaviour of the pedestrians. For these reasons the dynamics have to be understood on different levels: physical, social and psychological. The aim of the research of pedestrian dynamics is really important in order to develop elements that allow the increase of the efficiency and safety of pedestrian facilities. This study [5] is developed in 3 steps: 1) understanding of several collective phenomena of the pedestrian dynamics (Section 1.2), 2) development and calibration of models that are able to reproduce the dynamics in a realistic way (Chapters 2-4), 3) application of these models to design facilities for the pedestrians and to prepare and manage emergencies.

For these reasons in the last decades a lot of physicist worked on the creation of models to replicate the pedestrian behaviour in normal and panic situations.

The first models were based on fluid-dynamics and gas-kinetic models, because of the similarity in some aspects of the pedestrian dynamics with the one of fluid and gases. In 1971 Henderson did the first studies on these kind of models [13],[14].

Based on the traffic models made years before, in 1998 and 2000 the first models introduced respectively the idea of "social-forces" [16],[17] and stochasticity [21]-[31]. The first one was introduced by Helbing and is based on the idea that velocity and direction of people are influenced by the presence of other pedestrians, obstacles and points of interest. The second kind of models are called Cellular Automata. A lot of different versions of this model were made in the last decade, but the last one developed was the one based on the idea of the *floor fields*. The simulations in this paper are based on this last model. The reasons for this choice were essentially two: 1)despite its simplicity, this model is able to reproduce the real behaviour with a high accuracy; 2)being one of the last models developed, it has more potentiality of being improved, in order to create a really simple model able to reproduce even complex situations.

All these models will be described more accurately in the next chapters: the fluid-dynamics and gas-kinetic based models and the social force model in Chapter 2; the cellular automata models, in particular the one based on the *floor fields*, in Chapter 3.

In order to create models that are able to predict real data, it is necessary to understand deeply the real pedestrian behaviour. This study will be described in Section 1.2.

1.1 Reason of the research

As already mentioned, nowadays it is really important that architects and engineers, who project buildings, shopping centres, airports, railway stations or stadiums as well as organizers of big events are able to understand and prevent problems caused by evacuations in emergency situations. The simulation of pedestrian dynamics is an important, sometimes required, stage to understand these problems. Because of the complex and chaotic nature of pedestrian dynamics, simple analysis are not enough to understand the real behaviour of people in these situations. Evacuation exercises are too expensive, time consuming and dangerous to be a standard measure for evacuation analysis. For example, the UK Marine Coastguard Agency in 1996 [1] made an evacuation exercise that costed more than 10000 £. These exercises are although useful to be used as empirical data for the construction of the model [5] in three ways: 1) identify the parameters (factors that influence the evacuation process, e.g. capacity and width of the bottlenecks), 2) quantify those parameters (e.g. flow through the bottleneck in persons per meter and seconds), 3)validate the simulation results (compare the overall evacuation time measured with the one simulated).

1.2 Empirical observations

The first step of the creation of more efficient and safe pedestrian facilities is to understand the several collective phenomena of the pedestrian dynamics.

Pedestrian crowds dynamics have been studied since 1958 by Hankin and Wright [2], but a real extensive summary was done the first time by Helbing in 2002 [4]. They studied many self-organization phenomena on the base of observations, photographs and time-lapse movies. The idea is to understand deeply the dynamics of the pedestrian in order to recreate a mathematical model able to reproduce these features in a realistic way. This gives the possibility to study different other cases in an easier and more economic way, indeed computer simulations are a really powerful tool for designing and planning pedestrians facilities. This second part will be discussed in the following Chapters 2-4, while in this section only the empirical results will be described. The empirical study is not only important for the creation of the model but also for applications like safety study and legal regulations. At the beginning the collective phenomena in normal situations will be described. Some of these are common from everyday experience. This will be an initial benchmark test for the models used. In earlier days investigations of self-organization phenomena were based on qualitative empirical observations and video-based analysis [37]. They include:

1. bidirectional pedestrian streams in corridors or alleys [42],[44],[45]
2. four intersecting pedestrian streams with and without guidance through obstacles and railings [45]
3. the movement of pedestrians through a waiting crowd [45],[46]
4. the escape of students from a room with a narrow exit, without pushing [47]
5. uni- and bidirectional pedestrian streams in corridors with and without bottlenecks [37]
6. two intersecting pedestrian streams [37]

Some of these experiments will be used in Chapter 4 in order to calibrate the model and to be sure that the model used is able to recreate the phenomena observed in the reality.

It is mode difficult to understand the behaviour of the pedestrian in panic situations. Obviously it is difficult to recreate situations of emergency in a simulation of an escape without putting in danger people. Most of the results of the behaviour in these situations are qualitative observations, though there are a couple of experiments [37] that try to reproduce those situations like:

1. the escape of disoriented people from a room (where some effects of dense smoke or an outage of power supply were imitated by wearing eye masks) [48]
2. pushy pedestrians rushing toward an exit with and without an obstacle in front of it [37]

1.2.1 Behaviour in normal situations

Though the dynamics of the pedestrians can be sometimes chaotic and irregular, it is possible to find some regularities and rules, some of which become more visible in time-lapse films. The following list is a summary result of some other pedestrians studies and observations [2]-[7]:

1. Pedestrians prefer to walk with an individual pedestrian speed, that normally is the least energy consuming and comfortable one. Normally this speed is the minimum one in order to arrive to the destination in time. Considering that the speed of walking within pedestrian crowds depends on the situation, age, sex, purpose of the trip, time of the day, etc., it is possible to observe that the velocity is distributed as a Gaussian with average value of approximately 1.34 $\frac{m}{s}$ and a standard deviation of 0.26 $\frac{m}{s}$.
2. Many pedestrians show a strong aversion to detours or moving in the opposite direction than the desired one, even if the direct route is crowded. However there is also some evidence that normally they choose the fastest way and not the shortest one. The consequence of this is that it is possible to approximate the shape of their ways as a polygon. People always prefer to walk straight ahead as far as they can and change direction as late as possible, if the alternative routes are of the same length and not more attractive, for example, because of a friendlier environment, more light, less noise, etc. .
3. Normally pedestrian try to keep a certain distance from other pedestrians and from the environment (walls, obstacles, etc.). This distance is smaller if the pedestrian is in hurry and with the increase of the pedestrians density. This density is higher around particularly attractive places. Another interesting observation is that individuals knowing each other can form a group that behaves like a single pedestrian. Some studies modelled the size of groups as a Poisson distribution.
4. Pedestrian always act more or less automatically, even if the situation is new. An example of this behaviour are pedestrians that cause delays or

obstructions, by entering a train or an elevator before other pedestrians went out of them.

1.2.2 Behaviour in panic situations

Typically "panic situations" are those, where people compete for scarce or dwindling resources (e.g. safe space and access to an exit), which leads to selfish, asocial or even irrational behaviours and contagion that affects large groups. This phenomena is understandable in life threatening situations, like a fire in a crowded building, but sometimes it occurs even in unreasonable situations like in cases of a rush for good seats at concerts.

As mentioned before it is difficult to understand this behaviour, but some features appear to be typical [2]-[7]:

1. People try to move considerably faster than in normal situations
2. Moving and passing through bottlenecks becomes uncoordinated and hard
3. Escape is slowed down by fallen or injured pedestrians turning into obstacles
4. Alternative exits are often overlooked or inefficiently used in these situations
5. Individuals start pushing and physical interactions between pedestrians can cause dangerous pressures up to 4500 $\frac{N}{m}$.

The following quotations of "The Who concert disaster" give a more personal impression of the conditions during escape panics:

- "They just kept pushin' forward and they would just walk right on top of you, just trample over ya like you were a piece of the ground."
- "People were climbin' over people ta get in ... an' at one point I almost started hittin' 'em, because I could not believe the animal, animalistic ways of the people, you know, nobody cared."
- "Smaller people began passing out. I attempted to lift one girl up and above to be passed back ... After several tries I was unsuccessful and near exhaustion."

1.2.3 Collective Phenomena

One of the main reasons why physicists are interested in pedestrians dynamics is because under certain conditions, pedestrian flows form collective effects and self-organization phenomena, such as:

- clogging and jamming effects or oscillatory flows at bottlenecks
- density waves in dense crowds
- lanes of uniform walking directions in pedestrian counter-flows
- circulating flows intersections

With self-organization [37] it is meant that these patterns are not externally planned, prescribed or organized, for example by traffic signs, laws, behavioural conventions, or previous organization. This patterns are created by the non-linear interaction between the pedestrians and the environment. Physicist are able to study and reproduce mathematically by simulations this phenomena, only because these interactions are more reactive and subconscious than based on strategical considerations or communication.

Jamming, clogging and oscillation

Jamming and clogging typically occur for high densities at locations where the inflow exceeds the capacity of the passage. These locations with a reduced capacity are called *bottlenecks*. In Fig.1.2 it is possible to see how the pedestrians are jamming next to a bottleneck. When several pedestrians reach the bottleneck at the same time , their mutual blockage leads to a deadlock that none of them can pass through the passage. This is a typical situation in which it is possible to observe the clogging phenomena. The consequence of this effect is the exclusion principle: the space occupied by one particle is not available for others.

Figure 1.2: People jamming at the entrance of the Apple Store in Sanlitun, China

Other types of jamming occur in the case of counter-flows at bottlenecks. In this case it is possible to oscillatory changes of the passing direction, in the case that people don't panic. Once a pedestrian is able to pass through the narrowing, the other pedestrian with the same walking direction are facilitated in following him and pass through the bottleneck until somebody is able to pass in the opposite direction.

Lane formation

In a room with counter-flow movements, i.e. two groups of people moving in opposite directions, lanes are formed where people move in just one direction [3]. In this way most of the interactions caused by the counter-flow are reduced, which is more comfortable and allows higher walking speeds. Pedestrians moving against the stream or in areas with mixed directions will have for sure more interactions with the pedestrians moving in the opposite direction. In each interaction, the encountering pedestrians will move a little aside in order to pass each other. This sidewards movement tends to separate oppositely moving pedestrians, which leads to segregation. To understand better this phenomena, Fig.1.3 shows a lane formation in a crowded walkway in Bordeaux, France. The number of lanes can vary considerably with the total width of the flow. Usually this number is not constant and can change in time, even if there are small changes in the density of the environment. The number of lanes of opposite directions is not always the same.

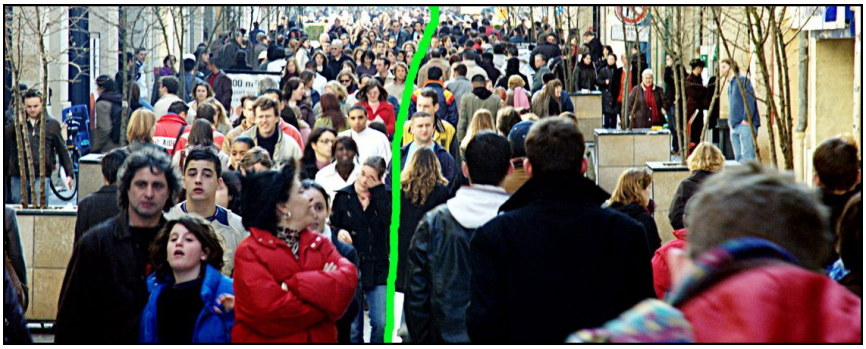

Figure 1.3: Lane formation phenomena in a crowded walkway in Bordeaux, France

Panic

This behaviour is usually characterized by selfish and anti-social behaviour, which through contagion afflicts large groups and even leads sometimes to

completely irrational actions. It occurs often in situations where people compete for scarce of dwindling resources, which in the case of an escape from a building are safe space or access to an exit. Different typical behaviours can be seen during this situation [6]:

- **Herding** — Herding is a term from zoology, that in this context means "go with the flow" or "follow the crowd". In many panic situations a lot of pedestrians tend to do what the majority of the other people is doing. A lot of times this causes some overcrowded exits, in which the majority of the people goes, and some other exits that are not used at all or not used in an optimized way.
- **Stampede** — Stampede, like herding, is a term from zoology used for crowd accidents too. In zoology, stampede defines a large herd of mammals like buffaloes collectively running in one direction and overrunning any obstacles. In panic situations this phenomena unfortunately happens even in human crowds. In the attempt to escape, many times humans trample other people.
- **Faster-is-slower effect** —Due to impatience caused by panic, pedestrian have an higher desired velocity, that leads to a slower movement of the crowd.
- **Freezing-by-heating effect** — In counter-flows, at sufficiently high densities, lanes are destroyed by the increasing fluctuation strength (which is similar to the temperature). However,instead of the expected transition from the "fluid" lane state to a disordered, "gaseous" state, a solid state is formed. This is characterized by a blocked situation.

1.3 Observables

Before explaining the models and the experimental studies with the consequent calibration of the model, it is important to introduce the commonly used observables. The flow J of a pedestrian stream gives us the number of people crossing a fixed location of a facility per unit of time. Usually it is taken as a scalar value since only the normal flow to the crossing section is considered. In order to calculate the flow, it is necessary to determine the times t_i at which pedestrian pass through the fixed location. The time gaps $\triangle t_i = t_{i+1} - t_i$ between two consecutive pedestrians $i+1$ and i are strictly related to the flow:

$$J = \frac{1}{\overline{\triangle t}} \qquad with \qquad \overline{\triangle t} = \frac{1}{N}\sum_{i=1}^{N} \triangle t_i = \frac{t_{N+1} - t_i}{N} \tag{1.1}$$

Another way to measure this flow is with a fluid dynamic approach. The flow J through a facility of width b determined by the average density ρ and the average speed v can be calculated with the following formula:

$$J = \rho v b = J_s b \tag{1.2}$$

where the specific flow:

$$J_s = \rho v \tag{1.3}$$

gives the flow per unit-width. This relation is also known as *hydrodynamic relation.*

Another way to quantify these quantities was proposed by Helbing [39]. The local density at place $\vec{r} = (x, y)$ and time t was obtained with the following formula:

$$\rho(\vec{r}, t) = \sum_j f(\vec{r}_j(t) - \vec{r}) \tag{1.4}$$

In the equation $\vec{r}_j(t)$ represents the position of the pedestrians j in the surrounding of $\vec{r}$ and

$$f(\vec{r}_j(t) - \vec{r}) = \frac{1}{\pi R^2} e^{-\frac{\|\vec{r}_j(t) - \vec{r}\|}{R^2}} \tag{1.5}$$

is a Gaussian distance-dependent weight function. R is a measurement parameter.

1.3.1 Fundamental diagram

The fundamental diagram describes the empirical relation between the pedestrian flux J and the density ρ. Due to hydrodynamic relation 1.3 there are three equivalent forms: $J_s(\rho)$, $v(\rho)$ and $v(J_s)$. As suggested by the name, this diagram is really important in the study of the pedestrian dynamics. In applications the relation is a basic input for engineers to design and dimension the pedestrian facilities. Furthermore it is a quantitative benchmark for models, since it is possible to calibrate them thanks to the fundamental diagram.

Fig.1.4 shows different fundamental diagrams used in planning guidelines and measurements in some similar empirical studies. It is possible to notice that the results disagree considerably. In particular the maximum value of the specific flow $J_{s,max}$ ranges from 1.2 $\frac{1}{ms}$ to 1.8 $\frac{1}{ms}$ and the values of the density in which the maximum is reached ρ_c ranges from 1.75 $\frac{1}{m^2}$ to 7 $\frac{1}{m^2}$. Many explanations have been suggested for these huge differences in the fundamental diagrams such as:

- cultural and population differences

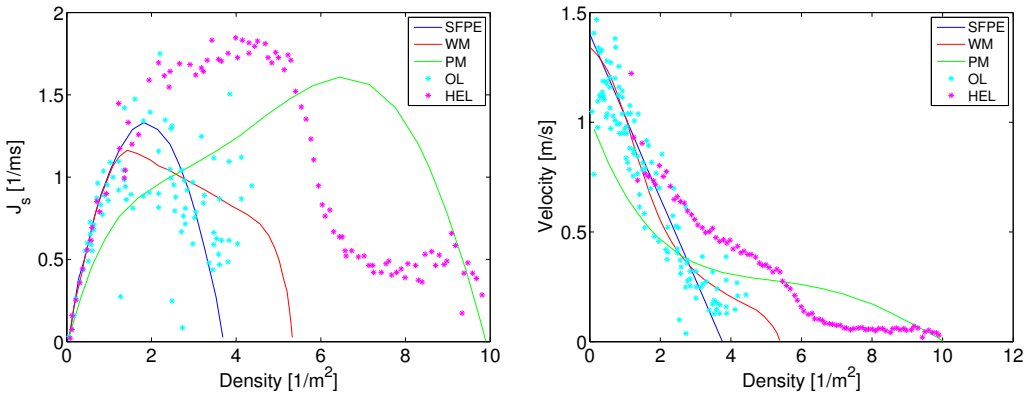

(a) Specific flow against density in the room (b) Velocity against density in the room

Figure 1.4: Fundamental diagrams for pedestrian movement in planar facilities. Data: SFPE Handbook (SFPE) [3], Predtechenskii and Milinskii (PM) [10], Weidmann (WM) [9], Older (OL) [11], Helbing (HEL) [12]

- short-ranged fluctuations
- influence of psychological factors given by the incentive of movement
- type of traffic (commuters, shoppers, etc.)

However all the diagrams agree at least in one characteristic: the velocity decreases with increasing density. The reason of this speed reduction is not completely clear yet. One reason could be that the walking speed of the pedestrian depends linearly on the step size and the inverse of the density can be regarded as the required length of one pedestrian to move. Thus it seems that smaller step sizes caused by a reduction of the available space with increasing densities is one cause of the reduction of speed.

Now that all the empirical observations and the most important physical quantities were described, it is possible to introduce the modelling of pedestrian dynamics. At the beginning of the next chapter the most important characteristics of the models will be introduced, with all their positive and negative sides. The successive sections will describe the most important models developed in the last years, except by the Cellular Automata model, that will be described in Chapter 3.

Chapter 2

Modelling

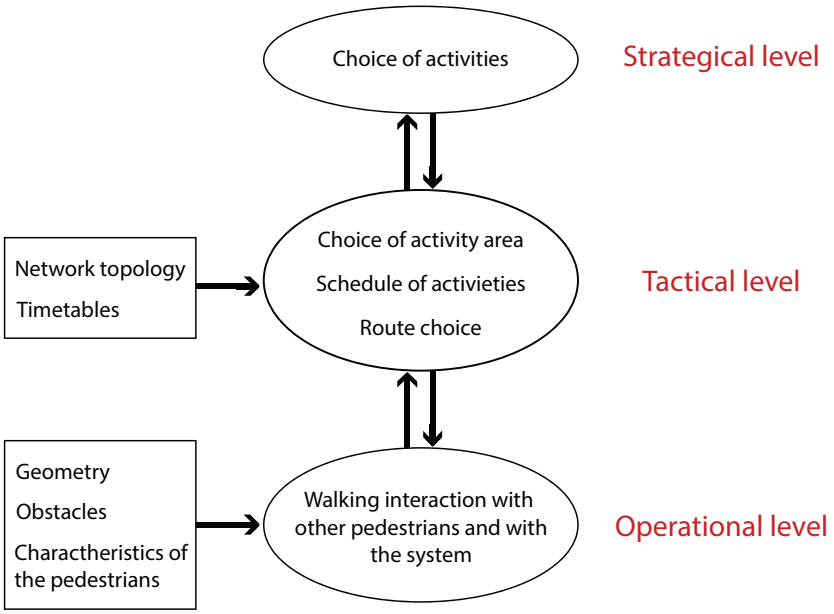

Figure 2.1: Different levels of modelling pedestrian behaviour

In order to understand the pedestrian dynamics in a global way it is necessary to take into account three levels of behaviour [5] (Fig.2.1). First of all it is necessary to understand which activities the pedestrians decide to do and the time in which they do these. This first level is called the *strategical level*. After the choices made in the strategical level, the *tactical level* concerns the short-term decisions of the pedestrians, like choosing precise routes in order to arrive in the desired place in the fastest and most comfortable way. Finally the *operational level* describes the actual walking behaviour of the pedestrians in order to avoid collision with the environment and other pedestrians.

The first 2 levels are usually considered exogenous to the pedestrian dynamics simulations, even if there are some models that take into account certain elements of these two levels. The first macroscopic observations of the operational level have been already described in 1.2. Modelling the operational level is usually based on the variations of models from physics. The reason of this is the fact that the motion of pedestrian crowds have similarities with the fluid, gases and granular material flow [4]:

- the emergence of pedestrian streams through standing crowds appears analogous to the formation of river bed
- footprints of pedestrians in snow look similar to streamlines of fluids
- at borderlines between opposite directions of walking one can observe "viscous fingering", i.e. the formation of patterns in a morphologically unstable interface between two fluids in a porous medium
- when the density is high enough, pedestrians spontaneously organize in lanes of uniform walking directions like the segregation or stratification phenomena in granular material
- at bottlenecks, the passing direction of pedestrian oscillates and can be compared to the granular "tickling of the hourglass"
- the propagation of shock waves can be seen in dense pedestrian crowds pushing forward

The aim is to find a model that is as simple as possible, but at the same time can reproduce in a realistic way the behaviour of the pedestrians observed in empirical studies. Therefore, taking inspiration from physics, pedestrians are often modelled as simple "particles" that interact with each other. All these models have characteristics [5] that can be used to classify the modelling approaches:

- **macroscopic vs. microscopic** — In macroscopic models different pedestrians can not be distinguished, but instead the state of the system is described by densities, usually a mass density derived from the position of the particles and a corresponding locally averaged velocity. In contrast, in microscopic models each individual is considered separately. This kind of models allow to introduce different types of characteristics to the single pedestrian, like the desired route or the desired velocity.
- **discrete vs. continuous** — All the variables in the models for the description of the system of pedestrian are time and state variables

(e.g. velocities). These variables can be either discrete or continuous. Cellular automata models are by definition discrete, but it is possible to implement it even in a continuous way. In computer simulations this is realized through a *random-sequential update* where at each time step the particle or site to updated is chosen randomly from the set of all particles and sites respectively. The discrete time version is usually implemented through a *parallel* or *synchronous update* where all the particles are moved in the same time. With this approach it is necessary to introduce a time-scale.

- **deterministic vs. stochastic** — The dynamics of pedestrians can be described either in a deterministic or a stochastic way. In the deterministic way the behaviour of the particle is determined by the present state. This means that if a particle is in a certain state, it will react always in the same way. Differently in stochastic models the behaviour is controlled by certain probabilities in order that pedestrians can react differently in the same state. The introduction of this stochasticity, even in really simple models, can generate really complex behaviours. But thanks to this stochastic behaviours it becomes often possible to generate rather realistic representations of complex systems like pedestrian crowds. The introduction of these probabilities reflects our lack of knowledge of the underlying physical process, e.g. determines the decision-making of the pedestrians.

- **rule-based vs. force-based** — The difference between rule-based and force-based models is that the interaction of the pedestrian with the environment and other particles is implemented in two different ways. In the first one all the pedestrian make their movement decision based on their current and neighbourhood situation, so it focuses on the local situation of the pedestrian. In contrary the force-based models are implemented taking into account the global situation of the system. In these models particles "feel" a force exerted by others and the infrastructure and act accordingly. It is a physical approach based on the observation that the presence of others leads to a deviation from a straight movement.

All the cellular automata (CA) models will be described accurately in Chapter 3, while in the following the other models will be briefly described.

MODEL				
Fluid-dynamics models	macroscopic	continuous	deterministic	force-based
Social-force models	microscopic	continuous	semi-stochastic	force-based
Optimal velocity model	microscopic	continuous	deterministic	force-based
CA Fukui-Ishibashi model	microscopic	discrete	deterministic	rule-based
CA Blue-Adler model	microscopic	discrete	stochastic	rule-based
CA floor field model	microscopic	discrete	stochastic	rule-based

Table 2.1: Summary of all the most important models with their usual characteristics.

2.1 Fluid-dynamics and gas-kinetic models

Similarly to many vehicular dynamics models, the first pedestrian dynamics models took inspiration from hydrodynamic and gas-kinetic theory. Henderson [13],[14] was the first one who tried to establish an analogy of large crowds with a classic gas. The result of his first work [13] was that the velocity vector V of a particle is considered to be the sum of a mean steady velocity transition $\overline{V}$ and a random fluctuation part v':

$$V = \overline{V} + v' \tag{2.1}$$

Taken over a crowd, $\overline{V}$ represents the average velocity of convection along a footpath. The random part v' is built under the hypothesis that all the particles are statistically independent of one another. Physically speaking, all the particles are free to select their V without any interference. Under these assumptions he found a good agreement of the p.d.f. of v' with Maxwell-Boltzmann distribution:

$$f(v) = \sqrt{\left(\frac{m}{2\pi kT}\right)^3} 4\pi v^2 e^{-\frac{mv^2}{2kT}} \tag{2.2}$$

where m is the particle mass and kT is the product of Boltzmann's constant and thermodynamic temperature. This p.d.f. gives the probability, per unit speed, of finding the particle with speed near v.

In a later work [14] Henderson tried to improve his model developing a fluid-dynamic theory of pedestrian flow. He described an homogeneous crowd by the well-known kinetic theory of gases, representing the interactions between the pedestrians as a collision process where the particles exchange momenta and energy. The kinetic theory of gases is based on several conservation laws. The conservation of mass, corresponding to the conservation of pedestrians in this case of study, is expressed with the following formula:

$$\frac{\partial \rho(\vec{r}, t)}{\partial t} + \nabla \cdot J(\vec{r}, t) = 0 \tag{2.3}$$

which connects the local density $\rho(\vec{r},t)$ with the current $J(\vec{r},t)$ (in position $\vec{r}$ and time t). However the hypothesis of conservation of energy and momenta, made to apply the kinetic theory of gases, is not true for interactions between pedestrians, which in general do not even satisfy the Newton's third law ("actio=reactio").

In [15] a better fluid-dynamical description was derived on the basis of a gas-kinetic model which describes the system in terms of a density function. First of all the pedestrians are divided into groups of different types μ of motion, e.g. by their different intended directions $\vec{e}_\mu := \frac{\vec{v}_\mu^0}{\|\vec{v}_\mu^0\|}$ of motion. With this method all the pedestrian are distinguished in several disjoint and complementary sets Φ_μ.

Thanks to a suitable choice of these sets it was possible to get approximately unimodal densities $\hat{\rho}_\mu(\vec{x},\vec{v}_\mu,\vec{v}_\mu^0,t)$ and therefore to obtain appropriate mean value equations. This function describes the number N_μ of pedestrians of type μ around a place $\vec{x}$ having approximately the intended velocity $\vec{v}_\mu^0$ but approximately the actual velocity $\vec{v}_\mu$:

$$\hat{\rho}_\mu(\vec{x},\vec{v}_\mu,\vec{v}_\mu^0,t) \equiv \hat{\rho}_\mu(\vec{x},\vec{u}_\mu,t) := \frac{N_\mu(U(\vec{x})\times S(\vec{u}_\mu),t)}{A\cdot V} \tag{2.4}$$

where:

- $U(\vec{x})$ is a neighbourhood around the position $\vec{x}$ of all accessible places. $A = A(\vec{x})$ denotes the area of $U(\vec{x})$.
- $S(\vec{u}_\mu)$ is a neighbourhood of $\vec{u}_\mu := (\vec{v}_\mu,\vec{v}_\mu^0)$ with a volume $V = V(\vec{u}_\mu)$.

The density function $\hat{\rho}_\mu$ changes in time due to four different effects:

1. A relaxation term with characteristic time τ describes the tendency of pedestrians to approach their intended velocity.
2. The interaction between pedestrians is modelled like in the Boltzmann equation. In this case pair interactions between types μ and ν occur with a total rate that is proportional to the densities $\hat{\rho}_\mu$ and $\hat{\rho}_\nu$.
3. Pedestrians are allowed to change from type μ to ν.
4. Additional gain and loss terms allow to model entrances and exits where pedestrians can enter or leave the system.

To conclude, the resulting equations derived from this gas-kinetic approach are similar to the equations of hydrodynamics (Euler equations for the motion of the gases).

2.2 Social force model

The social force model [16],[17] is a deterministic continuum model in which the interactions between pedestrians are implemented by using the concept of a *social force* or *social field*. This model is based on the idea that it is possible to put the rules of the pedestrian behaviour into an equation of motion. This equation will describe the temporal change $\frac{d\vec{v}_\alpha}{dt}$ of the velocity $\vec{v}_\alpha$ of a pedestrian α and depends on a vectorial quantity $\vec{F}_\alpha$ called *social force*. Clearly, this social force must represent the effect of the environment, e.g. other pedestrians or borders, on the behaviour of the described pedestrian:

1. Let us consider a pedestrian α that wants to reach a certain destination $\vec{r}^0_\alpha$ as comfortable as possible. Therefore he/she will take the shortest way possible, that usually has the shape of a polygon with edges $\vec{r}^0_\alpha := \vec{r}^1_\alpha, \ldots, \vec{r}^n_\alpha$. If $\vec{r}^k_\alpha$ is the next edge of the polygon the pedestrian will have a desired direction $\vec{e}_\alpha(t)$:

$$\vec{e}_\alpha(t) := \frac{\vec{r}^k_\alpha - \vec{r}_\alpha}{\|\vec{r}^k_\alpha - \vec{r}_\alpha\|} \tag{2.5}$$

   If the pedestrian is not disturbed, he/she will walk in the desired direction $\vec{e}_\alpha(t)$ with the desired speed v^0_α. A deviation of the actual velocity $\vec{v}_\alpha$ from the desired one $\vec{v}^0_\alpha := v^0_\alpha \vec{e}_\alpha(t)$ due to necessary deceleration, leads to a tendency to approach again $\vec{v}^0_\alpha$ within a certain relaxation time τ_α. This can be described by an acceleration term:

$$\vec{F}^0_\alpha(\vec{v}_\alpha, \vec{v}^0_\alpha) := \frac{1}{\tau_\alpha}(\vec{v}^0_\alpha - \vec{v}_\alpha) \tag{2.6}$$

2. The pedestrian α is influenced even by the presence of other pedestrians, e.g. pedestrian β. He/she keeps a certain distance from other pedestrians, that depends on the pedestrian density and on the desired speed v^0_α. This results in a repulsive force:

$$\vec{f}_{\alpha\beta}(\vec{r}_{\alpha\beta}) := -\nabla_{\vec{r}_{\alpha\beta}} V_{\alpha\beta}[b(\vec{r}_{\alpha\beta})] \tag{2.7}$$

   where:

   - $V_{\alpha\beta}(b)$ is a monotonic decreasing function of b with equipotential lines having the form of an ellipse that is directed into the direction of motion
   - b denotes the semi-minor axis of the ellipse and is give by:

$$2b(\vec{r}_{\alpha\beta}) := \sqrt{(\|\vec{r}_{\alpha\beta}\| + \|\vec{r}_{\alpha\beta} - v_\beta\ \Delta t\ \vec{e}_\beta\|)^2 - (v_\beta\ \Delta t)^2}$$

with $\vec{r}_{\alpha\beta} := \vec{r}_\alpha - \vec{r}_\beta$ and $s_\beta := v_\beta\ \Delta t$ that represents the step width of the pedestrian β.

In the same way the pedestrian α is influenced by *borders* of buildings, walls, streets, obstacles, etc. . Therefore a border B evokes a repulsive effect that can be described by:

$$\vec{F}_{\alpha B}(\vec{r}_{\alpha B}) := -\nabla_{\vec{r}_{\alpha B}} U_{\alpha B}(\|\vec{r}_{\alpha B}\|) \tag{2.8}$$

where:

- $U_{\alpha B}(\|\vec{r}_{\alpha B}\|)$ is a monotonic decreasing function
- $\vec{r}_{\alpha B} := \vec{r}_\alpha - \vec{r}_B^{\,\alpha}$, where $\vec{r}_B^{\,\alpha}$ denotes the location of that piece of border that is nearest to the pedestrian α

3. Pedestrians are sometimes attracted by other pedestrians, e.g. friends, or objects, e.g. exits. These *attractive effects* can be modelled in a similar way like the repulsive effects:

$$\vec{f}_{\alpha i}(\|\vec{r}_{\alpha i}\|, t) := -\nabla_{\vec{r}_{\alpha i}} W_{\alpha i}(\|\vec{r}_{\alpha i}\|, t) \tag{2.9}$$

where $\vec{r}_{\alpha i} := \vec{r}_\alpha - \vec{r}_i$ and $W_{\alpha i}(\|\vec{r}_{\alpha i}\|, t)$ is a monotonic increasing function.

The formulas described above for attractive and repulsive effects only hold for situations that are perceived in the desired direction $\vec{e}_\alpha(t)$ of motion. Situations located behind a pedestrian will have a weaker influence c with $0 < c < 1$. To take this effect into account it is necessary to introduce an effective angle of sight 2φ and the weights:

$$w(\vec{e}, \vec{f}) := \begin{cases} 1\ if\ \vec{e} \cdot \vec{f} \geqslant \|\vec{f}\| \cos\varphi \\ c\ otherwise \end{cases} \tag{2.10}$$

In conclusion, the repulsive and attractive forces are give by:

$$\vec{F}_{\alpha\beta}(\vec{e}_\alpha, \vec{r}_{\alpha\beta}) := w(\vec{e}_\alpha, -\vec{f}_{\alpha\beta})\vec{f}_{\alpha\beta}(\vec{r}_{\alpha\beta}) \tag{2.11}$$

$$\vec{F}_{\alpha i}(\vec{e}_\alpha, \vec{r}_{\alpha i}, t) := w(\vec{e}_\alpha, \vec{f}_{\alpha i})\vec{f}_{\alpha i}(\vec{r}_{\alpha i}, t) \tag{2.12}$$

Therefore the social force model is now defined by:

$$\frac{d\vec{v}_\alpha(t)}{dt} := \vec{F}_\alpha(t) + fluctuations \tag{2.13}$$

where:

$\vec{F}_\alpha(t) := \vec{F}_\alpha^0(\vec{v}_\alpha, \vec{v}_\alpha^0) + \sum_\beta \vec{F}_{\alpha\beta}(\vec{e}_\alpha, \vec{r}_{\alpha\beta}) + \sum_B \vec{F}_{\alpha B}(\vec{e}_\alpha, \vec{r}_{\alpha B}) + \sum_i \vec{F}_{\alpha i}(\vec{e}_\alpha, \vec{r}_{\alpha i}, t)$

The fluctuation term takes into account random variations of the behaviour of the pedestrian α.

2.3 Optimal-velocity model

The optimal-velocity (OV) model [18],[19] for pedestrian dynamics is based on the one dimensional one thought for traffic flow. So first of all is important to briefly present the one dimensional OV model [18] to understand the two-dimensional one applicable for pedestrian dynamics. The basic concept of the model is that each driver controls the acceleration in order to reduce the difference between the optimal velocity and his/her real velocity. This can be expressed by the equation of motion:

$$\frac{d^2x_n(t)}{dt^2} = a\left[V(\Delta x_n(t)) - \frac{dx_n(t)}{dt}\right] \tag{2.14}$$

where:

- x_n and Δx_n are the position and the headway of the nth vehicle
- a is the *sensitivity*, which represents the strength of reaction of each driver
- $V(\Delta x) := \alpha[\tanh\beta(\Delta x - b) + c]$ is the OV function, which indicates the optimal velocity of the driver depending on the headway

This model has a trivial homogeneous flow solution:

$$x_n = hn + V(h)t + const \tag{2.15}$$

where all vehicles run with the same velocity $V(h)$ and the same headway h.

In order to apply this model to the pedestrian dynamics it is necessary to construct a two-dimensional OV model [19]. The equation of motion for a pedestrian j is given by:

$$\frac{d^2\vec{x}_j(t)}{dt^2} = a\left[\left\{\vec{V}_0 + \sum_k \vec{F}(\vec{x}_k(t) - \vec{x}_j(t))\right\} - \frac{d\vec{x}_j(t)}{dt}\right] \tag{2.16}$$

where:

- $\vec{x}_j := (x_j, y_j)$ and $\vec{x}_k := (x_k, y_k)$ are the positions of the jth and kth pedestrian
- $\vec{F}$ expresses the interaction between pedestrians and has the following form:

$$\vec{F}(\vec{x}_k - \vec{x}_j) = f(r_{kj})(1 + \cos\varphi)\vec{n}_{kj}$$

with $r_{kj} = \|\vec{x}_k - \vec{x}_j\|$, $\vec{n}_{kj} = \frac{(\vec{x}_k - \vec{x}_j)}{r_{kj}}$ and φ is the angle between the vectors $(\vec{x}_k - \vec{x}_j)$ and $\vec{V}_0$. $f(r_{kj}) = \alpha[\tanh \beta(r_{kj} - b) + c]$ represents the OV function like in the one-dimensional model.

The next chapter will introduce the last kind of models described at the beginning of this chapter, the Cellular Automata model. Differently from the models described in the previous sections this model is discrete and stochastic.

Chapter 3

Cellular automata model

Cellular automata (CA) [5]-[30] are rule-based models that are discrete in space and time. The structure is a two-dimensional grid, that describes the size and the shape of the room, which can be closed periodically in one or both directions.

Each cell can only be occupied by one particle so that this space requirement can be identified with the size of the cell. A natural space discretization can be calculated from the maximal densities observed in crowds which gives the minimal space occupied by one person. Empirical results showed that the maximum density is 6.25 per/m^2 that leads to a cell size of 40×40 cm^2, that is the typical space occupied by a person in a dense crowd [24]-[30].

The update of the position of every particle is done in parallel, this introduces a time scale into the dynamics which can be identified with the reaction time t_{reac}. In the model used in this work, a single particle, that doesn't interact with others, moves with a velocity of one cell per time step. The average velocity of a pedestrian observed in this kind of situations is about 1.3 m/s that leads to $t_{reac} \approx 0.3$ s [24]-[30].

The next section will discuss the general basic rules applicable in any kind of CA model. Sections 3.2-3.4 will focus on the CA model with *floor fields*. The chapter will end with a study made on the *dynamic floor field*, that will improve the accuracy of the calibration in Chapter 4.

3.1 Basic rules

All the particles are able to move in one of the four neighbouring sites, if they are free, or to stay in the same cell. The dynamics is defined by rules which specify transition probabilities for the motion of the particle (Fig.3.1). In each update step, for each particle a desired move is chosen randomly

according to these probabilities. If no other particle targets the same cell, the move is executed, otherwise there is a conflict and only one or none can move. This argument will be discussed deeper in Section 3.3.1 [24]-[30].

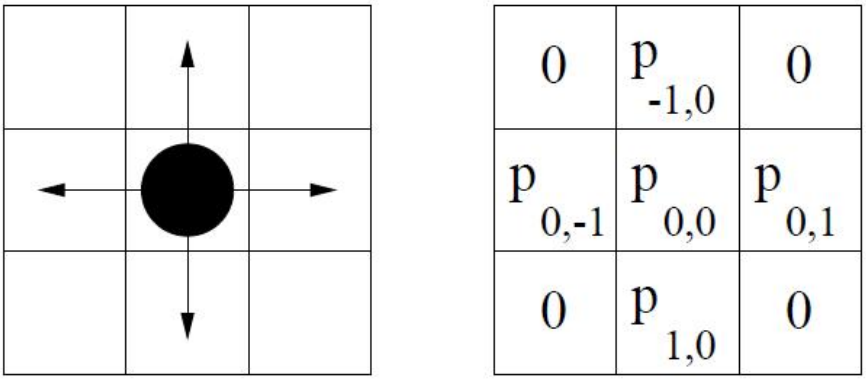

Figure 3.1: Possible directions of motion of a particle and the corrisponding transition probabilities p_{ij} [26]

The transition probabilities can be determined in different ways, according to the kind of CA model, but are always defined by three factors [5] : (1) the desired direction of motion, (2) interactions with other particles, and (3) interactions with the infrastructure (walls, doors , etc.). The model used in this work is a specific one, namely the floor field model (Sec.3.2-3.3). The probabilities in this model are calculated through a coupling to so-called *floor fields*. A couple of other examples of CA models are the following:

Fukui-Ishibashi Model

In this model [22]-[23] the pedestrians are divided in two groups. One group moves from east to west and the other one in the opposite direction on the same passageway. The passageway of length L and width W is defined by a two-dimensional lattice of L $\times$ W. The pedestrians of the east bound group E_g on each of W lanes of the passageway walk from west to east and encounter the pedestrians of the other group W_g, that are walking in the opposite direction. All pedestrians advance by one cell on one time step. On every odd time step, the pedestrians of the E_g group advance eastbound by one site. The pedestrians of the W_g group advance westbound at each even time step, if the site in front of them is empty. If the site in front of a pedestrian is occupied by a particle of the same group, he stops there, whereas is the site is occupied by a particle of the other group he'll change lane to avoid collision. The two following rules are applied:

1. *Sidestepping model*: If the site just beside the concerned pedestrian is empty, he sidesteps there. If both sides are empty, he chooses one randomly, while if both are occupied, he doesn't change the lane. The pedestrian going forward is given priority over the pedestrian changing lane.
2. *Diagonal sidestepping model*: If the diagonal front site is empty, the particle moves there. All the other rules are the same as 1.

Blue-Adler Model

The Blue-Adler CA model [20]-[21] is based on three fundamental elements: side stepping (lane changing), forward movement (breaking, acceleration), and conflict mitigation. Side stepping refers to the desire of the pedestrian to switch lane. Forward movement must be adaptable to the desired velocity of the pedestrian and the placement of the other particles in the neighbourhood. Conflict mitigation refers to the manner in which pedestrians approaching each other from opposite directions try to avoid a head-on deadlock. The basic rules of this model were developed around these three elements and were designed to work in a framework with parallel updates. To avoid the problem of head-on conflicts the use of a probability p_{exch} was introduced. When opposing pedestrians are within one cell of each other, the two particles will swap their positions with probability p_{exch}.

Each pedestrian is randomly assigned a desired speed of 2, 3, or 4 cells per time step. The rule set for the Blue-Adler CA model [20] is the following:

- *LANE CHANGE (parallel update 1)*
    1. Eliminate conflicts: two walkers that are laterally adjacent may not sidestep into one another
        (a) An empty cell between two walkers is available to one of them with 50/50 random assignment
    2. Identify gaps: same lane or adjacent (left or right) lane is chosen that best advances forward movement up to v_{max} according to the gap computation sub-procedure that follows the step forward update
        (a) For dynamic multiple lanes (DML)
            i. Step out of lane of a walker from opposite direction by assigning gap=0 if opposing pedestrian is within 8 cells
            ii. Step behind a same direction walker when avoiding an opposite direction walker by choosing any available lane with $gap_{same,dir} = 0$ when gap=0

(b) Ties of equal maximum gaps ahead are resolved according to:

i. Two-way tie between the adjacent lanes: 50/50 random assignment

ii. Two-way tie between current lane and single adjacent lane: 80/20 random assignment for stay in lane/adjacent lane

iii. Three-way tie: 80/10/10 assignment for stay in lane or either adjacent lane

3. Move: each pedestrian p_n is moved 0, +1, or -1 lateral sidesteps after 1. and 2. are completed

- *STEP FORWARD (parallel update 2)*

1. Update velocity: Let $v(p_n) = gap$, where gap was calculated with "gap computation" below
2. Exchanges:

if *(gap=0 or gap=1) AND* $gap = gap_{opp}$ **then**
  with probability p_{exch} $v(p_n) = gap + 1$;
else
  $v(p_n) = 0$
end

3. Move: each pedestrian p_n is moved $v(p_n)$ cells forward on the lattice after 1. and 2. are completed

- *SUB-PROCEDURE : GAP COMPUTATION*

1. Same direction: Look ahead a max of 8 cells ($8 = 2\ largest(v_{max})$)

if *occupied cell found with same direction* **then**
  set gap_{same} to number of cells between entities;
else
  $gap_{same} = 8$
end

2. Opposite direction:

if *occupied cell found with opposite direction* **then**
  set $gap_{opp} = ceil(0.5\ number\ of\ cells\ between\ entities)$;
else
  $gap_{opp} = 4$
end

3. Assign $gap = min(gap_{same}, gap_{opp}, v_{max})$

In the first parallel update, a set of lane changing rules is applied to each pedestrian to determine the next lane of each pedestrian based on the current condition. The lane that offers the best forward movement, between the left, same or right lane, is chosen as the next lane of the pedestrian. Once all the sidesteps are decided, all the pedestrian are moved to the new cells.

In the second parallel update, a set of forward movement rules is applied to each pedestrian. The allowable movement of each pedestrian is based on the pedestrian's desired speed and the available gap in the lane he chooses. Once speeds are found for every particle, all of them execute their forward movement to the new cells [21].

3.2 Floor fields

In order to reproduce certain collective phenomena it is necessary to introduce longer-ranged interactions. In some continuous models this is done using the idea of social force. Since we want to keep the model as simple as possible we introduce in the CA model the concept of *floor field* [5], [24]-[30].

This kind of approach allows us to take into account the interactions between particles and the geometry of the system, without loosing the advantage of the local transition rules, that is the reason why this model was chosen. The two floor fields are called the *static floor field* and the *dynamic floor field*. These two fields are going to influence the transition probabilities in such a way that a motion into the direction of a larger field is preferred.

3.2.1 Static floor field

The static floor field S does not evolve in time and is not changed by the presence of the particles. Such a field is used to specify some region of the system of particular interest for the pedestrians, such as emergency exits or shop windows. In case of an evacuation, the static floor field describes the shortest distance to an emergency exit. The values of S in each cell

are calculated due to a certain distance metric so that the field values are increased in the direction to the door.

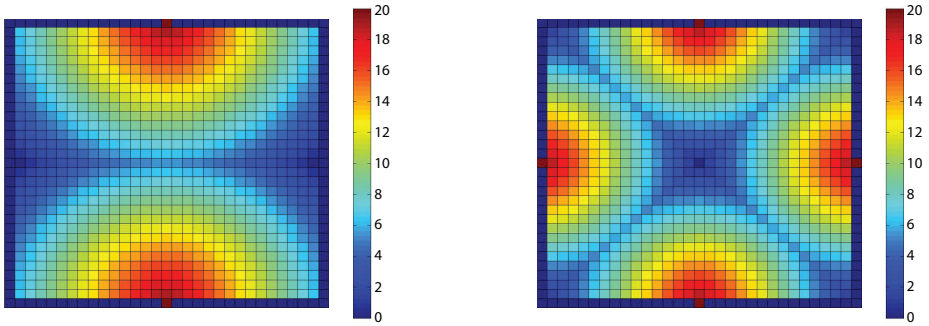

(a) Two doors (b) Four doors

Figure 3.2: Examples of static floor fields

In this work the values of S_{ij} are calculated in the following way [25] : The pedestrian can leave the room only through a number of door cells $\{(i_{T_1}, j_{T_1}) \cdots (i_{T_k}, j_{T_k})\}$ and can move only on the cells (i_l, j_l) with no obstacles. The explicit values of S are calculated with a distance matrix:

$$S_{ij} = \min_{(i_{T_s}, j_{T_s})} \{\max_{(i_l, j_l)} [\sqrt{(i_{T_s} - i_l)^2 + (j_{T_s} - j_l)^2} - \sqrt{(i_{T_s} - i)^2 + (j_{T_s} - j)^2}]\}$$

This means that the value of the static floor field depends on the shortest distance to an exit. The value $\max_{(i_l, j_l)} \sqrt{(i_{T_s} - i_l)^2 + (j_{T_s} - j_l)^2}$ is the largest distance of any cell to the door (i_{T_s}, j_{T_s}). This is used to normalize the values of the field so that they increase with the decreasing distance $\sqrt{(i_{T_s} - i)^2 + (j_{T_s} - j)^2}$ to a door and are equal to zero for the cell farthest away from the exit as it is shown in Fig.3.2.

3.2.2 Dynamic floor field

The dynamic floor field D is modified by the presence of the pedestrians and evolves in time. The chosen approach is very similar to the one used by some insects for communication [31]. They create a chemical trace to guide other individuals to food sources. In this case pedestrians also create a trace, that differently from the one created by insects is only virtual, although one can assume that it corresponds to some abstract representation of the path in the mind of the pedestrians. Since the total transition probability is proportional

to the dynamic field every particle becomes more attracted to follow other particles. At the beginning of the simulation all cells are empty of this trace. Whenever a pedestrian jumps from site (i,j) to one of the four neighbours, the trace in the cell (i,j) is increased by one.

$$D_{ij} \longrightarrow D_{ij} + 1$$

The dynamic floor field is also subject to diffusion and decay which leads to a dilution and finally yo the vanishing of the trace after some time [24]-[25] . After all motions of the pedestrians during one time step have been performed, the oldest trace of each cell is destroyed with probability α, the destruction parameter. With probability δ, the diffusion parameter, the trace diffuses randomly to one of the neighbouring cells I=[(p,k)∈(neighbouring cells of (i,j))].

$$\alpha : D_{ij} \longrightarrow D_{ij} - 1$$
$$\delta : D_{ij} \longrightarrow D_{ij} - 1 \; and \; D_{pk} \longrightarrow D_{pk} + 1 \; with \; (p,k) \in I$$

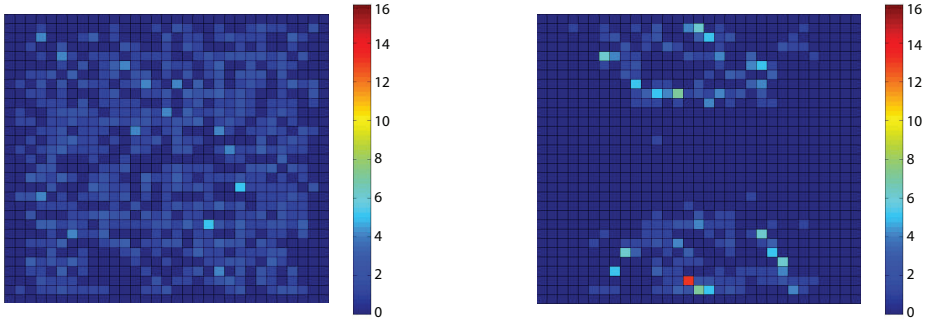

(a) t=1.5s (b) t=150s

Figure 3.3: Examples of dynamic floor fields (two doors)

3.3 Movement rules

The movements of all the particles is driven by the *transition probability matrix*. In order to reproduce certain collective phenomena and to give an intelligence to the particles, this matrix must be dependent from the two floor fields. At each time step for each particle a matrix is created in order to choose where to move [26],[29] :

$$p_{ij} = Ne^{k_S S_{ij}} e^{k_D D_{ij}} (1 - \eta_{ij}) p_{ij}^I p_{ij}^D \tag{3.1}$$

Here η_{ij} is the occupation of the target cell in direction (i,j). A cell is occupied if there is a particle or an obstacle on it.

$$\eta_{ij} = \begin{cases} 1 \; if \; (i,j) \; is \; occupied \\ 0 \; if \; (i,j) \; is \; empty \end{cases}$$

N is a normalization constant to ensure that $\Sigma_{ij} p_{ij} = 1$, where the sum is over the five possible targets.

k_S and k_D are the coupling strength of the two fields. This two parameter drive the influence that the two fields have on the probabilities (see 3.4). S_{ij} and D_{ij} are the values of the static and the dynamic fields in the cell (i,j). For a strong coupling to the static field pedestrians will choose the shortest way to the exit. This represents a normal situation. A strong coupling with the dynamic field instead implies a strong herding effect behaviour leading the pedestrians to follow the others. This often happens in emergency situations.

The inertia factor p_{ij}^I is equal to e^{k_I} , where k_I is the inertia parameter, if during the time step from t-1 to t the particle has moved in the same direction, so that this movement is enhanced. Otherwise the inertia factor is equal to 1 [29].

The correction factor p_{ij}^D is equal to e^{-k_D}, if in the time step t-1 the particle was in (i,j). Otherwise it is equal to 1. This factor avoids the risk of a particle being influenced by the trace that he left in the previous time step. The update rules Z [25] of the full model including the interaction with the floor fields have the following structure:

1. For each pedestrian, the transition probability matrix for a move to an unoccupied neighbour cell is determined.
2. Each pedestrian chooses a target cell based on the probabilities of the transition matrix.
3. The conflicts arising by two or more pedestrians attempting to move to the same target are resolved like in 3.3.1.
4. The pedestrians allowed to move execute their step.
5. The pedestrians change the dynamic floor field of the cell they occupied before the move.
6. The dynamic floor field is modified according to its diffusion and decay rules described in 3.2.2.

3.3.1 Conflicts

In each time step, a desired move is chosen according to the transition probability matrix, like described in the previous section. This is done in parallel for all the particles, therefore conflicts can occur where different particles choose the same destination cell. If the target cell is empty and no other particle targets the same cell, the move is executed. In case two or more particles choose the same cell, a conflict arises which can be solved in two ways:

1. While one particle is picked randomly and execute the move, the other particles involved in the conflict don't move. This can be simply done by updating the move of the pedestrian sequentially and not in parallel. At every time step the order of move of the particles is randomly picked.

2. For the floor field model it has been shown that the behaviour becomes more realistic if not all conflicts are resolved. This means that one pedestrian for sure is allowed to move whereas the others stay at their position [28]. That is why it is possible to introduce to the model a new parameter, the so called friction parameter $\mu \in [0, 1]$. With probability μ the movement of *all* involved pedestrians is denied (Fig.3.4). This allows to describe clogging effects between the pedestrians in a much more detailed way, but the computational time using μ is much higher than without.

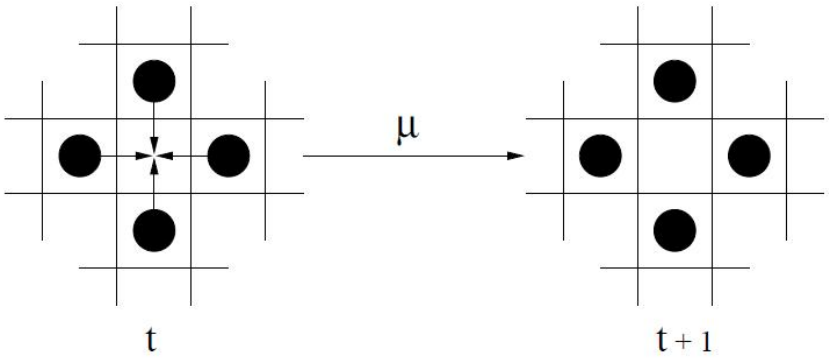

Figure 3.4: Refused movement due to the friction parameter μ [28]

C++ Implementation

Parameters

- $xsize \in \mathbb{Z}_+$: size of the room in the x axes
- $ysize \in \mathbb{Z}_+$: size of the room in the y axes
- $\rho \in [0,1]$: density of pedestrians in the room
- $numcells \in \mathbb{Z}_+$: number of cells with no obstacles and doors on it
- $numped = \rho\ numcells$: number of pedestrian in the room
- $\alpha \in [0,1]$: destruction parameter
- $\delta \in [0,1]$: diffusion parameter
- $k_S \in \mathbb{R}_+$: coupling strength to the static floor field
- $k_D \in \mathbb{R}_+$: coupling strength to the dynamic floor field
- $k_I \in \mathbb{R}_+$: inertia parameter

Variables

- $E_S \in \mathbb{R}_+^{xsize \times ysize}$: static floor field matrix
- $E_D \in \mathbb{R}_+^{xsize \times ysize}$: dynamic floor field matrix
- $E_O \in \{0,1,2,3\}^{xsize \times ysize}$: occupation matrix
  (0=empty, 1=occupied by a pedestrian, 2=occupied by an obstacle, 3=door)
- $P^i \in \mathbb{R}^{3\times 3}$ *with* $p^i_{-1-1} = p^i_{11} = p^i_{-11} = p^i_{1-1} = 0$:
  probability matrix of the ith pedestrian
- $pedinroom \in \mathbb{N}$: number of pedestrians still in the room
- $PED \in \mathbb{N}^{pedinroom}$: vector containing the indices of the pedestrian still in the room
- $DM \in \mathbb{N}^{pedinroom \times 2}$: matrix containing the desired moves of all the particles

Functions

- *assignfp* : function that assigns the first position to all pedestrians and updates E_O
- *createstatic* : function that creates E_S with the metric described in 3.2.1, and assigns the right value to *maxstat* (Sec. 3.4)
- *probmatrix* : function that calculates the probability matrix of a particle
- *permutation* : function that permutes the elements of the vector

- *move* : function that executes the move of the pedestrians
- *desmove* : function that decides the desired move of a particle
- *moveconflicts* : function that evaluates all the desired moves and executes them, taking into account the conflicts arisen
- *updatedynamic* : function that updates the matrix E_D with the diffusion and decay rules described in 3.2.2

$E_S = createstatic(xsize, ysize);$
$E_O = assignfp(numped);$
while *pedinroom!=0* **do**
  $PED = permutation(PED);$
  for *k=1:pedinroom* **do**
    $i = PED(k);$
    $P^i = probmatrix(E_O, E_S, E_D, k_D, k_S, k_I);$
    $[E_O, E_D] = move(P^i);$
  end
  $E_D = updatedynamic(\alpha, \delta);$
end

Algorithm 1: Without friction

$E_S = createstatic(xsize, ysize);$
$E_O = assignfp(numped,);$
while *pedinroom!=0* **do**
  for *i=1:pedinroom* **do**
    $P^i = probmatrix(E_O, E_S, E_D, k_D, k_S, k_I);$
    $DM^i = desmove(P^i)$
  end
  $[E_O, E_D] = moveconflicts(DM);$
  $E_D = updatedynamic(\alpha, \delta);$
end

Algorithm 2: With friction

3.4 Dynamic floor field study

The purpose of this study is to understand how the average maximum value of the floor field varies in function of the parameters of the system in a simulation of an evacuation from a room. The idea is to find a suitable upper

limit for the static floor field to avoid overflow problems in the simulation with C++. Once the two coupling strengths $k_S = k_D = 1$ are fixed, we expect that the movement of the particles depends from the two fields more or less in the same way, but that is not true if one of the fields is much stronger than the other one. Normalizing the static floor field with the average maximum value of the dynamic floor field with a fixed combination of parameters should equalize the strength of the two floor fields, so that the two terms $e^{k_S S}$ and $e^{k_D D}$ depend only from the two coupling strengths and not from the parameters of the system.

Another useful aspect of this normalization can be seen in the calibration of the model. The experimental data of the evacuation are considered in a certain system. Once the right proportion of k_S and k_D to reproduce the experimental data is found, it is not sure that this proportion is correct changing the system, because the maximum values of the two floor fields change their intensities. This problem can be solved partially with the normalization described in this section.

The maximum value of the static floor field $maxstat = maxstat(siz)$, with the metric used in this work, depends from the size of the room, because the value $\max_{(i_l,j_l)} \sqrt{(i_{T_s} - i_l)^2 + (j_{T_s} - j_l)^2}$ describes the maximum distance from one door to each cell. The average maximum value of the dynamic floor field $\overline{maxdyn} = \overline{maxdyn}(siz, \rho, \alpha, \delta)$ is a function of the four parameters of the system, but does not change significantly for different simulation with a fixed combination of those parameters. The parameters of the system are: a)the size of the room: $siz \times siz$; b)the initial density of pedestrians in the room ρ ; 3)the destruction parameter α ; d)the diffusion parameter δ.

The maximum values of the dynamic floor field at each time step, while the field is stationary, $maxdyn_t(siz, \rho, \alpha, \delta)$ are averaged in time for every combination of the four parameters.

$$\overline{maxdyn}(siz, \rho, \alpha, \delta) = E_t[maxdyn_t](siz, \rho, \alpha, \delta) \tag{3.2}$$

The maximum value of the static floor field $maxstat$ and the inertia parameter k_I are fixed to the values $maxstat = 20$ and $k_I = 1$. The value 20 has been determined observing the average maximum values of the dynamic floor field in some preliminary simulations. After finding the values $\overline{maxdyn}(siz, \rho, \alpha, \delta)$, a second simulation is done changing the maximum values of the static field for every combination of the parameters: $maxstat_i = \overline{maxdyn}_{i-1}$ where i are the simulations. This process is repeated until the succession of all the $\overline{maxdyn}_i(siz, \rho, \alpha, \delta)$ converge to certain points.

3.4.1 Geometry

In order to understand the dependence of the dynamic floor field to the number and the position of the doors, two different geometries of the system were tried. The dynamic field is for sure dependent on the number and the positions of the doors, but if the results with the two systems are similar, it is possible to conclude that this dependence is not strong enough to influence this study, that is only qualitative.

One door

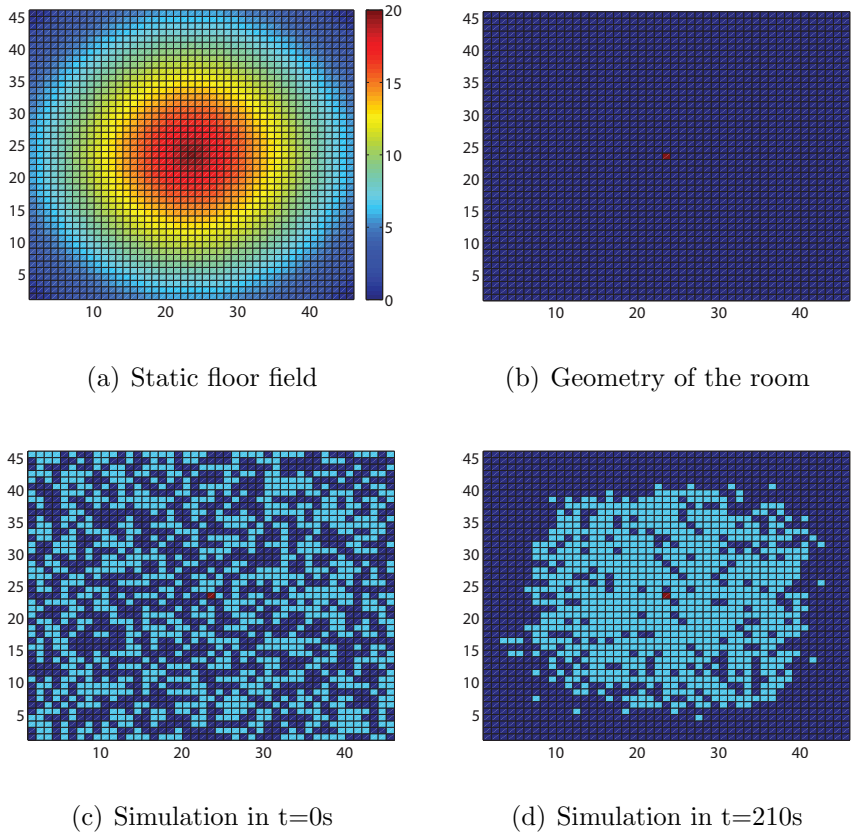

(a) Static floor field

(b) Geometry of the room

(c) Simulation in t=0s

(d) Simulation in t=210s

Figure 3.5: Dynamic floor field study: one door geometry

The system is symmetric with one door and with periodic boundary conditions in all directions (Fig. 3.5), in order to investigate a general case. The door is placed in the middle of the square in order to maintain the symmetry of the system. From now on blue, light blue, yellow and red cells represent

the free cells, the pedestrians, the obstacles (walls, columns, etc.) and the doors respectively.

Two doors

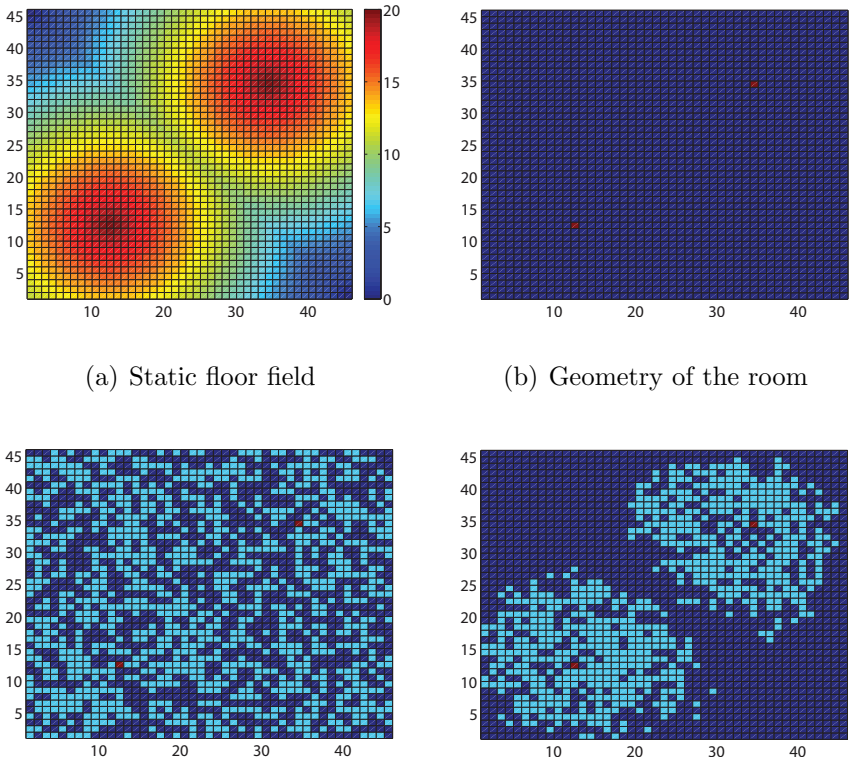

(a) Static floor field

(b) Geometry of the room

(c) Simulation in t=0s

(d) Simulation in t=210s

Figure 3.6: Dynamic floor field study: two doors geometry

The second system is also symmetric and with periodic boundary conditions but with two doors placed in the first and third quarter of the system always to maintain the symmetry (Fig. 3.6).

3.4.2 1-dimensional study

In the first simulations only the dependence of $\overline{maxdyn}$ from one of the 4 parameters is studied. The purpose of this is to have a preliminary understanding of the dependence of each parameter singularly to the dynamic floor field to control that the 4-dimensional study is correct.

PARAMETERS	VARIABLE
ρ=0.5 ; α=0.4 ; δ=0.2	siz
siz=45 ; α=0.4 ; δ=0.2	ρ
siz=45 ; ρ=0.5 ; δ=0.2	α
siz=45 ; ρ=0.5 ; α=0.4	δ

Table 3.1: Parameters used for the 1-dimensional dynamic floor field study

One Door

The function $\overline{maxdyn}(siz)$ (Fig.3.7.a) is constant around the value 4.5 for every size of the room. Even if the pedestrians in the room are more, with a bigger room, the effect seen in the function $\overline{maxdyn}(siz)$ is not of particular influence in this case.

In Fig.3.7.b the function $\overline{maxdyn}(\rho)$ is shown. The average value and standard deviation of the dynamic floor field increases with the initial density. The increase of the number of pedestrian inside the room brings to a higher probability that a pedestrian walks on the cells near the door and this causes an increase of $\overline{maxdyn}$. The minimum value is obtained in $\rho = 0.2$ and is equal to 2.5, while the maximum is obtained in $\rho = 0.9$ and equals 5.7.

In Fig.3.7.c it is possible to observe, that the values of $\overline{maxdyn}$ and the standard deviation decrease with the increase of α. This result was predictable, because α is the probability that the oldest trace is destroyed. The shape of the function remembers an exponential function. The maximum value is 17, while the minimum is 1, and are obtained respectively for $\alpha = 0.1$ and $\alpha = 0.9$.

The maximum average value of the dynamic floor field decreases with the increase of δ (Fig.3.7.d). If the diffusion probability is higher, the traces of the pedestrians diffuse more easily and this brings to a decrease of the dynamic floor field. Even if the trend seems to be monotonic decreasing, the maximum is obtained in $\delta = 0.1$ and $\delta = 0.7$ and equals 4.3, while the minimum equals 3 and is obtained in $\delta = 0.9$.

In the following Table 3.2 all the values of the non-linear regression of the four functions $\overline{maxdyn}(\cdot)$ are listed. For each variable the best function that suits the values of $\overline{maxdyn}(\cdot)$ is chosen for the non-linear regression.

Two Doors

In the 2 doors system the function $\overline{maxdyn}(siz)$ (Fig.3.8.a) is not constant in a unique value. In this case the enlargement of the room brings to an increase of the average maximum value of the dynamic field. These values

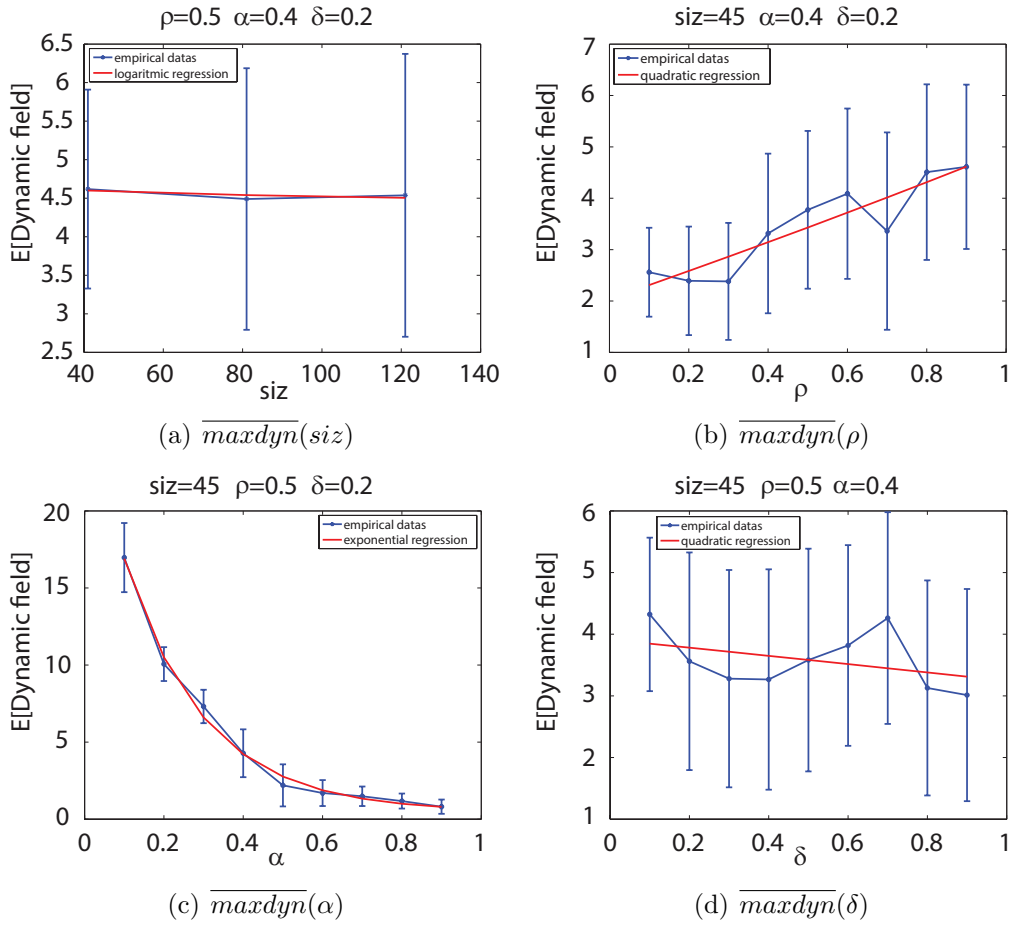

(a) $\overline{maxdyn}(siz)$ (b) $\overline{maxdyn}(\rho)$

(c) $\overline{maxdyn}(\alpha)$ (d) $\overline{maxdyn}(\delta)$

Figure 3.7: 1-dimensional study: one door

VARIABLES	FUNCTION	COEFFICIENTS
siz	$f(x) = aln(x) + b$	a=-0.087294 b=4.9237
ρ	$f(x) = ax^2 + bx + c$	a=0.20073 b=2.6805 c=2.04
α	$f(x) = ae^{bx} + c$	a=26.892 b=-4.9345 c=0.48061
δ	$f(x) = ax^2 + bx + c$	a=-0.019458 b=-0.64989 c=3.9122

Table 3.2: One door: Non-linear regression coefficients of the 1-dimensional dynamic floor field study

go from 2.9 in $siz = 80$ to 4 in $siz = 120$.

For the same reason as before the function $\overline{maxdyn}(\rho)$ (Fig.3.8.b) and the standard deviation is increasing with the initial pedestrian density ρ. The minimum value is obtained in $\rho = 0.3$ and the maximum in $\rho = 0.9$ and they are equal to 1.9 and 3.5 respectively.

The function $\overline{maxdyn}(\alpha)$ is shown in Fig.3.8.c. The results are exactly the same as in the one door system.

The function $\overline{maxdyn}(\delta)$ is increasing with δ as in the one door system. The maximum value is 3.5, while the minimum value is 2.1, and are obtained respectively in $\delta = 0.1$ and $\delta = 0.8$.

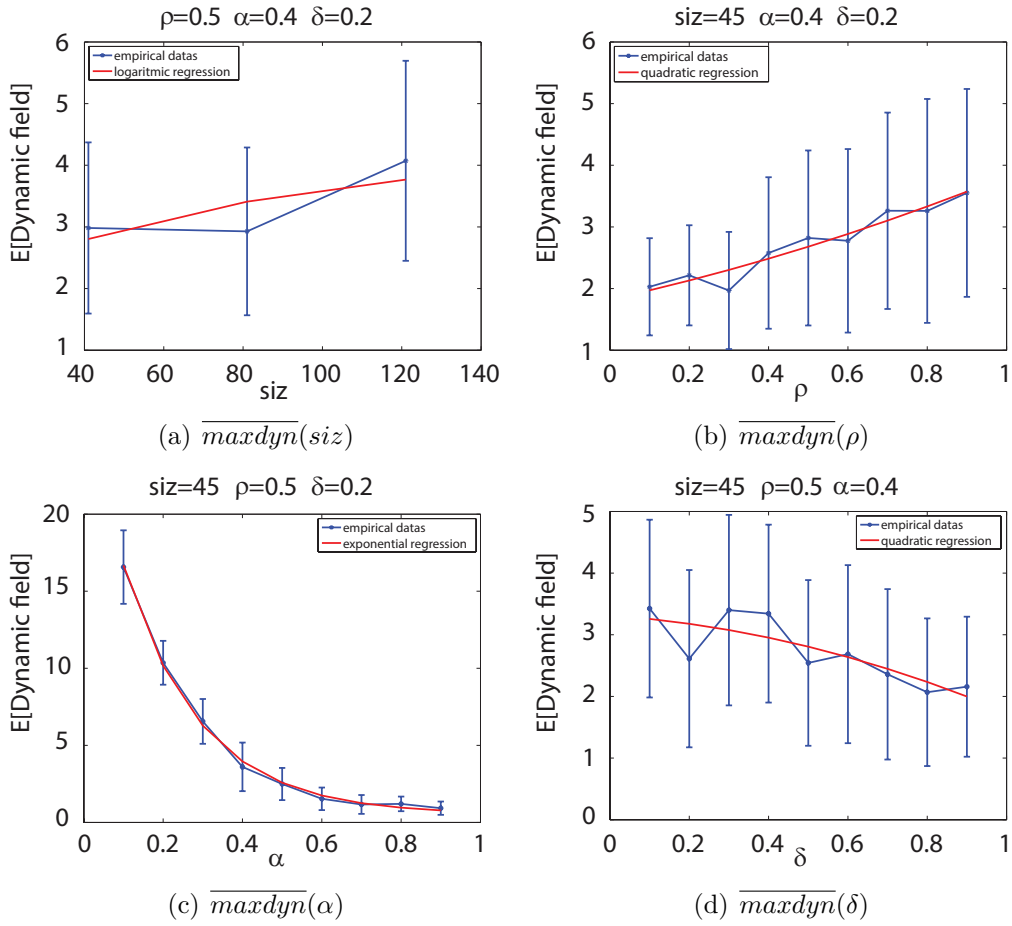

(a) $\overline{maxdyn}(siz)$ (b) $\overline{maxdyn}(\rho)$

(c) $\overline{maxdyn}(\alpha)$ (d) $\overline{maxdyn}(\delta)$

Figure 3.8: 1-dimensional study: two doors

VARIABLES	FUNCTION	COEFFICIENTS
siz	$f(x) = aln(x) + b$	a=0.8911 b=-0.50539
ρ	$f(x) = ax^2 + bx + c$	a=0.57579 b=1.4243 c=1.823
α	$f(x) = ae^{bx} + c$	a=27.062 b=-5.1572 c=0.51949
δ	$f(x) = ax^2 + bx + c$	a=-1.1175 b=-0.45604 c=3.3143

Table 3.3: Two doors: Non-linear regression coefficients of the 1-dimensional dynamic floor field study

3.4.3 4-dimensional study

In this section the results of the 4-dimensional simulation are shown. After the preliminary results, all the points of the function $\overline{maxdyn}(siz, \rho, \alpha, \delta)$ are calculated. For computational time problems it was not possible to have a really dense grid, but this problem has been avoided, interpolating the simulated values in a denser grid. The following table shows the values of the parameters used for the simulation.

VARIABLE	POINTS
siz	[17,33,65,129]
ρ	[0.1,0.3,0.5,0.7,0.9]
α	[0.1,0.3,0.5,0.7,0.9]
δ	[0.1,0.3,0.5,0.7,0.9]

Table 3.4: Parameters used for the 4-dimensional dynamic floor field study

One door

As mentioned before this simulation is repeated until the average of the difference between the last simulation and the previous one over all combinations of the four parameters $(siz, \rho, \alpha, \delta) \in C = \{$ *all possible combinations* $\}$ is not so high:

$$E_{(siz,\rho,\alpha,\delta)\in C} \; |\overline{maxdyn}_i(siz, \rho, \alpha, \delta) - \overline{maxdyn}_{i-1}(siz, \rho, \alpha, \delta)| < \varepsilon$$

After the second simulation we can observe that the average difference observed between the second and the first simulation is 0.84959. This value is still a bit high even assuming that there is a bit of variance between the two simulations and that the values are rounded up. It is possible to see in Fig.3.9.a, where the probabilities of a certain difference between the two simulation are plotted, that there are still many combinations where the difference is 1 and 2.

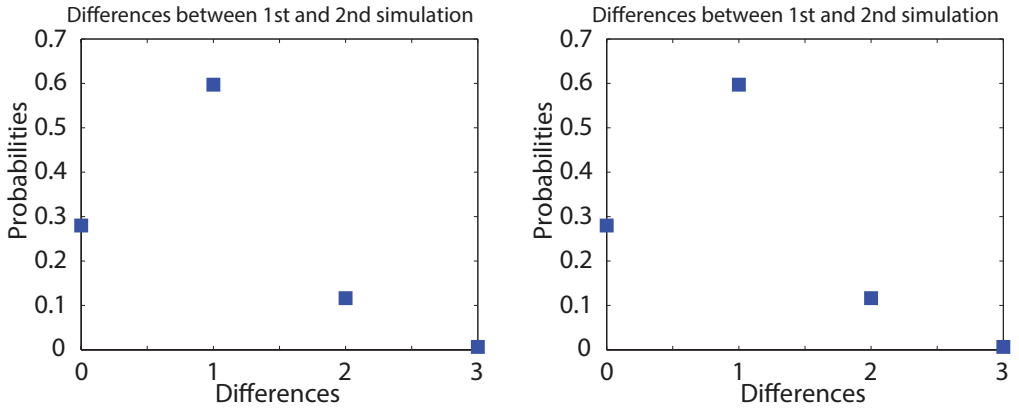

(a) 1_{st} and 2_{nd} simulation (b) 1_{st} and 2_{nd} simulation

Figure 3.9: One door: probability density function of the differences between 2 consecutive simulations

Repeating again the simulation changing the values of $maxstat_3 = \overline{maxdyn}_2$ the average value decreases to 0.32051. This value is acceptable and in Fig.3.9.b it is even possible too see that almost all the probability density function is concentrated in 0, that was the desired result.

In Fig.3.10.a-b the values of the dynamic field as a function of α and respectively the density and the size of the room are shown. For small values of α the two functions are increasing in density and size, as predicted from the 1-dimensional study. For higher values of α this dependence is weaker, and the values of $\overline{maxdyn}$ don't change so much, increasing ρ and siz. This result is understandable, because if α is high, the dynamic field can not grow, even with higher values of ρ and siz. The maximum values for the two functions are obtained in $(\rho, \alpha) = (0.9, 0.1)$ and $(siz, \alpha) = (129, 0.1)$ and are equal to 16 and 17 respectively. The minimum values are equal to 1 and are obtained for both the functions in $\alpha = 0.9$. The function $\overline{maxdyn}(siz, \rho)$ (Fig.3.10.c) is increasing with both siz and ρ and has a maximum value equal to 5 and a minimum value equal to 1.

In Fig.3.11 are plotted the functions $\overline{maxdyn}(siz)$, $\overline{maxdyn}(\rho)$, $\overline{maxdyn}(\alpha)$ and $\overline{maxdyn}(\delta)$ fixing the other parameters like in 3.4.2, to compare the results with the 1-dimensional study. All four functions have almost the same behaviour as in 3.4.2. The following table shows the coefficients of the non-linear regression made on the 1-dimensional functions:

The results of the regression are similar to the one obtained in the 1-dimensional study, this confirms that the 4-dimensional study is correct.

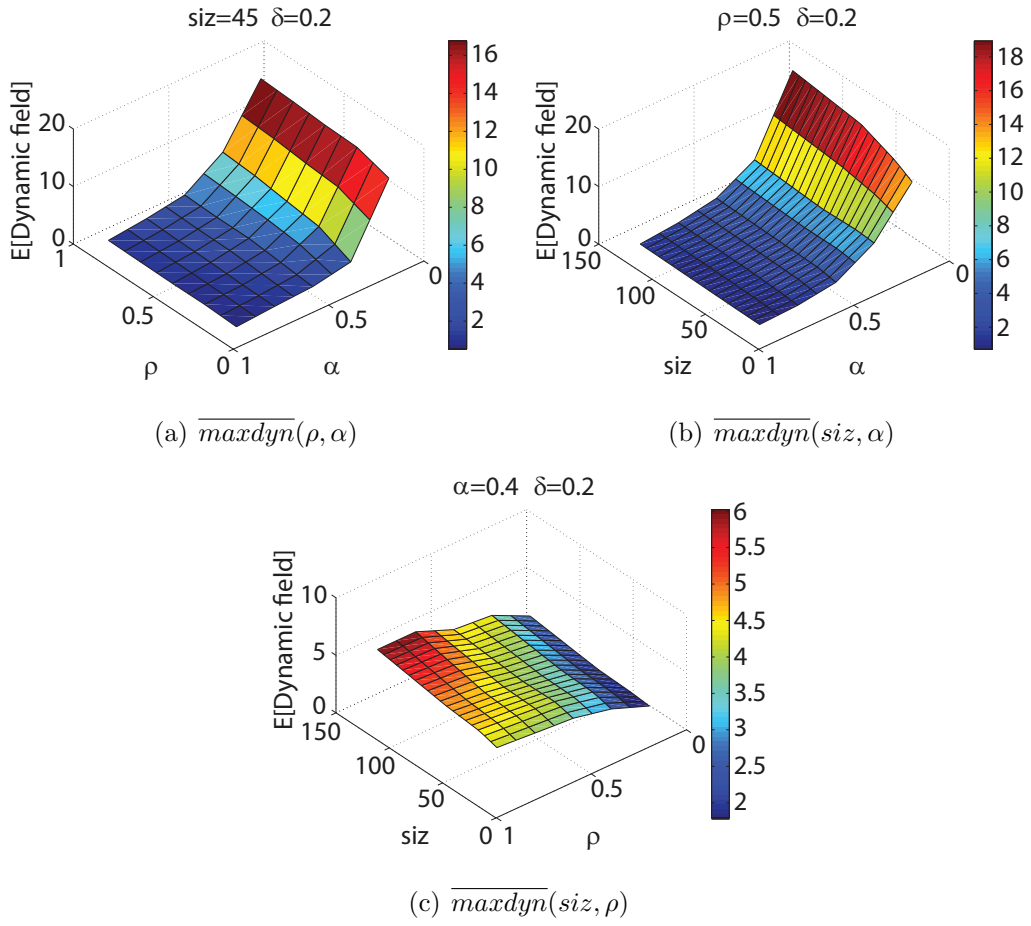

(a) $\overline{maxdyn}(\rho, \alpha)$

(b) $\overline{maxdyn}(siz, \alpha)$

(c) $\overline{maxdyn}(siz, \rho)$

Figure 3.10: 4-dimensional study (2 variable dependence) : one door

VARIABLES	FUNCTION	COEFFICIENTS
siz	$f(x) = aln(x) + b$	a=0.36737 b=2.7443
ρ	$f(x) = ax^2 + bx + c$	a=-4.5827 b=7.922 c=1.3513
α	$f(x) = ae^{bx} + c$	a=25.77 b=-4.8672 c=0.43673
δ	$f(x) = ax^2 + bx + c$	a=-1.4855 b=1.6792 c=3.8561

Table 3.5: One door: Non-linear regression coefficients of the 4-dimensional dynamic floor field study

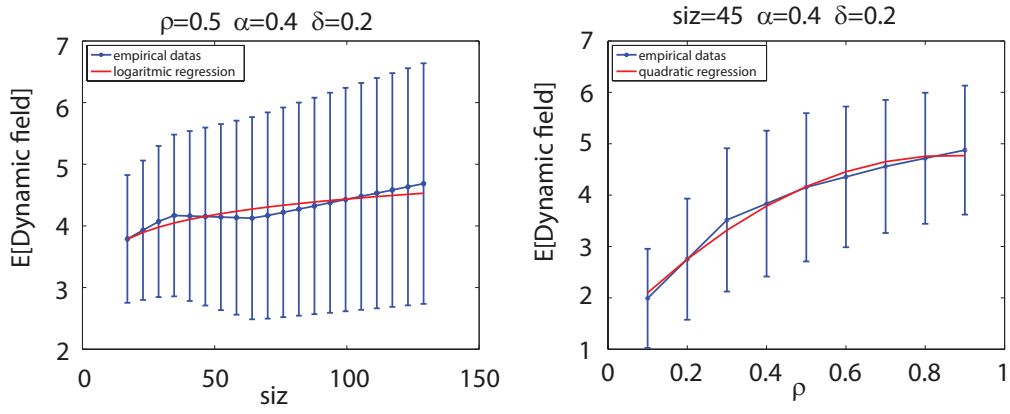

(a) $\overline{maxdyn}(siz)$ (b) $\overline{maxdyn}(\rho)$

(c) $\overline{maxdyn}(\alpha)$ (d) $\overline{maxdyn}(\delta)$

Figure 3.11: 4-dimensional study (1 variable dependence) : one door

Two doors

Even in the two doors system the simulation is repeated until the average of the difference between the last simulation and the previous one over all combinations of the four parameters $(siz, \rho, \alpha, \delta) \in C = \{\ all\ possible\ combinations\ \}$ is not so high.

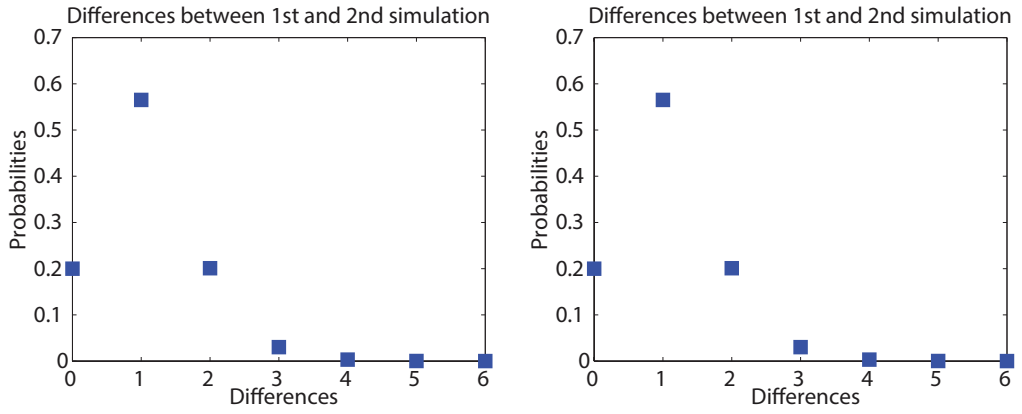

(a) 1_{st} and 2_{nd} simulation

(b) 1_{st} and 2_{nd} simulation

Figure 3.12: Two doors: probability density function of the differences between 2 consecutive simulations

Like in the one door system after the second simulation the mean difference with the first are a bit too high: 1.0726, and the combinations with differences equal to 1 and 2 are still plenty (Fig.3.12.a).

Repeating again the simulation, changing the values of $maxstat_3 = \overline{maxdyn}_2$, the average value decreases to 0.28182. This value is acceptable and in Fig.3.12.b is even possible too see that almost all the probability density is concentrated in 0.

In Fig.3.13 the 3 functions $\overline{maxdyn}(\rho, \alpha)$, $\overline{maxdyn}(siz, \alpha)$ and $\overline{maxdyn}(siz, \rho)$ are shown. It is possible to notice that the results are approximately the same as in the system with one door.

In Fig.3.14 are plotted the functions $\overline{maxdyn}(siz)$, $\overline{maxdyn}(\rho)$, $\overline{maxdyn}(\alpha)$ and $\overline{maxdyn}(\delta)$ fixing the other parameters like in 3.4.2. Even in the two doors system all four functions have almost the same behaviour as in 3.4.2. The following table shows the coefficients of the non-linear regression made on the 1-dimensional functions:

Even in this case the non-linear regressions are similar to the one of the 1-dimensional study, confirming that the 4-dimensional one is correct.

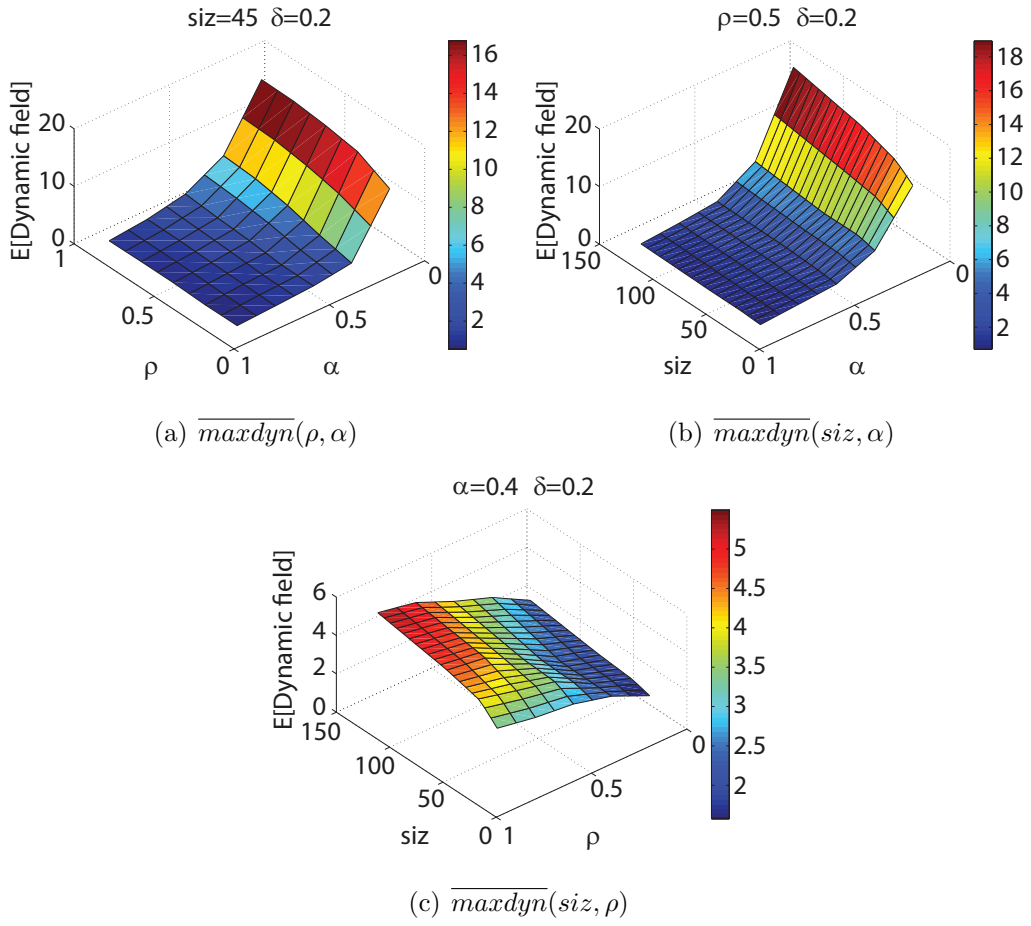

(a) $\overline{maxdyn}(\rho, \alpha)$

(b) $\overline{maxdyn}(siz, \alpha)$

(c) $\overline{maxdyn}(siz, \rho)$

Figure 3.13: 4-dimensional study (2 variable dependence) : two doors

VARIABLES	FUNCTION	COEFFICIENTS
siz	$f(x) = aln(x) + b$	a=0.55032 b=1.4316
ρ	$f(x) = ax^2 + bx + c$	a=-1.4249 b=5.0427 c=1.2969
α	$f(x) = ae^{bx} + c$	a=27.081 b=-5.5426 c=0.62374
δ	$f(x) = ax^2 + bx + c$	a=-2.5562 b=1.5109 c=3.3864

Table 3.6: Two doors: Non-linear regression coefficients of the 4-dimensional dynamic floor field study

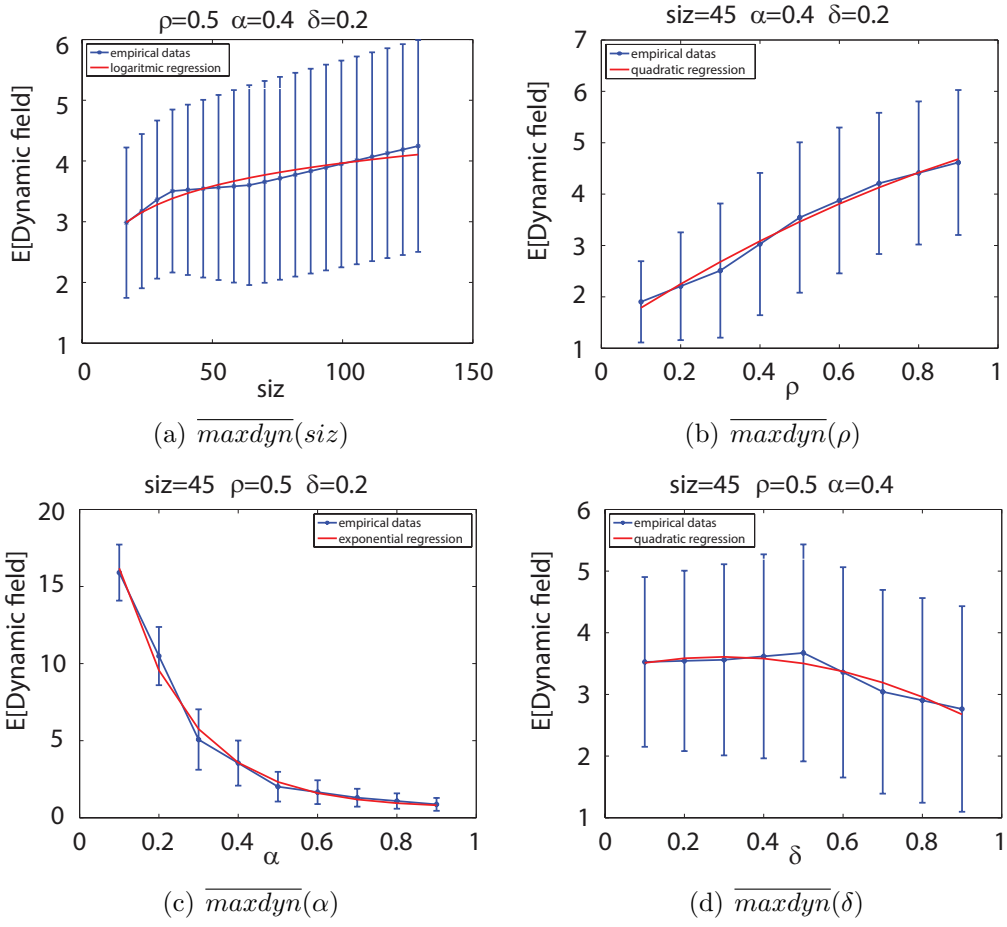

(a) $\overline{maxdyn}(siz)$ (b) $\overline{maxdyn}(\rho)$

(c) $\overline{maxdyn}(\alpha)$ (d) $\overline{maxdyn}(\delta)$

Figure 3.14: 4-dimensional study (1 variable dependence) : two doors

Conclusion

The difference between the one door and the two doors geometries is not so high. It is not possible to say that for all number of doors and for each position of these, the average value of the dynamic floor field does not change, but we can conclude that it is not so influential in this qualitative study.

Once the right value of the 4 movement parameters (k_S, k_D, k_I and μ) are found, in order to reproduce in a correct way the real data for a fixed geometry, therefore with the 4 fixed system parameters (siz, ρ, α and δ), it is possible, thanks to the values found for each system parameters combination, to use the same movement parameters in different geometries obtaining the right desired movement of the pedestrians. As already mentioned in 3.4 this is done, using the normalization of the static floor field so that its strength is comparable to the one of the dynamic floor field. These considerations will be important in the next chapter, where the calibration of the model will be discussed.

C++ Implementation

```
xsize = ysize;
for xsize = 17 : 129 do
    for ρ = 0.1 : 0.9 do
        for α = 0.1 : 0.9 do
            for δ = 0.1 : 0.9 do
                Algorithm 1;
            end
        end
    end
end
```

Algorithm 3: Dynamic floor field study

Chapter 4

Calibration

The aim of this chapter is to calibrate the model, i.e. finding the right values of the movement parameters in order to reproduce correctly the real pedestrian dynamics. Past works about the cellular automata model focused on the study of these parameters, but none of them found precise values. For this reason there are no information about the right values of the different parameters.

The calibration is made using the Montecarlo method and a statistical estimation method that has as input the experimental data. The aim of this operation is to calculate the values of the parameters of the model in order to minimize the difference between the modelled values and the experimental values of some variables of interest.

Let us assume $x^i = [x_1^i, \ldots, xn^i]$ the points in which the variable i is calculated, $f_r^i = f_r^i(x^i)$ the real values of the variable i taken from the experiments and $f^i_{(k_S,\mu,k_I)} = f^i_{(k_S,\mu,k_I)}(x^i)$ the simulated variables for each combination of the parameters. The method used is the following:

Minimize the average on x^i of the ratio between the absolute error between the simulated and the real value of the variable i and the real value of the variable i:

$$minerr_1^i = \min_{(k_S,\mu,k_I,c)} E_{x^i}\left[\frac{|f^i_{(k_S,\mu,k_I)} - f_r^i|}{f_r^i}\right]$$

To determinate the parameters that better fix different variables i, the following equation was used:

$$mintot_1 = \min_{(k_S,\mu,k_I,c)} E[minerr_1^1, \ldots, minerr_1^n]$$

As already explained in Section 3.4, the parameters of the environment are: the size of the room, the decay parameter α, the diffusion parameter

δ and the initial density of pedestrians in the room ρ. These values will be fixed in order to study the other parameters of the model that concern the movement of the pedestrians. The values of α and δ are fixed to 0.4 and 0.2 respectively, while the size of the room and the initial density of the pedestrians in the room change according to the experiment used. The parameters of the movement are the following:

- **Dynamic coupling strength** k_D — This parameter controls the influence that pedestrians have from the dynamic floor field. It is really important to understand the right value in order to reproduce different behaviours observed in real dynamics, like the herding effect. The value of $k_D \in \mathbb{N}$.
- **Static coupling strength** k_S — Exactly like k_D, the static coupling strength controls the influence of the pedestrians from the static floor field. After a preliminary study on the movement of the particles is possible to conclude that the value of $k_S \in \mathbb{N} \cap [k_D, \infty]$, otherwise the particles begin to move randomly without aiming to the exits.
- **Inertia parameter** k_I — This parameter describes the will of the particles of moving in the same direction of the previous step. The value of $k_I \in \mathbb{N}$.
- **Friction parameter** μ — The value of the friction parameter describes the probability, in case of conflicts between different particles, that nobody moves. Clearly $\mu \in [0, 1]$.

Since we have already studied the dynamic floor field (3.4), it is not necessary to study both k_D and k_S separately, but it is possible to consider the ratio $\frac{k_S}{k_D}$. This is done fixing the value of k_D to 1 and changing the value of k_S. After this is fixed it is necessary to understand the sensitivity of this ratio, studying how the movement changes, increasing the value of c in $c\frac{k_S}{k_D}$. This will be done equalizing c to k_D and putting the value of the static coupling strength equal to ck_S

Changing the combination of the values of these 3 movement parameters and the sensitivity parameter, it is possible to reproduce different scenarios and different collective phenomena described in chapter 1 like:

- **Normal situation** — In this scenario the pedestrians are walking normally without a particular hurry. As already described in section 1.2 pedestrians normally head to the exit creating a jam next to the bottleneck. In this scenario they will try to walk with a certain distance to each other to avoid collisions, so it can be expected to obtain a not so high value of μ and a quite a high value of the ratio $\frac{k_S}{k_D}$.

- **Panic situation** — In panic situations pedestrians begin to push and to walk faster. In contrast with the normal scenario, the value of the friction parameter has to be high in this case, in order to reproduce even collective phenomena like the freezing by heating effect (Section 1.2.2). It is even reasonable to expect an increase of both the parameters k_D and k_S, therefore an increase of the sensitivity parameter.

In this work we will focus on the calibration of the normal situation, because it is the benchmark for all the other scenarios and because of the lack of experiments for the panic situation.

4.1 Normal situation

In order to calibrate the model in a accurate way, we will use an experiment that will calculate different fundamental quantities for the understanding of the dynamics. The experiment will study the flow and the total time of evacuation in function of the size of the bottleneck b and the number of initial pedestrians in the room N. Since in an evacuation simulation the dynamics of the pedestrian near the bottleneck are the most important things to study, this first experiment will be the benchmark for our calibration. The final decision will be taken considering which combination of parameters will produce the results of the variable of interest, that best fit the experimental data, both separately and in average. At the beginning of the study we will first find the optimal value of the combination of parameters with fixed $c = k_D = 1$ (Sec.4.1.1). Once found the optimal values, we are going to change the value of the sensitivity parameter in a neighbourhood of these parameters to see if this change brings to a more accurate model. This study will be done even on another experiment in order to improve the accuracy of the model even more.

4.1.1 Fixed sensitivity parameter c

Because of the lack of information of the right values of the 3 parameters, at the beginning of the calibration a preliminary study to understand which parameters were surely not correct for the reproduction of the experimental data was necessary. This preliminary study brought to the values listed in Table 4.1.

Starting from these values, all the combinations of k_S, k_I and μ were tried.

The experimental data taken are considered in a room with a variable bottleneck [36]. The students have to evacuate from a corridor through an

PARAMETERS	POINTS
k_S	[1,25]
k_I	[1,13]
μ	[0,0.6]

Table 4.1: Parameters used for the calibration in the normal situation fixed c

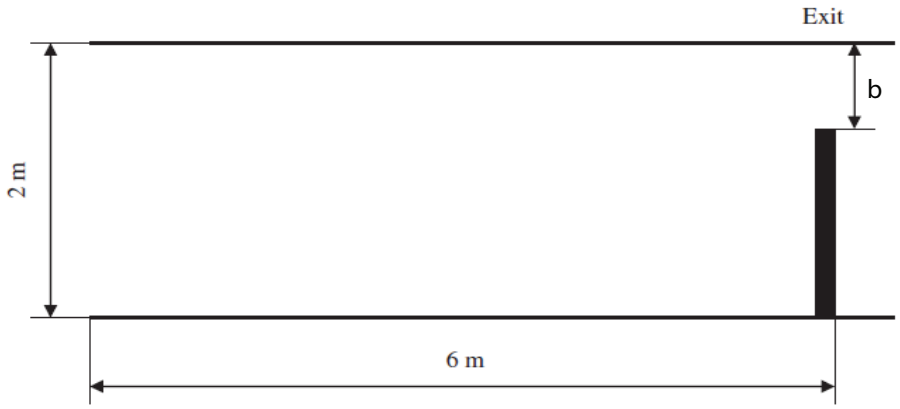

Figure 4.1: Schematic illustration of the first experiment

exit walking normally. The schematic illustration of the experimental set-up is shown in Fig.4.1. The exact width of the channel is W=2m and its length L=6m. All the students stand in a random place at the beginning of the experiment and after a signal they begin to walk through the exit. The following table describes the settings in which this experiment was taken:

PARAMETERS	POINTS
Number of initial students	[5,10,20,30,40,60]
Width of the bottleneck	[0.4,0.8,1.2,1.6]

Table 4.2: Experiment settings for the flow through a bottleneck

The first physical quantity, that has been tried to reproduce, is the number of escaped pedestrians in function of the escape time. The experimental results for the fixed bottleneck width $b = 0.4m$ and $b = 1.2m$ respectively and changing the number of initial pedestrians are shown in Fig.4.2.a-b.

Clearly it is possible to see that the escape time increases with the order of escaped pedestrians. For each fixed initial number of walkers we can see that the dependence is linear. The slopes of these straight lines increase with the initial number of pedestrians in the room, which means that the flow of

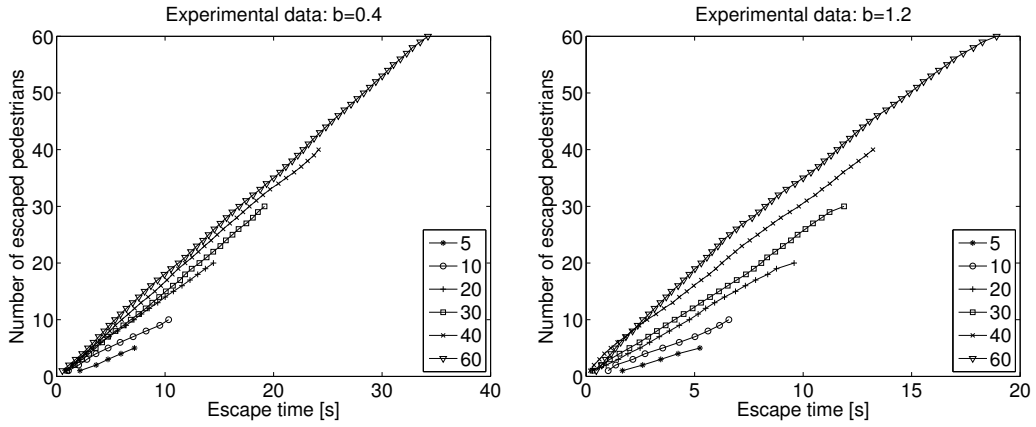

(a) $b = 0.4m$ (b) $b = 1.2m$

Figure 4.2: Number of escaped pedestrians in function of the escape time, changing the number of initial pedestrians in the room (experimental results)

the pedestrians is higher with higher initial number of walkers. This result is even more clear with higher values of the width of the bottleneck. It is even clear that the total time of evacuation decreases with the increase of the bottleneck width. It is possible to see that for $b = 1.2m$ the escape time of all the pedestrians is almost half of that with $b = 0.4m$ for each fixed number of initial pedestrians in the room.

In the following plots (Fig.4.3) the simulation of the evacuation of 5 pedestrians in the room with bottleneck width equal to $0.4m$ are shown. All the sub-plots try to reproduce the same experimental values in function of the 3 parameters k_S, k_I and μ. The plots are ordered in the following way: for a fixed value k_I and row the plots represent the values for increasing μ; for a fixed column and friction parameter the plots represent the values for increasing k_I, while in each sub-plot there are the variation of the function for increasing k_S. It is possible to see how for each fixed value of k_I and μ the pedestrians evacuate faster for increasing parameter k_S. This was predictable assuming that, increasing the static coupling strength, the pedestrians move more direct to the exit. Clearly there is the opposite effect for increasing values of μ. For increasing value of k_I, until $k_I = 5$, the pedestrians are faster for each value of k_I and μ, while they walk almost in the same way for higher values of k_I.

Table 4.3 lists all the combination of the four parameters that best reproduce the functions described before fixing the initial number of pedestrians in the room. In addiction there is even the combination that best reproduces

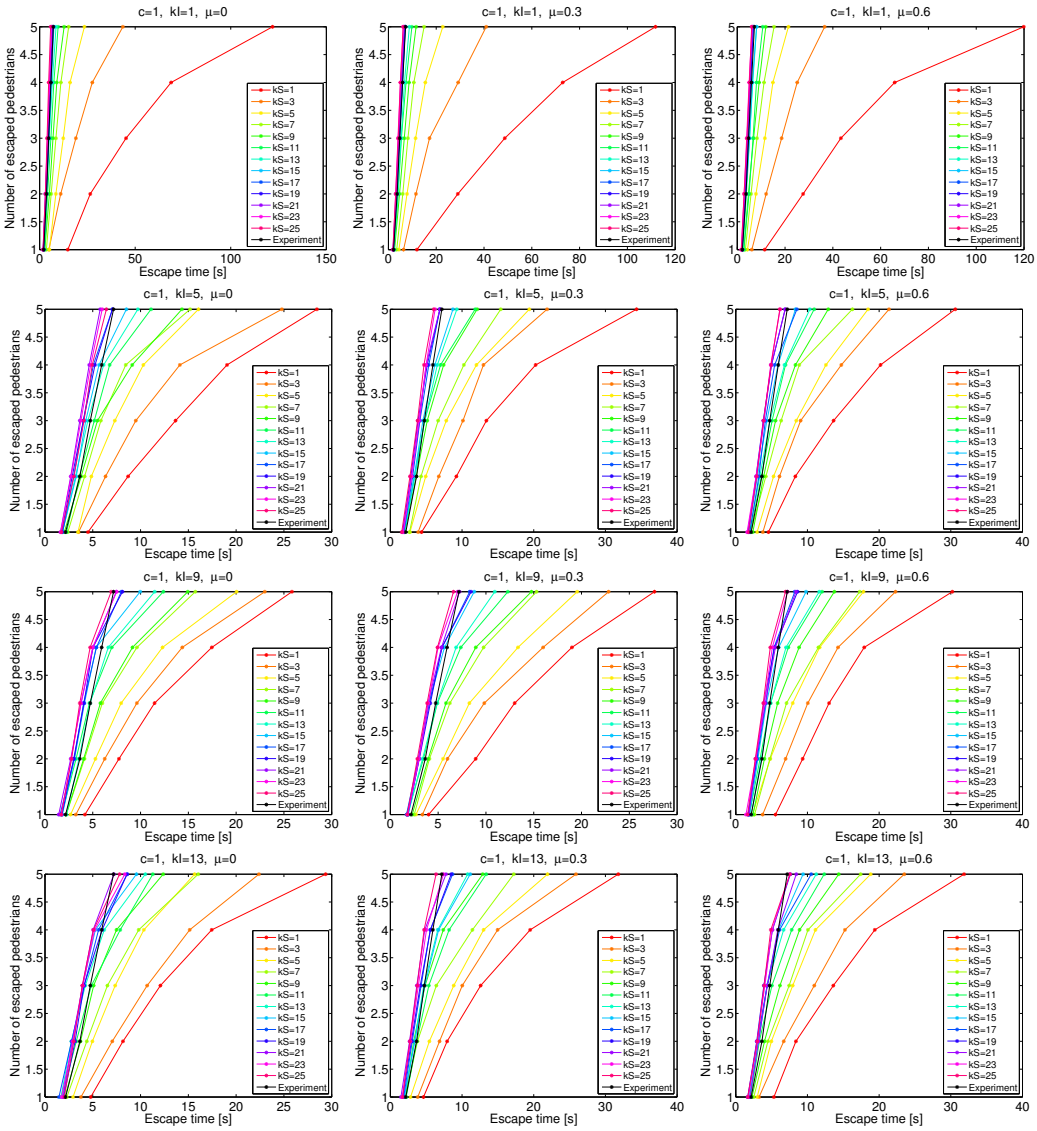

Figure 4.3: 5 pedestrians through a bottleneck with width $b = 0.4m$ (sensitivity parameter $c = 1$)

all the functions in average. It is possible to see how for each value of N the best combination of parameters varies. There is not a clear trend of the best combinations of parameters, but it is clear that this can be caused by the high stochasticity of the cellular automata model. This effect was reduced a bit through the use of the Montecarlo method, but the number of simulations for a fixed combination of parameters was not so high due to computational problems.

N	PARAMETERS
5	$\frac{k_S}{k_D} = 17$ $k_S = 17$ $\mu = 0$ $k_I = 1$
10	$\frac{k_S}{k_D} = 21$ $k_S = 21$ $\mu = 0.3$ $k_I = 7$
20	$\frac{k_S}{k_D} = 15$ $k_S = 15$ $\mu = 0$ $k_I = 1$
30	$\frac{k_S}{k_D} = 17$ $k_S = 17$ $\mu = 0.3$ $k_I = 5$
40	$\frac{k_S}{k_D} = 25$ $k_S = 25$ $\mu = 0$ $k_I = 9$
60	$\frac{k_S}{k_D} = 25$ $k_S = 25$ $\mu = 0$ $k_I = 13$
Average best	$\frac{k_S}{k_D} = 19$ $k_S = 19$ $\mu = 0$ $k_I = 11$

Table 4.3: Best combination of parameters with fixed value of $b = 0.4m$, varying N

In Fig.4.4 the comparisons of the simulated and experimental number of evacuated pedestrian in function of time, using the combination of parameters listed in Table 4.3 are shown. We can see that the model is able to reproduce the experimental data almost perfectly, except for $N = 40$ and $N = 60$ (Fig.4.4.d and Fig.4.4.f respectively), in which the model overestimates a bit the total time of evacuation. This result, however, is not so important, because our goal is to find a unique combination of parameters that are able to reproduce in a acceptable way all the situations and characteristics of the pedestrian dynamics.

Fig.4.5 shows this comparison for all the initial number of pedestrians in the room, using the combination of parameters with the lowest average relative error. Obviously the approximation is worse than the one using the best combination with a fixed number of initial pedestrians, anyway it is in average acceptable. We can see that the model overestimates the total time for $N \geqslant 10$. This overestimation is caused by the decrease of velocity of the last pedestrians, indeed the simulated curves are not completely straight lines, but have a slight curvature for the last escaped pedestrians. The reason of this is that sometimes the last pedestrians have some difficulties in finding the exit in a fast way like the other particles at the beginning of the simulation. This is caused by the high value of the inertia parameter, that, at the beginning of the simulation, helps the pedestrians to increase their velocities,

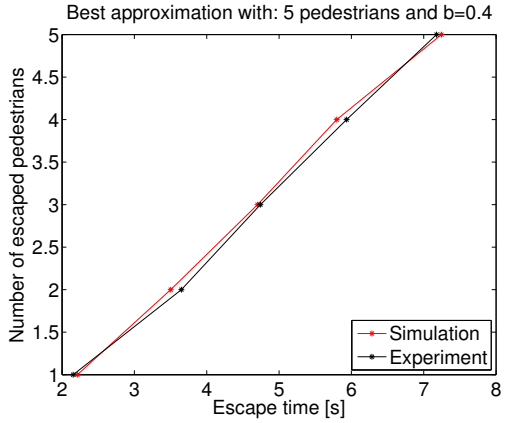

(a) $N = 5$

(b) $N = 10$

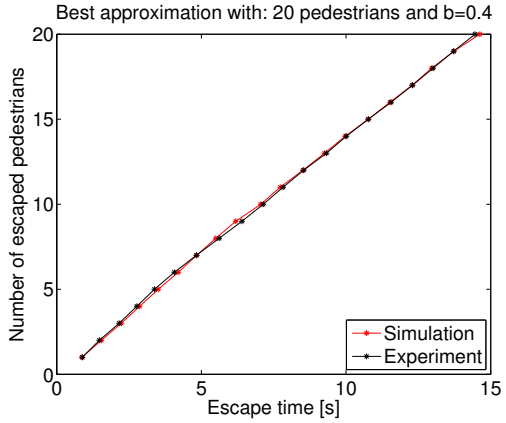

(c) $N = 20$

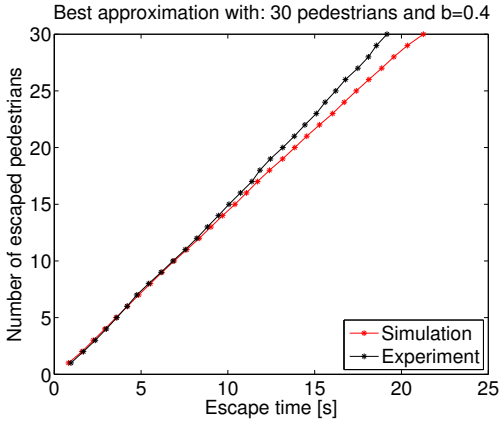

(d) $N = 30$

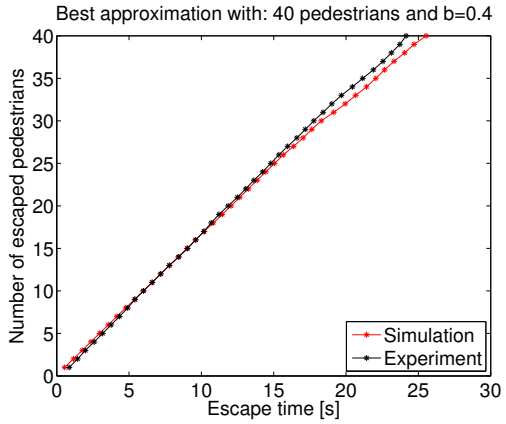

(e) $N = 40$

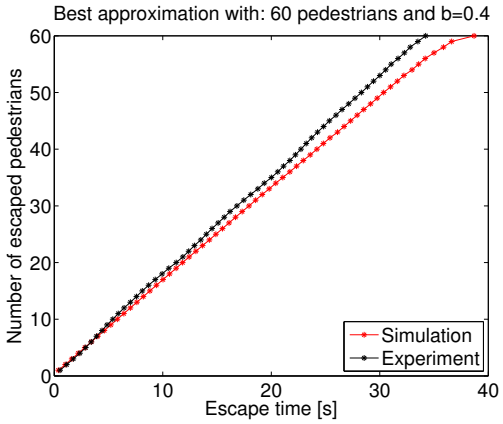

(f) $N = 60$

Figure 4.4: Best approximations of the number of escaped pedestrians as function of time with fixed N and $b = 0.4m$

but with few particles in the system causes a wrong dynamic of the pedestrians, that begin to walk next to the walls of the room until they hit the corner with the exit. This effect is not so evident in this experiment because the exit is set on the corner of the room, but as we will see in the Sec.4.1.2, this wrong dynamic brings to an high increase of the error for experiments in which the exit is not situated in a corner of the room.

The average relative error is equal to 0.0825, indeed it is possible to see that the absolute total time of evacuation error goes from $0s$ to almost $5s$ for 5 initial pedestrians to 60 respectively.

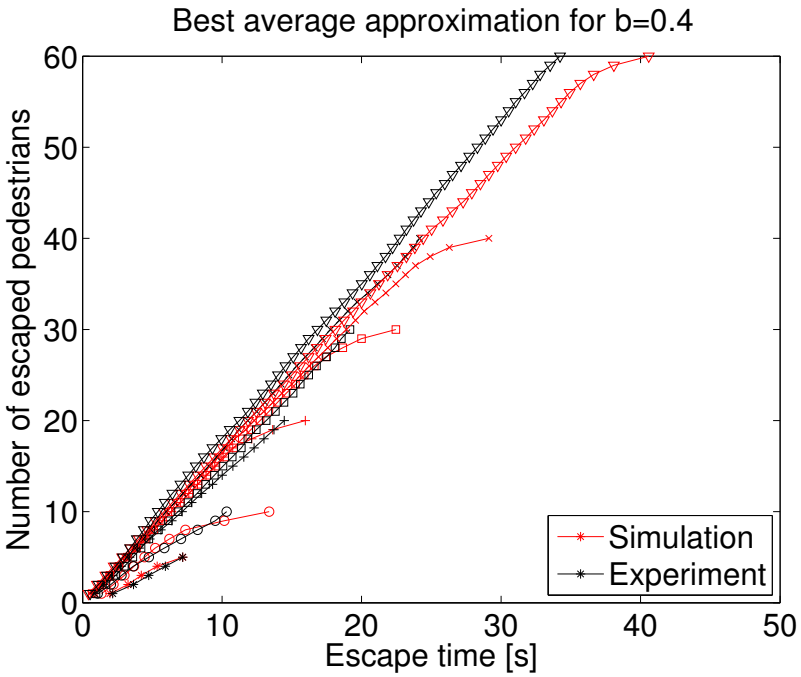

Figure 4.5: Best average approximation of the number of escaped pedestrians as function of time with $b = 0.4m$, varying N

Almost the same results are visible in the flow with the bigger bottleneck width (Fig.4.6). As mentioned before the velocity of evacuation of the pedestrians increases with the increase of k_S and the decrease of μ. In this case the increase of the value k_I enhances the velocity of the pedestrians with more influence than in the case of $b = 0.4m$. This is caused by the fact that having more space to exit, the pedestrians are more free to flow straight.

Like for the $b = 0.4m$ case, Table 4.4 shows the best combination of parameters to reproduce the number of evacuated pedestrians against the evacuation time for each value of N and for fixed $b = 1.2m$. It is possible to notice that except for $N = 5$, the value of the ratio $\frac{k_S}{k_D}$ is lower than in the

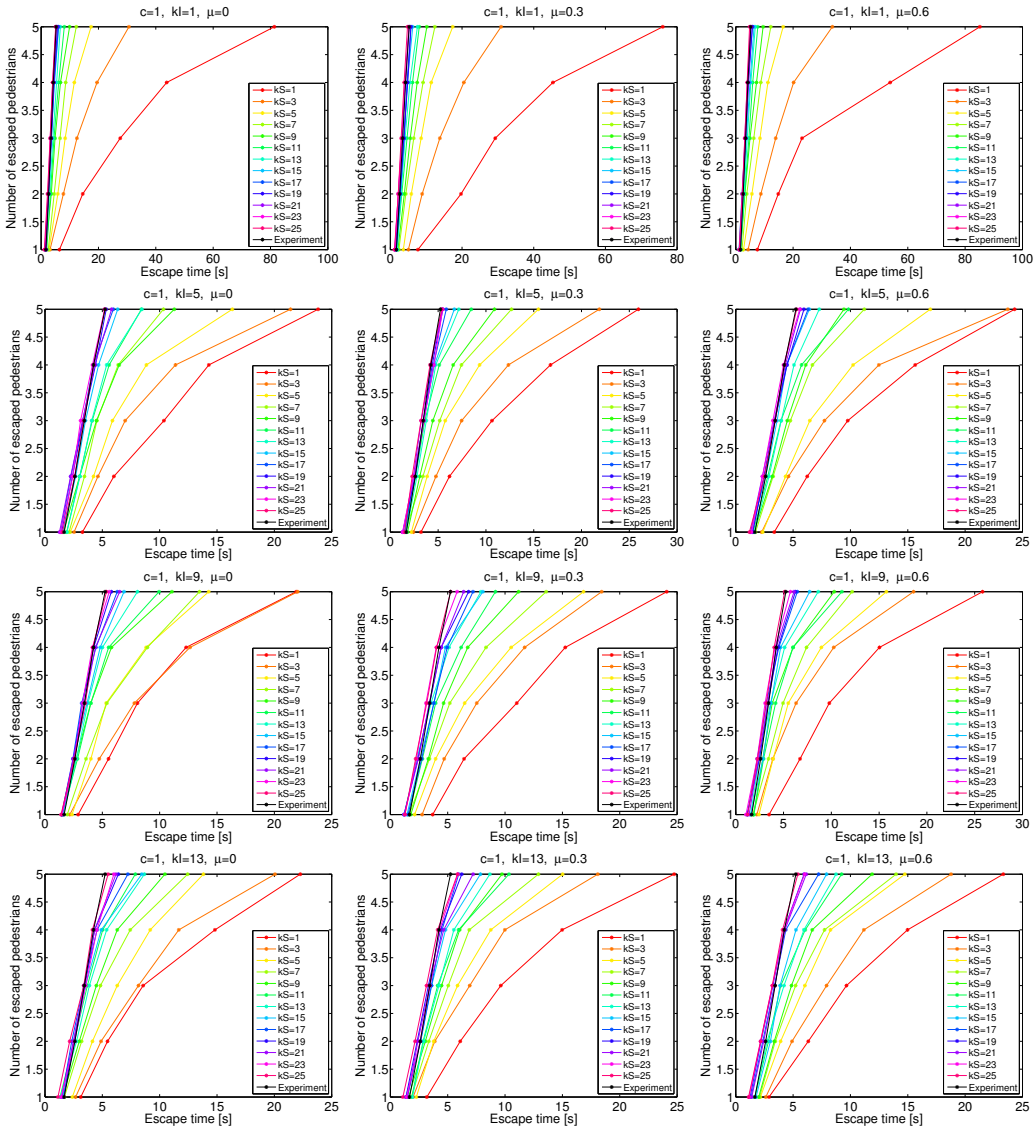

Figure 4.6: 5 pedestrians through a bottleneck with width $b = 1.2m$ (sensitivity parameter $c = 1$)

previous case with the smaller exit. In this case the pedestrians exit from the room in a much easier way than in the previous one due to the bigger width of the bottleneck. This is the reason for the decrease of the ratio, because with higher values the simulated pedestrians exit too fast from the room compared to the real ones.

N	PARAMETERS
5	$\frac{k_S}{k_D} = 19\ k_S = 19\ \mu = 0\ k_I = 3$
10	$\frac{k_S}{k_D} = 17\ k_S = 17\ \mu = 0.6\ k_I = 1$
20	$\frac{k_S}{k_D} = 7\ k_S = 7\ \mu = 0\ k_I = 1$
30	$\frac{k_S}{k_D} = 7\ k_S = 7\ \mu = 0.3\ k_I = 1$
40	$\frac{k_S}{k_D} = 9\ k_S = 9\ \mu = 0.3\ k_I = 1$
60	$\frac{k_S}{k_D} = 7\ k_S = 7\ \mu = 0.3\ k_I = 5$
Average best	$\frac{k_S}{k_D} = 19\ k_S = 19\ \mu = 0.6\ k_I = 11$

Table 4.4: Best combination of parameters with fixed value of $b = 1.2m$, varying N

The simulations (Fig.4.7) of the single cases of N separately show that the model is able to reproduce correctly even the case with the bottleneck equal to $1.2m$. For the same reason explained before, even here it is possible to notice how the velocity of evacuation is correct, expect for the last pedestrians that decrease a bit their velocity.

The result of the simulation with the combination that gives the lowest average relative error with $b = 1.2m$ is shown in Fig.4.8. Clearly even in this case the approximation is worse than the one using the best combination with a fixed number of initial pedestrians. The average relative error is equal to 0.1299, this confirms that the simulation is able to reproduce the evacuation in a correct way. Anyway even in this case for $N \geqslant 10$, for the same reason as before, the simulated pedestrians have a tendency in decreasing the flow with the increasing time of evacuation. The absolute total time of evacuation errors go from 1 to 3 for $N = 30$ and $N = 10$ respectively. As we can see, the total times of evacuation are almost correct, but the simulated pedestrians flow faster than the real ones at the beginning of the simulation and decrease their velocity in the end, giving to the functions a curvilinear shape instead of straight one.

The same quantity is calculated changing the width of the bottleneck with the fixed number of initial pedestrians equal to 60. Fig.4.9 shows the experimental results of the number of evacuated pedestrian against the escape time with $N = 60$ and changing the bottleneck width. Clearly even here it is possible to see how the time of escape decreases with the increase of b.

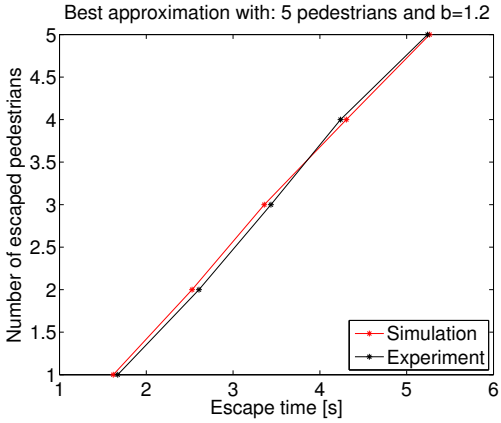

(a) $N = 5$

(b) $N = 10$

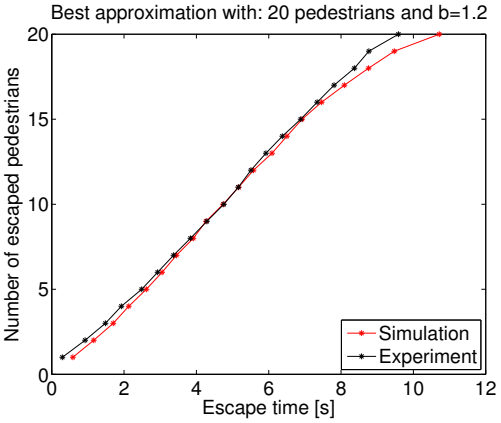

(c) $N = 20$

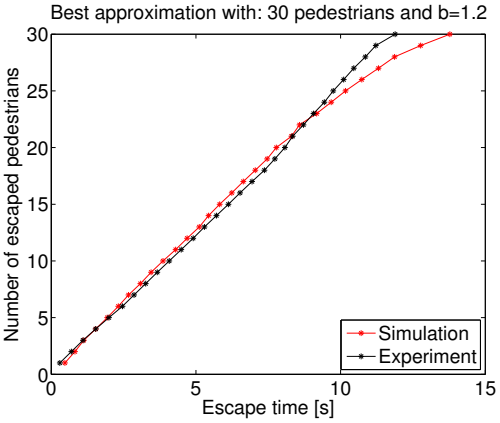

(d) $N = 30$

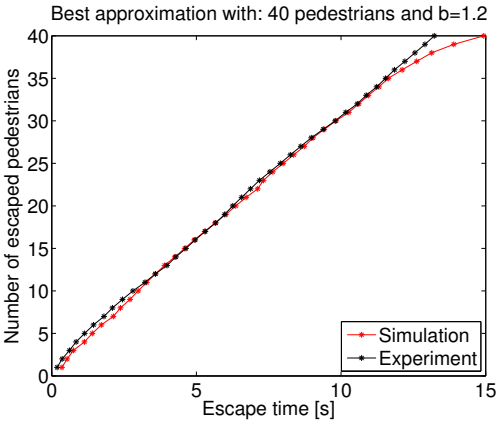

(e) $N = 40$

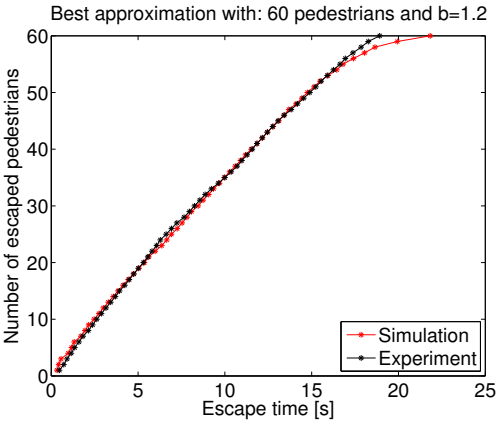

(f) $N = 60$

Figure 4.7: Best approximations of the number of escaped pedestrians as function of time with fixed N and $b = 1.2m$

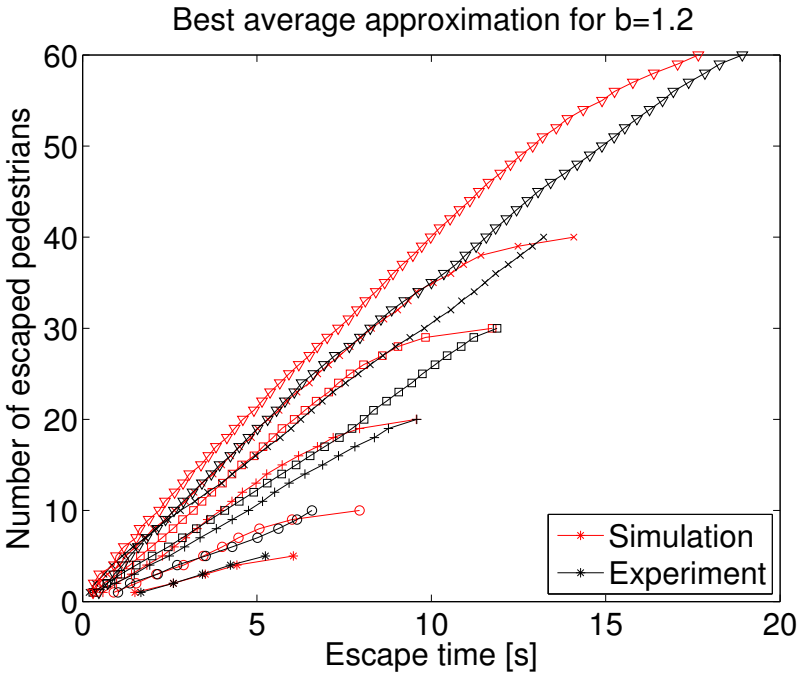

Figure 4.8: Best average approximation of the number of escaped pedestrians as function of time with $b = 1.2m$, varying N

As shown previously in Fig.4.3, for the case of 5 pedestrians with bottleneck width of $b = 0.4m$, even in this case (Fig.4.10) the total evacuation time decreases with the increase of the ratio $\frac{k_S}{k_D}$. As mentioned before for small bottlenecks the influence in the increase of velocity due to high values of the inertia parameter is less visible than for higher values of b. The influence of the friction parameter μ is exactly the same as in the previous case.

Table 4.5 shows the values of the combination of parameters that best reproduce the experimental data, both with fixed values of the bottleneck width and in average. As already mentioned before, it is possible to see how the model needs a high value of the ratio $\frac{k_S}{k_D}$ to reproduce the correct flow of the pedestrians through bottlenecks with a small width: $b \leqslant 0.8m$. For higher values of b the optimal value of the ratio decreases, because the particles do not need a high value of the static coupling strength in order to find the right position of the door. Higher values of this ratio would cause an underestimation of the total time of evacuation due to an excessive increase of the velocity of the pedestrians.

Fig.4.11 shows the simulations of the quantity studied, varying the width of the bottleneck with fixed number of initial pedestrians equal to 60. Like before the model, using different combinations of parameters for each fixed

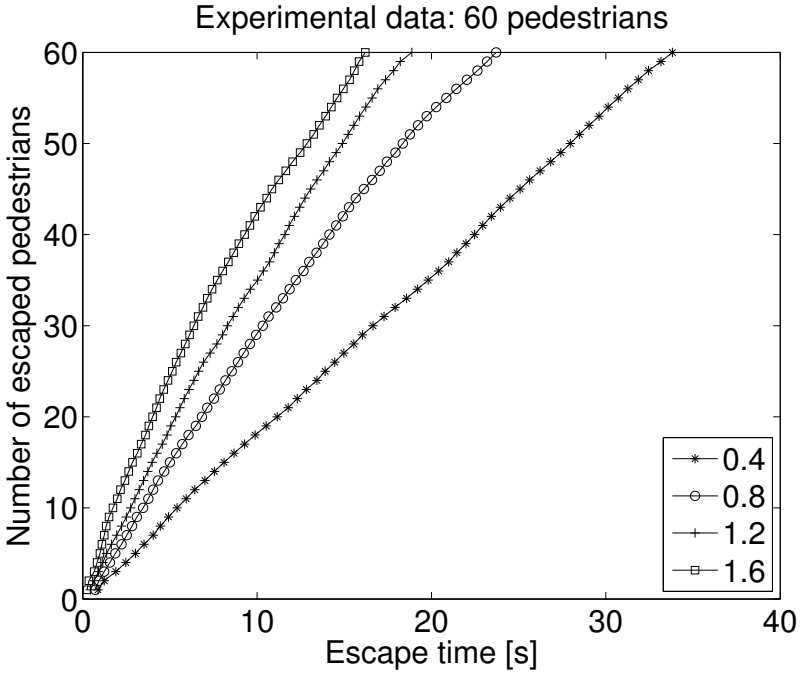

Figure 4.9: Number of escaped pedestrians in function of the escape time, changing the bottleneck width with $N = 60$ (experimental results)

$b[m]$	PARAMETERS
0.4	$\frac{k_S}{k_D} = 25$ $k_S = 25$ $\mu = 0$ $k_I = 13$
0.8	$\frac{k_S}{k_D} = 19$ $k_S = 19$ $\mu = 0.3$ $k_I = 1$
1.2	$\frac{k_S}{k_D} = 7$ $k_S = 7$ $\mu = 0.3$ $k_I = 5$
1.4	$\frac{k_S}{k_D} = 5$ $k_S = 5$ $\mu = 0$ $k_I = 5$
Average best	$\frac{k_S}{k_D} = 7$ $k_S = 7$ $\mu = 0$ $k_I = 7$

Table 4.5: Best combination of parameters with fixed value of $N = 60$, varying b

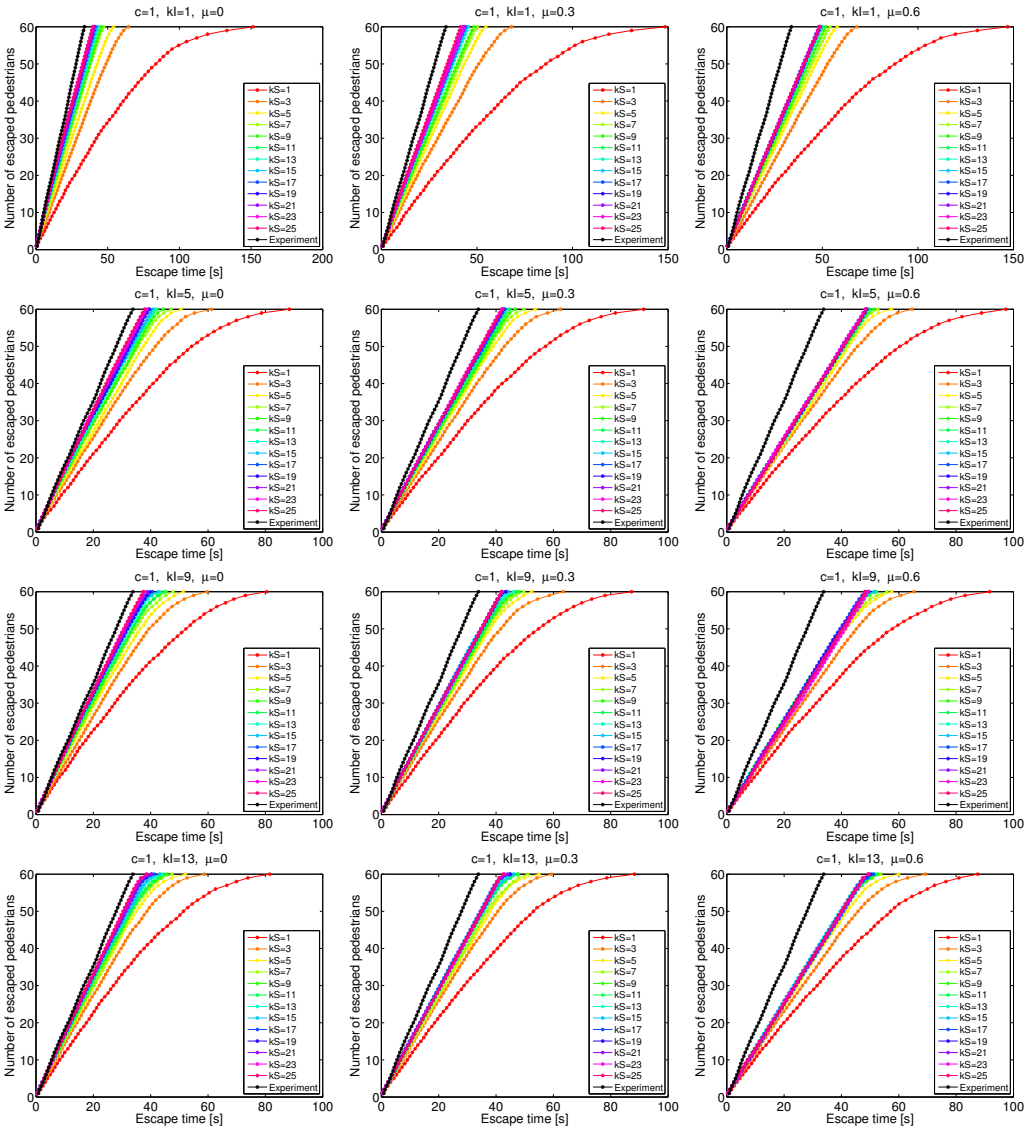

Figure 4.10: 60 pedestrians through a bottleneck woth width $b = 0.4m$ (sensitivity parameter $c = 1$)

value of b, is able to reproduce the experimental data almost correctly, except for the decrease of velocity of the last pedestrians explained previously.

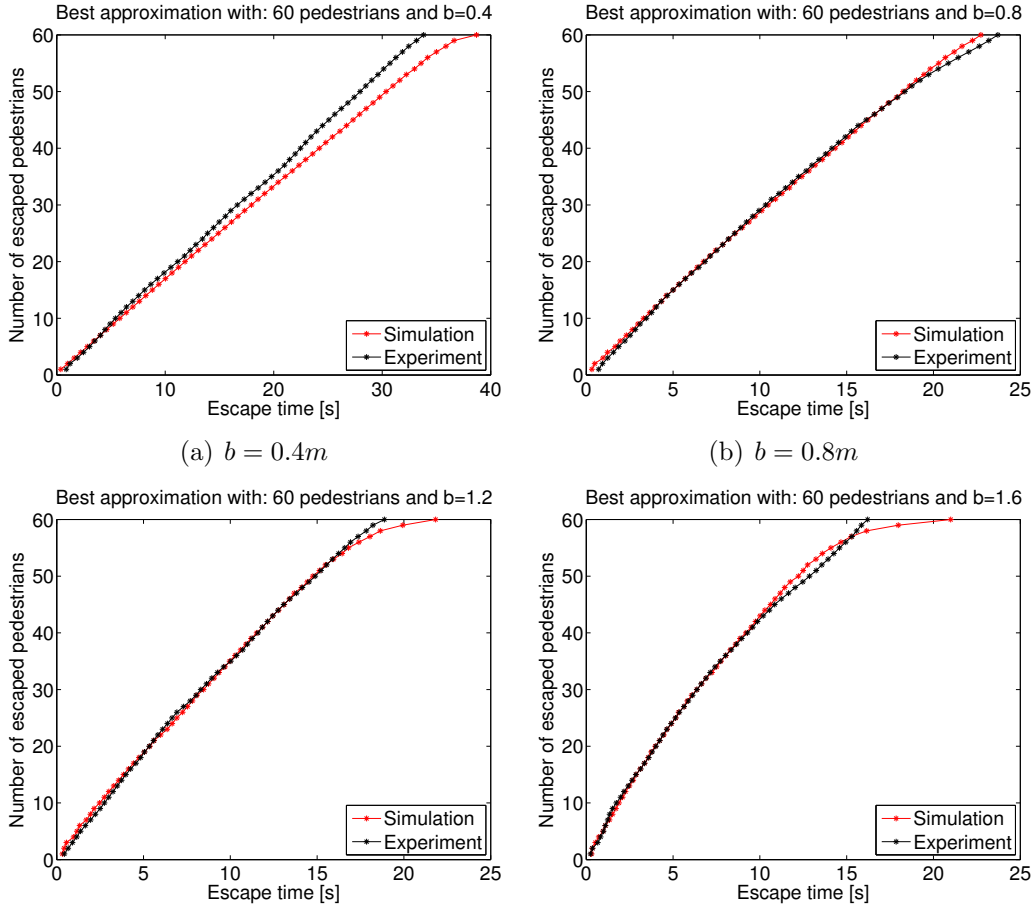

(a) $b = 0.4m$ (b) $b = 0.8m$

(c) $b = 1.2m$ (d) $b = 1.6m$

Figure 4.11: Best approximations of the number of escaped pedestrians as function of time with fixed b and $N = 60$

The result of the simulation with the combination that gives the lowest average relative error with $N = 60$ and changing the width of the bottleneck is shown in Fig.4.12. Even in this case the approximation is worse than the one using the best combination with a fixed number of initial pedestrians. As we can see in the plots, it is possible to notice that the model is able to reproduce correctly the experimental data and the decreasing tendency of the total evacuation time with the increase of the bottleneck width. The average relative error is equal to 0.1181. Anyway even in this case there is the decrease of the velocity of the pedestrians with the increase of the time. This

tendency is really visible with the smallest width of the bottleneck, because of the optimal ratio $\frac{k_S}{k_D}$ that is too low compared to the optimal value of k_I to allow the pedestrians to find the right position of the exit fast enough. The absolute error of the total time of evacuation varies from approximately $3s$ for $b = 1.6m$ to $15s$ for the smallest bottleneck width.

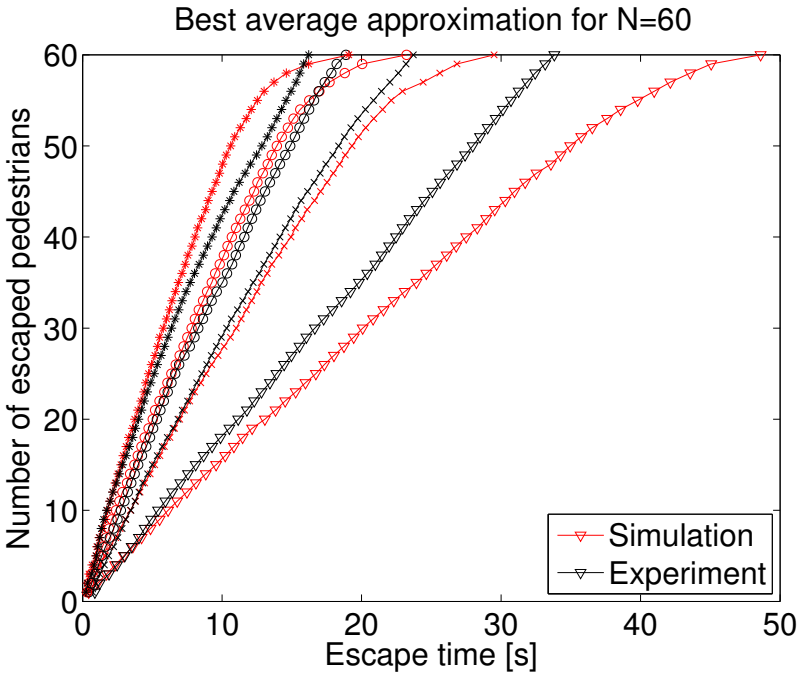

Figure 4.12: Best average approximation of the number of escaped pedestrians as function of time with $N = 60$, varying b

The last quantity that has been tried to reproduce, is the mean flow rate against the initial density of pedestrians in the room for $b = 0.4m$ and $b = 1.2m$. With increasing density, the mean flow rate increases and saturates at a value for narrow exit $b = 0.4m$. The saturation of the flow rate is caused by the clogging of walkers at the bottleneck. For a wider exit $b = 1.2m$, the mean flow rate increases with the density without saturating. Clearly the values of the mean flow increase with the increase of the bottleneck width. These results are visible in Fig.4.13 that shows the experimental result of this quantity.

The following table (Tab.4.6) describes the optimal values of the parameters for the correct reproduction of the mean flow of the pedestrians against the initial density changing the bottleneck width and in average. The decrease of the ratio $\frac{k_S}{k_D}$ due to an increase of b is visible even in this case, though the effect is weaker. This is caused by the fact that the calculation of

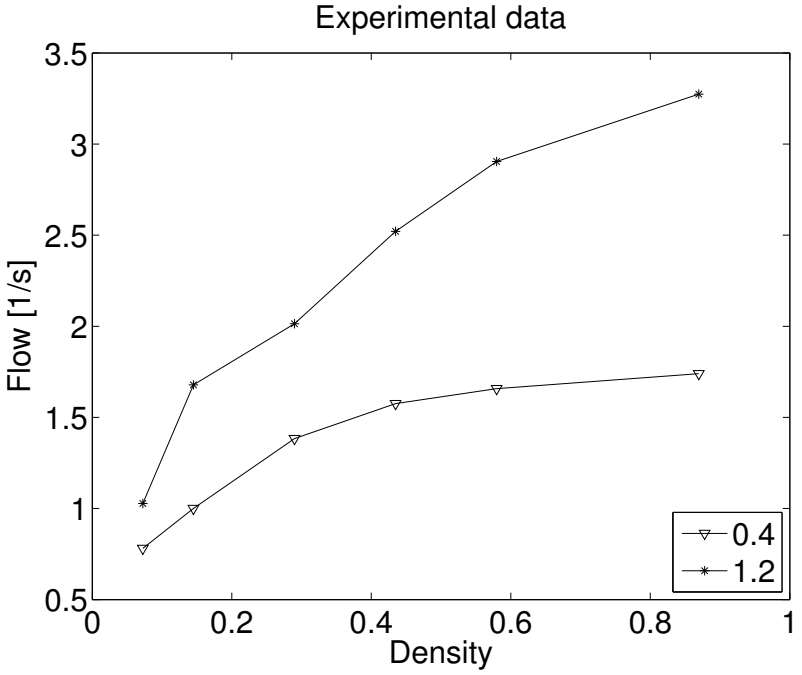

Figure 4.13: Mean flow rate in function of the initial pedestrian density in the room, varying the bottleneck width (experimental results)

the mean relative error is made averaging on the errors for each fixed density, i.e. the number of initial pedestrians in the room, while in the previous case (Tab.4.3-4.4), these were considered separately.

$b[m]$	PARAMETERS
0.4	$\frac{k_S}{k_D} = 23$ $k_S = 23$ $\mu = 0$ $k_I = 13$
1.2	$\frac{k_S}{k_D} = 19$ $k_S = 19$ $\mu = 0.6$ $k_I = 11$
Average best	$\frac{k_S}{k_D} = 17$ $k_S = 17$ $\mu = 0$ $k_I = 9$

Table 4.6: Best combination of parameters for the mean flow rate fixing b

The results of the simulations of the mean flow against the initial density made with the optimal parameters both with $b = 0.4m$ and $b = 1.2m$ are shown in Fig.4.14. Both cases are reproduced by the model in a correct way. In particular with $b = 0.4m$ the model is able to reproduce the mean flow perfectly for densities lower than 0.4, while for higher densities it saturates at a lower value than the experimental mean flow, underestimating it approximately of $0.1\frac{1}{s}$. Anyway in both cases the general trend of the mean flow is simulated in the correct way, indeed the mean flow increases with the

increase of the density and for a narrow exit it saturates at a certain value.

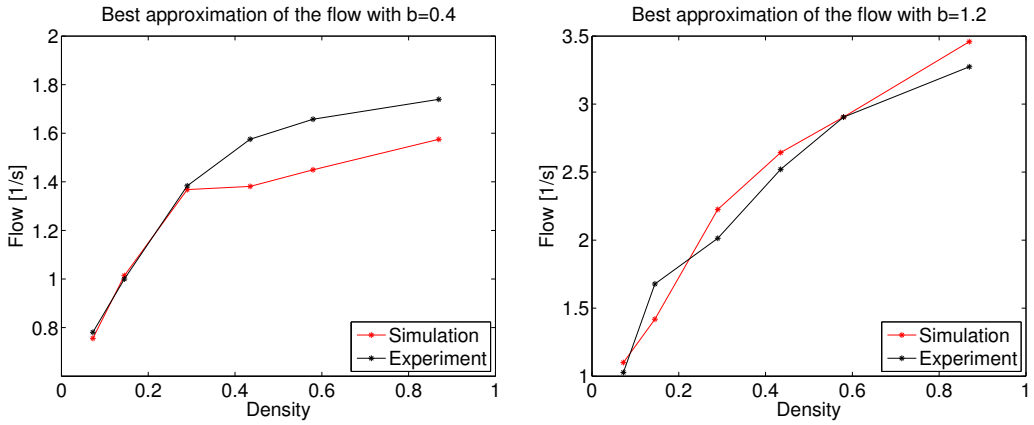

(a) $b = 0.4m$ (b) $b = 0.8m$

Figure 4.14: Best approximations of the mean flow as function of the initial density with fixed b

The plot of the simulation of the mean flow with the combination of parameters with the lowest average relative error is shown in Fig.4.15. The simulated values, even with this combination, describe in a correct way the trend of the real mean flow, except in $N = 10$ (density equal to 0.13), in which the increase of the flow is much lower than the real one in both cases $b = 0.4m$ and $b = 1.2m$. The average error is 0.1256, which confirms that the simulation is able to reproduce the data in a acceptable way.

Conclusion

We have obtained the optimal values of the parameters in order to reproduce four different quantities from the experimental data:

1. The number of evacuated pedestrians against the evacuation time with fixed bottleneck width equal to $0.4m$ and varying the number of initial number of pedestrians in the room
2. The number of evacuated pedestrians against the evacuation time with fixed bottleneck width equal to $1.2m$ and varying the number of initial number of pedestrians in the room
3. The number of evacuated pedestrians against the evacuation time with fixed number of initial pedestrians in the room equal to 60 and varying the bottleneck width

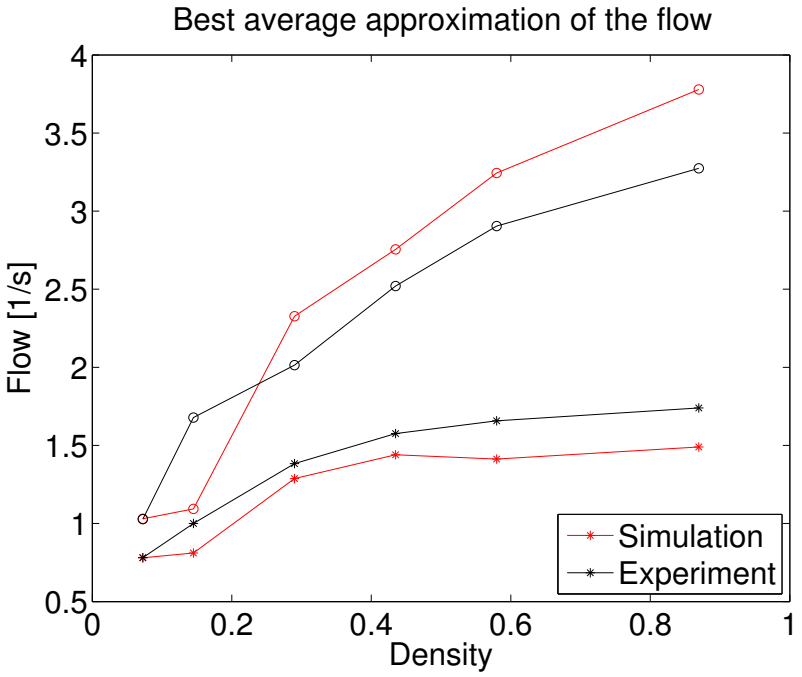

Figure 4.15: Best average approximation of the mean flow rate as a function of the initial pedestrian density, varying b

4. The mean flow rate as a function of the initial density of pedestrians in the room, varying the bottleneck width

Averaging the relative errors of the four quantities, we were able to find a unique optimal combination of parameters, that will be the starting point for the next section (Sec.4.1.2), in which we are going to study the dependence of the sensitivity parameter in order to describe in a more accurate way this experiment and a second one.

The optimal combination, that gives the lowest average relative error of the four quantities is:

$$\frac{k_S}{k_D} = 17 \quad k_S = 17 \quad \mu = 0 \quad k_I = 9$$

The total average error is 0.1416 and in the following plots (Fig.4.16) are represented all the four quantities calculated with the combination just showed. It is possible to see how the model describes in an acceptable way all the four quantities, but clearly still shows the mistakes described earlier.

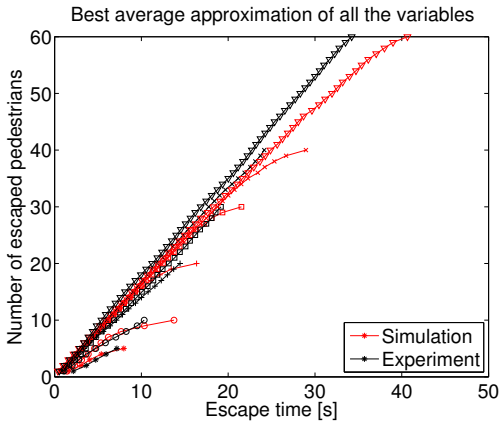

(a) Number of escaped pedestrians against evacuation time with $b = 0.4$, varying N

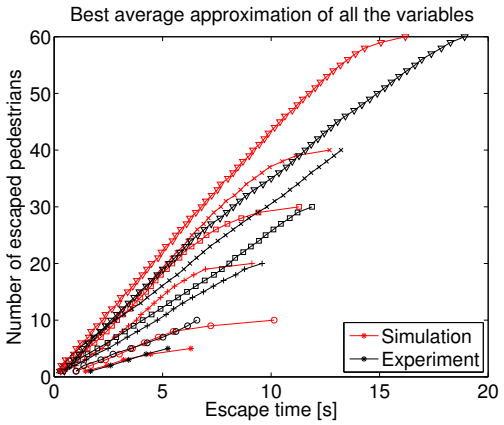

(b) Number of escaped pedestrians against evacuation time with $b = 1.2$, varying N

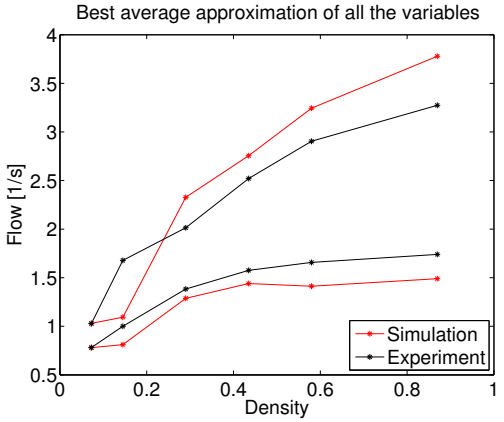

(c) Mean flow rate against initial density in the room with $b = 0.4$ and $b = 1.2$

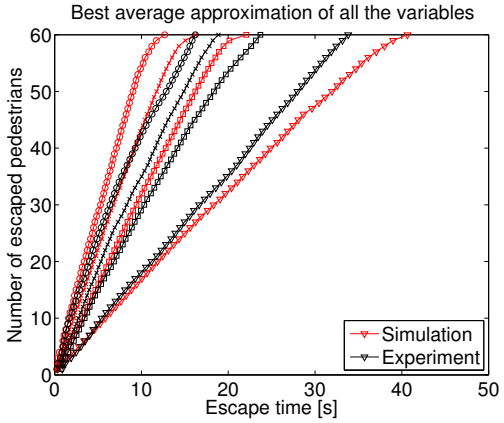

(d) Number of escaped pedestrians against evacuation time with $N = 60$, varying b

Figure 4.16: Best approximation of the four quantities studied in Sec.4.1.1

4.1.2 Variable sensitivity parameter c

In this section we will discuss the influence on the simulation of the sensitivity parameter c and we will try to improve the accuracy of the model introducing this parameter inside the simulation. As already mentioned in the previous section the simulated pedestrians sometimes begin to walk around the room next to the walls due to the high value of the inertia parameter k_I. However this effect is not so visible in the experiment used in the previous section (Sec.4.1.1), because the bottleneck is placed in the corner of the room, therefore the wrong dynamic of the pedestrians described before doesn't influence so much the total evacuation time and the correct flow of the particles. For this reason it is necessary to study even another case in which the system is different in order to calibrate the model, so that it is able to reproduce different scenarios. To do this we will first study qualitatively how the sensitivity parameter influences the dynamics of the simulated particles. Afterwards we will try to reproduce the dynamics of the second experiment using a neighbourhood of the optimal parameters found in the previous section changing the value of c. In the end we will find the the combination of parameters that will return the lowest average error between the two experiments.

Fig.4.17 shows the results of the simulation, with the optimal combination of parameters found in the end of the previous section, of the number of evacuated pedestrians against the evacuation time, fixing b and N and changing the sensitivity parameter. Increasing the value of the sensitivity parameter the particles walk much faster. This is caused by the beginning of the simulation, in which the increase of the value k_S is more influential by the one of k_D, because the matrix of the dynamic floor field is null at time 0. This effect is more evident with few pedestrians in the room, while it is possible to see how for $N = 60$ the sensitivity parameter has a little influence on the dynamics of the pedestrians. Another consequence of the increase of the sensitivity parameter is that both the values k_S and k_D increase their influence on the particles dynamics, reducing the dependence from the inertia parameter k_I. This fact solves partly the wrong dynamics explained before, but improves even the velocity at the beginning of the simulation, causing an underestimation of the total time of the evacuations.

In order to increase the accuracy of the calibration, the model has to be able to reproduce different experimental data compared to the one used previously. The second experiment considered [34] is the flow through bottlenecks with different widths ($b \in [0.4, 1.6]$) and with a depth of 0.4m. The difference between this experiment and the one seen in the previous section, is the position of the door. As we can see in Fig.4.18 the bottleneck is not placed in the corner of the room like in the previous experiment. The space

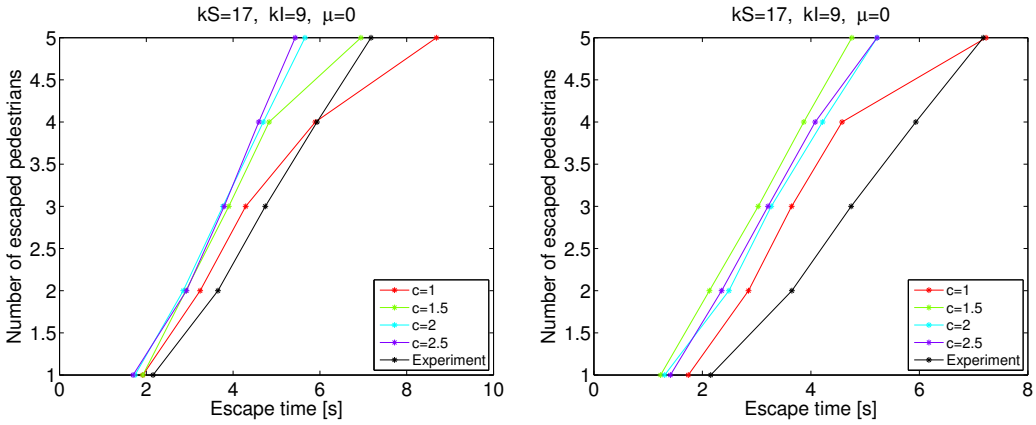

(a) $b = 0.4m$ and $N = 5$

(b) $b = 1.2m$ and $N = 5$

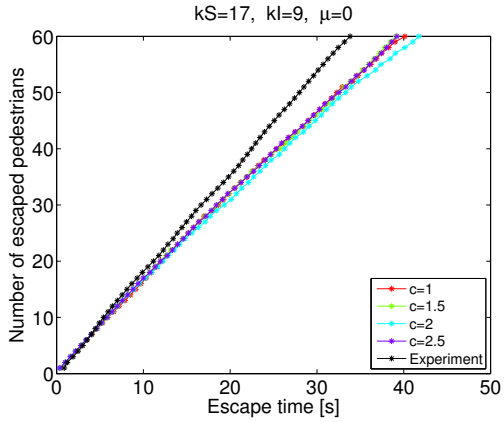

(c) $b = 0.4m$ and $N = 60$

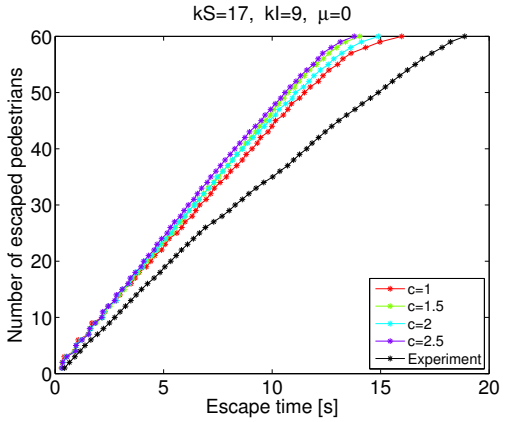

(d) $b = 1.2m$ and $N = 60$

Figure 4.17: Influence of the sensitivity paramter on the simulation of the number of escaped pedestrians against the evacuation time fixing b and N

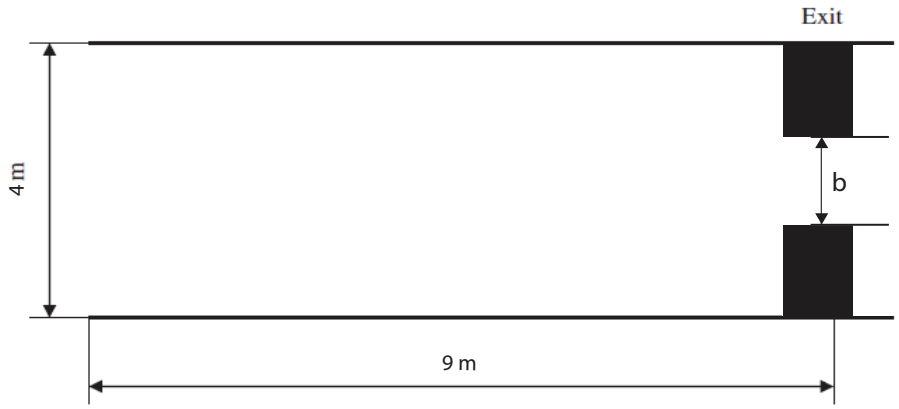

Figure 4.18: Schematic illustration of the second experiment

in front of the bottleneck is about 4m wide and 9m deep. At the beginning of each run the 100 pedestrians are standing in front of the bottleneck. The quantities calculated are the total time of evacuation and the flow, both as a function of the bottleneck width. Both cases are calculated considering firstly all the 100 pedestrians involved in the experiment and secondly considering the first 80 pedestrians passed through bottleneck. Thanks to this, we will be able to understand more deeply why and how the model errs in the reproduction of the dynamics of the last pedestrians in the room. We will see that to solve partly this problem the model needs a higher value of the sensitivity parameter, in order to increase the dependence of k_S enough, to be stronger than the one of k_I next to the bottleneck, but this will cause even an underestimation of the total time of evacuation of the first 80 pedestrians.

After the first preliminary simulations with the optimal combination of the parameters found in Sec.4.1.1 it is immediately clear that the inertia parameter k_I is too high compared to ratio $\frac{k_S}{k_D}$ (is equal to k_S for $c = k_D = 1$) in order to reproduce in a correct way this experimental data. The last pedestrians in the room begin to walk around it next to the walls and are not able to find the position of the bottleneck, causing an high overestimation of the total time of evacuation.

Taken into account the results of the calibration with fixed $c = 1$ and analysing the results of the preliminary study, the following parameters (Tab.4.7) were tried for the reproduction of the quantities of this second experiment. In this first simulation we will understand if the increase of c is able to increase the strength of the static floor in order to reduce the errors explained before. In case this increase of the sensitivity parameter does not solve the problem, another simulation will be run with lower values of k_I. As mentioned before, the inertia parameter found in the previous study is too

high for the right reproduction of this experiment, therefore it was useless to try higher values. On the contrary we increased the range of values of the friction parameter, in order to reduce the velocity of the pedestrians due to the increase of the sensitivity parameter.

PARAMETERS	POINTS
k_S	[13,19]
k_I	[5,7]
μ	[0,0.8]
c	[1,2.5]

Table 4.7: Parameters used for the calibration in the normal situation with variable c (first simulation)

The first quantity studied is the total time evacuation as a function of the bottleneck width. Clearly it is possible to see how the total time of evacuation decreases with the increase of the bottleneck width (Fig.4.19).

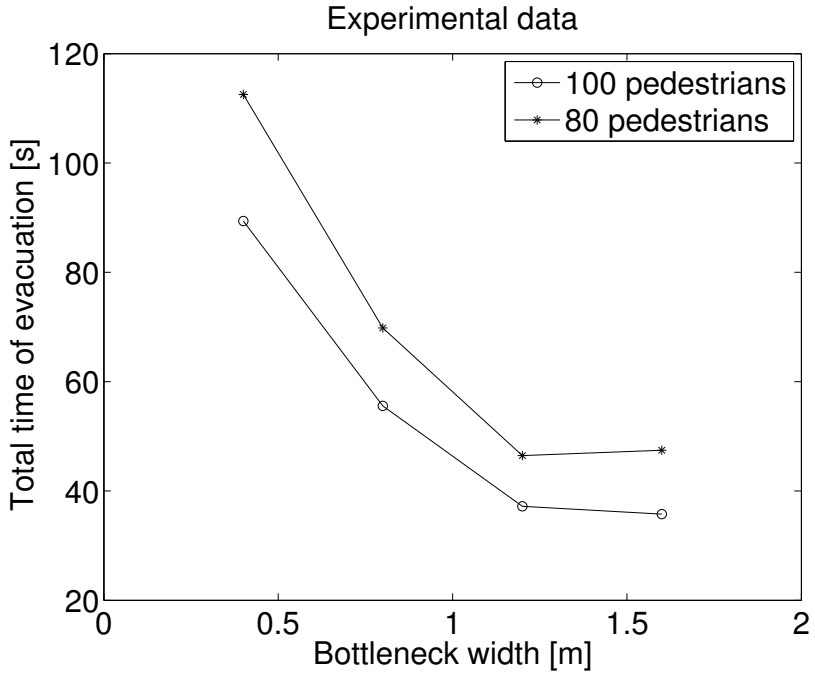

Figure 4.19: Total time of evacuation in function of the bottleneck width, varying the number of pedestrians considered (experimental results)

The following table (Tab.4.8) describes the best combination of parameters for the representation of the quantity just described, considering all the

100 pedestrians and the first 80 passed through the bottleneck. We can see how the optimal ratio $\frac{k_S}{k_D}$ is for both cases equal to 13, but if we consider all 100 pedestrians, they need a much higher value of the static coupling strength in order to avoid partly the wrong dynamics described before and this causes an increase of the sensitivity parameter. We can also see that the friction parameter for 80 pedestrians is the double of the one with 100. This confirms the fact that if there are still a lot of pedestrians in the room the model overestimates their velocities and therefore needs a low value of c and a high value of μ in order to replicate the real data.

PEDESTRIANS	PARAMETERS
100	$\frac{k_S}{k_D} = 13$ $k_S = 26$ $\mu = 0.4$ $k_I = 5$ $c = k_D = 2$
80	$\frac{k_S}{k_D} = 13$ $k_S = 13$ $\mu = 0.8$ $k_I = 7$ $c = k_D = 1$
Average best	$\frac{k_S}{k_D} = 13$ $k_S = 26$ $\mu = 0.8$ $k_I = 5$ $c = k_D = 2$

Table 4.8: Best combination of parameters for the total time of evacuation against the bottleneck width, varying the number of pedestrians considered

Fig.4.20 shows the simulation with the best combination for each fixed number of pedestrians considered in comparison with the experimental data. Both cases are reproduced in a good way by the model, expect for the final saturation of the total time of evacuation, that stops to decrease for $b > 1.2$ in the experiment, but still decreases in both cases in the simulation.

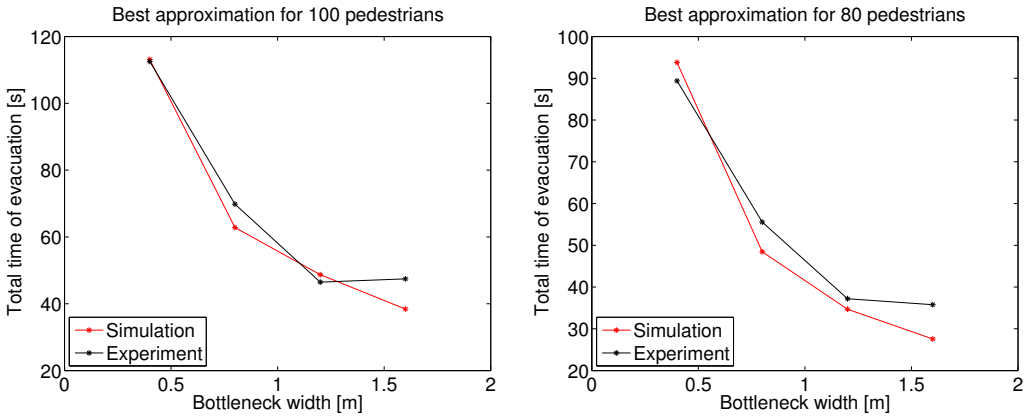

(a) 100 pedestrians considered

(b) 80 pedestrians considered

Figure 4.20: Best simulation of the total time of evacuation against the bottleneck width, fixing the number of pedestrians considered

The plots of both cases using the average best combination of the parameters are shown in Fig.4.21. As already shown in Tab.4.8 the average best

combination is really similar to the best combination considering all the 100 pedestrians, except for μ that is equal to the optimal one considering the first 80 pedestrians. The model, in order to reproduce both quantities in a acceptable way, increases the velocity of the pedestrians choosing an high value of the sensitivity parameter, but decreases their velocity when there are still many inside the room, opting for the highest value of the friction parameter. This brings to an overestimation for 100 pedestrians and a bottleneck width equal to $0.4m$, in which the effect of μ is really strong, and an underestimation of the total time of evacuation considering the first 80 particles and larger bottleneck widths. This confirms that even while using the average best combination of parameters for the optimal reproduction of both cases, the model is able to reproduce the total time in acceptable way, but lacks in the replication of the right dynamics of a group of pedestrians exiting through a bottleneck, that normally have a constant velocity in evacuating the room.

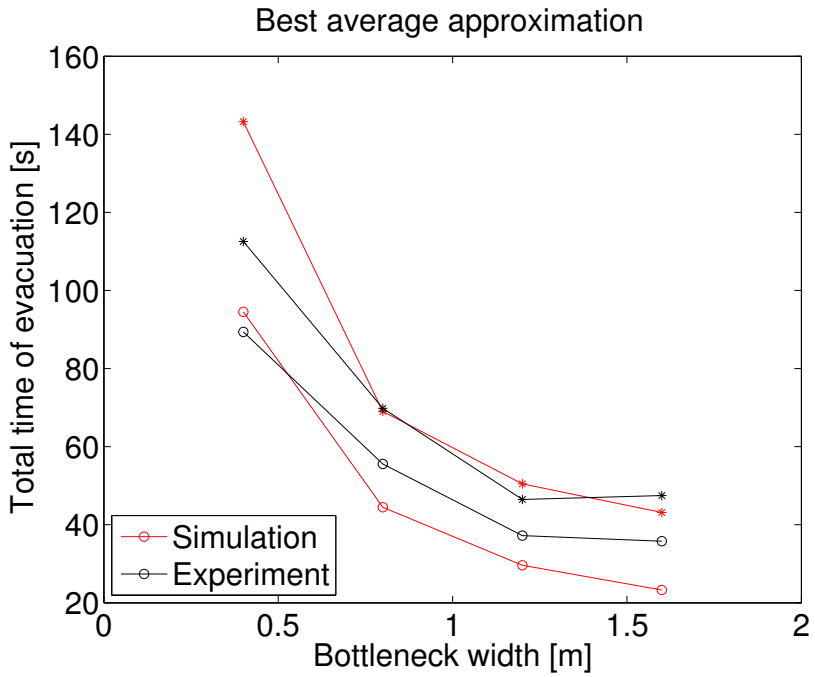

Figure 4.21: Best average approximation of the total time of evacuation against the bottleneck width

The experimental results of the mean flow are shown in Fig.4.22. It is possible to see that the flow is almost equal in both case, i.e. the pedestrians do not loose velocity in the end of the evacuation.

For the same reasons explained before, the model favours high values

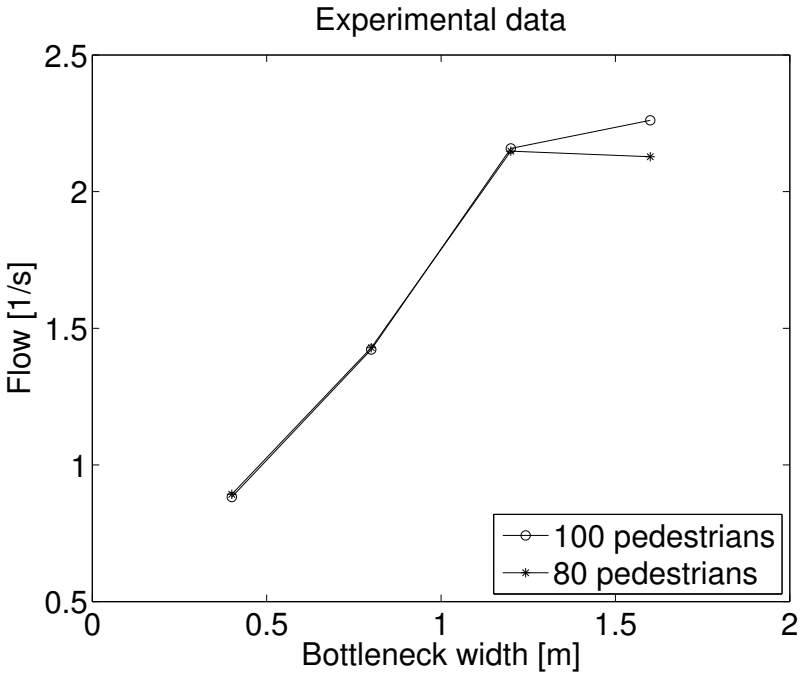

Figure 4.22: Mean flow rate in function of the bottleneck width, varying the number of pedestrians considered (experimental results)

of c and low values of μ if we consider all the 100 pedestrians and favours the opposite thing in the other case. The best average is, like before, a compromise between the two cases.

PEDESTRIANS	PARAMETERS
100	$\frac{k_S}{k_D} = 19$ $k_S = 38$ $\mu = 0$ $k_I = 7$ $c = k_D = 2$
80	$\frac{k_S}{k_D} = 13$ $k_S = 13$ $\mu = 0.8$ $k_I = 7$ $c = k_D = 1$
Average best	$\frac{k_S}{k_D} = 13$ $k_S = 26$ $\mu = 0.8$ $k_I = 5$ $c = k_D = 2$

Table 4.9: Best combination of parameters for the mean flow against the bottleneck width, varying the number of pedestrians considered

Fig.4.23 shows the results of the simulation with the best combinations fixing the number of pedestrians considered. For all the 100 pedestrians the mean flow is reproduced almost correctly, expect for the final saturation of the flow for $b \geqslant 1.2m$. The simulation considering only the first 80 pedestrians overestimates, for all b, the experimental mean flow of the pedestrians. This was predictable considering the results seen previously.

Using the combination with the minimum average error the model is able

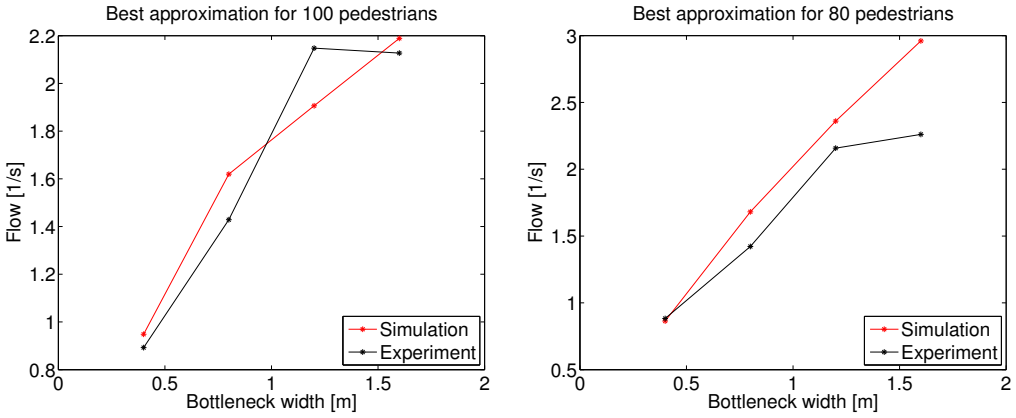

(a) 100 pedestrians considered (b) 80 pedestrians considered

Figure 4.23: Best simulation of the mean flow against the bottleneck width, fixing the number of pedestrians considered

to reproduce almost correctly the flow for 100 pedestrians, but lacks to reproduce in the correct way the mean flow considering the first 80 particles. As already explained before in order to reproduce the flow of the 100 pedestrians in a correct way, the model overestimates the flow of the first 80 because with the increase of the evacuation time the pedestrians decrease their velocity.

The optimal combination of parameters that best reproduces both the quantities in average is the following:

$$\frac{k_S}{k_D} = 13 \quad k_S = 26 \quad \mu = 0.8 \quad k_I = 5 \quad c = k_D = 2$$

The average relative error is equal to 0.2705, which confirms that the model is not able to reproduce both cases of both the quantities in an acceptable way. Most of the error is caused by the overestimation of the velocity of the first 80 pedestrians as we can see in Fig.4.25. The other results are completely similar to the ones explained before.

Analysing the plot of the time-gaps of evacuation between two consecutive pedestrians (Fig.4.26) it is possible to see even better the wrong dynamic of the pedestrians in the end of the simulation. The time-gaps should oscillate around a certain value without having this high variation. In Fig.4.26.b it is possible to see that this happens considering the first 80 pedestrians crossing the bottleneck. If we consider all the pedestrians, we have an high increase of the time-gaps for the last pedestrians. Indeed for $b = 0.4m$ the time-gaps oscillate around a value equal to approximately $1.25s$, while this value increases for the last pedestrians up to $16s$. This brings to an almost correct evaluation of the total time of evacuation also without reproducing well the real pedestrians dynamics.

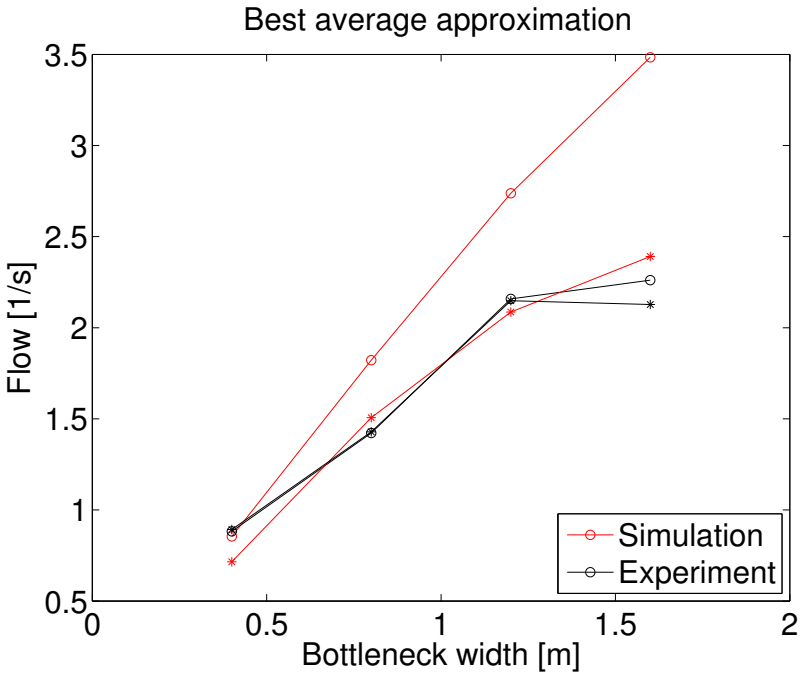

Figure 4.24: Best average approximation of the two

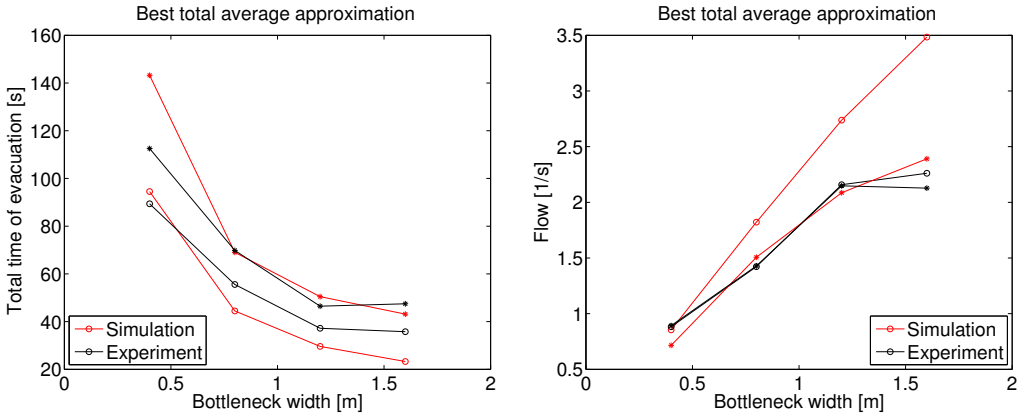

(a) Total time of evacuation against the bottleneck width

(b) Mean flow against the bottleneck width

Figure 4.25: Best approximation of the two quantities studied in Sec.4.1.2 (first simulation)

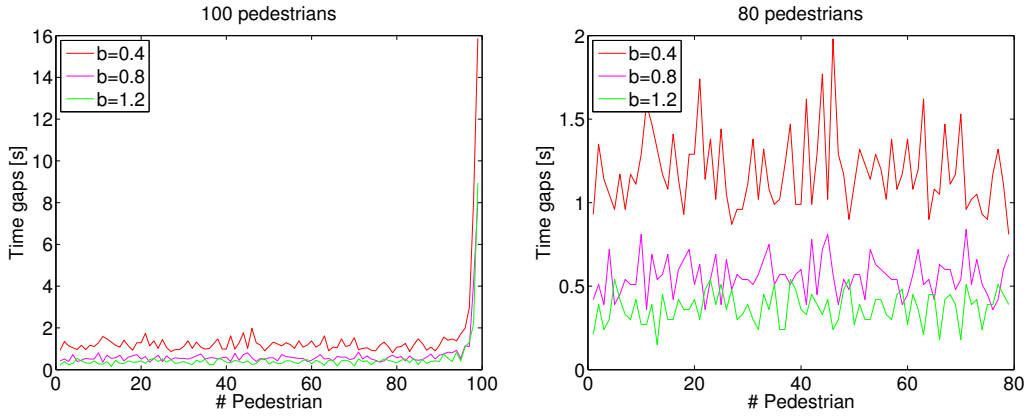

(a) 100 pedestrians considered (b) 80 pedestrians considered

Figure 4.26: Time-gaps between two consecutive pedestrians (first simulation)

For the reasons explained in the first simulation we will try to simulate again this experiment considering even lower values of the inertia parameter in order to try to reduce its effect on the dynamics of the last pedestrians. Table 4.10 shows the new ranges of the parameters tried in the simulation.

PARAMETERS	POINTS
k_S	[13,19]
k_I	[1,7]
μ	[0,0.8]
c	[1,2.5]

Table 4.10: Parameters used for the calibration in the normal situation with variable c (second simulation)

Since the single results of each quantity have been explained deeply in the first simulation, we will present only the final results of this second simulation. The result of the best combination of parameters that gives the lowest average error of all the quantities is the following:

$$\frac{k_S}{k_D} = 13 \quad k_S = 13 \quad \mu = 0.8 \quad k_I = 1 \quad c = k_D = 1$$

As we expected, the model advantages low values of the inertia parameter and therefore does not need a high value of the sensitivity parameter in order to reduce the effect of k_I.

Fig.4.27 shows the simulations of both the total time of evacuation and the mean flow against the bottleneck width using the combination of parameters

just mentioned. It is possible too see that the model is able to reproduce both cases in a much better way compared to the first simulation. The shape and the simulated values of the total time of evacuation are really similar to the real ones in both cases, expect for the final saturation of the function, that the model is not able to reproduce correctly. Like for the total time of evacuation the model is able to replicate the general trend of the mean flow, except for the final saturation. The mean flows of the two cases are really close like in the experiment, this confirms us that in this second simulation the mistake in the dynamics described in the first simulation is almost vanished, indeed the pedestrians have almost a constant velocity of escape during the whole simulation, differently from the first simulation made.

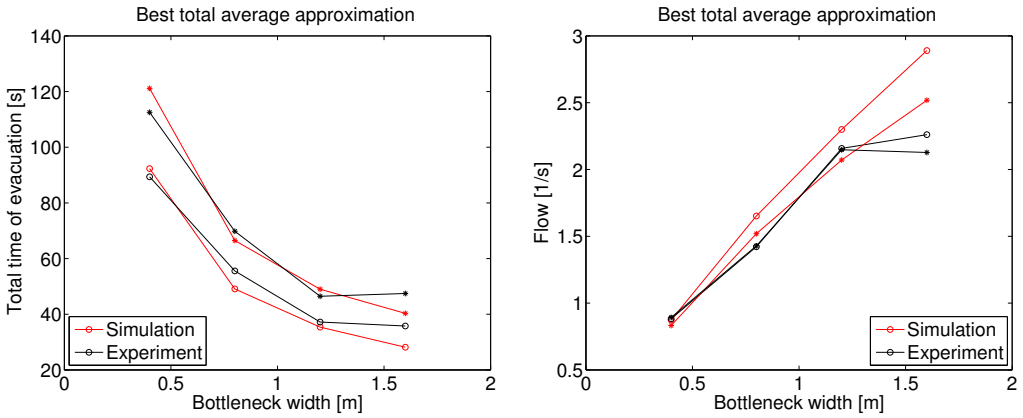

(a) Total time of evacuation against the bottleneck width

(b) Mean flow against the bottleneck width

Figure 4.27: Best approximation of the two quantities studied in Sec.4.1.2 (second simulation)

This is evident even analysing the time-gaps of evacuation between two consequent pedestrians. It is possible to see in Fig.4.28.a that even in this case the last pedestrians decrease a bit their velocity, increasing the time-gaps, but differently from before, this increase is really low. Indeed for $b = 0.4m$ the time-gaps of two consecutive pedestrians oscillate around the value $1.3s$, while the maximum value obtained for the last pedestrians is equal to $5s$. This result is acceptable because the decrease of velocity is quite low.

Conclusion

In the previous two sections we studied two different experiments in order to find the right values of the 3 movement parameters and the sensitivity param-

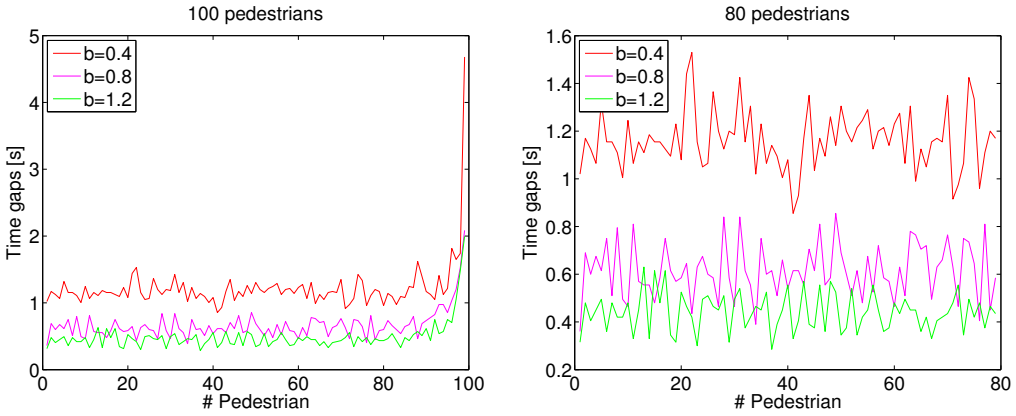

(a) 100 pedestrians considered (b) 80 pedestrians considered

Figure 4.28: Time-gaps between two consecutive pedestrians (second simulation)

eter. Averaging the relative errors of the quantities studied in each experiment, we found the optimal values of the combination of the four parameters in order to replicate in the best way the two experiments separately. Our aim is to find the right combination, so that the model is able to reproduce different experiments with different settings and quantities studied. Therefore we are going to simulate again the first experiment, using the ranges of the 4 parameters used in the second simulation of the second experiment (4.10). The combination of parameters that gives the lowest average error of the two experiments is the following:

$$\frac{k_S}{k_D} = 13 \quad k_S = 13 \quad \mu = 0.6 \quad k_I = 1 \quad c = k_D = 1$$

Fig.4.29 shows the results using the optimal combination of the quantities studied in the first experiment. It is possible to see that the model is able to reproduce in an acceptable way all the quantities studied, except for the number of escaped pedestrians against the evacuation time for $b = 0.4m$ and $N \geqslant 20$ (Fig.4.29.a). In this case the pedestrians flow too slowly to reproduce in the correct way the experimental data. As already seen in Sec.4.1.1 the model improved the quality of the approximation of the first experiment increasing the value of the inertia parameter to increase the velocity of the pedestrians. However the high value of k_I, useful to reproduce this quantity in the correct way, brought to high errors in different settings. This problem is even evident analysing the mean flow against the initial density (Fig.4.29.c). We can see that the model underestimates the flow for $b = 0.4m$ for densities higher than $3\frac{1}{s}$, i.e $N \geqslant 20$, however it is able to reproduce the

final saturation for increasing initial density. For higher bottleneck widths ($b = 1.2m$) the model reproduces almost perfectly the two quantities as we can see in Fig.4.29.b-c. For $N = 60$ (Fig.4.29.d) the simulated particles have almost the same behaviour as the real pedestrians for $b \geqslant 0.8$, however as already explained the model overestimates their time of evacuation for $b = 0.4m$.

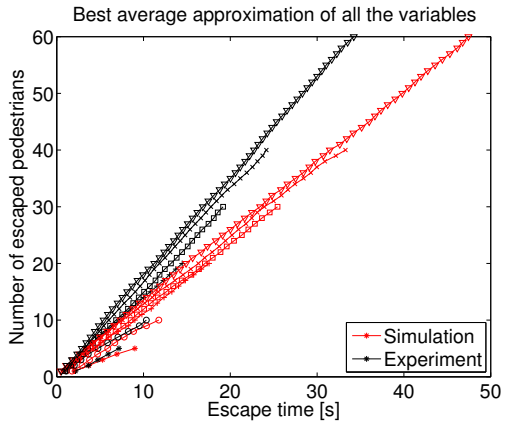

(a) Number of escaped pedestrians against evacuation time with $b = 0.4$, varying N

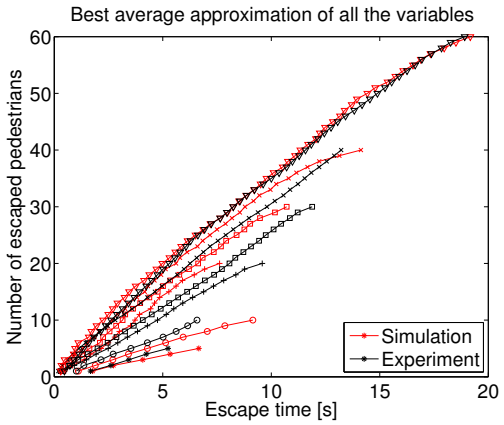

(b) Number of escaped pedestrians against evacuation time with $b = 1.2$, varying N

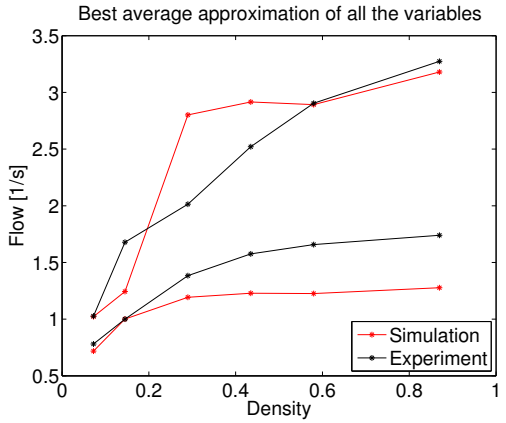

(c) Mean flow rate against initial density in the room with $b = 0.4$ and $b = 1.2$

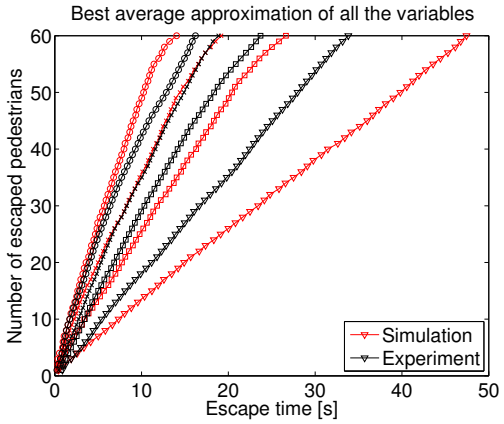

(d) Number of escaped pedestrians against evacuation time with $N = 60$, varying b

Figure 4.29: Approximation of the first experiment using the average best combination of the two experiments

The simulation results of the second experiment using the combination just found are shown in Fig.4.30. All the parameters are equal to the ones found in Sec.4.1.2, expect for the value of the friction parameter μ, that is equal to 0.6 instead of 0.8, therefore the results of the simulation are almost

the same. Even with this combination the total time of evacuation and the mean flow against the bottleneck width are replicated with low average errors by the model, except for the final saturation for both quantities. The mean flow (Fig.4.30.b) considering both the first 80 pedestrians flowing through the exit and all the 100 pedestrians are almost the same. This confirms that the mistake in the dynamics of the particles seen at the beginning of this study is almost vanished.

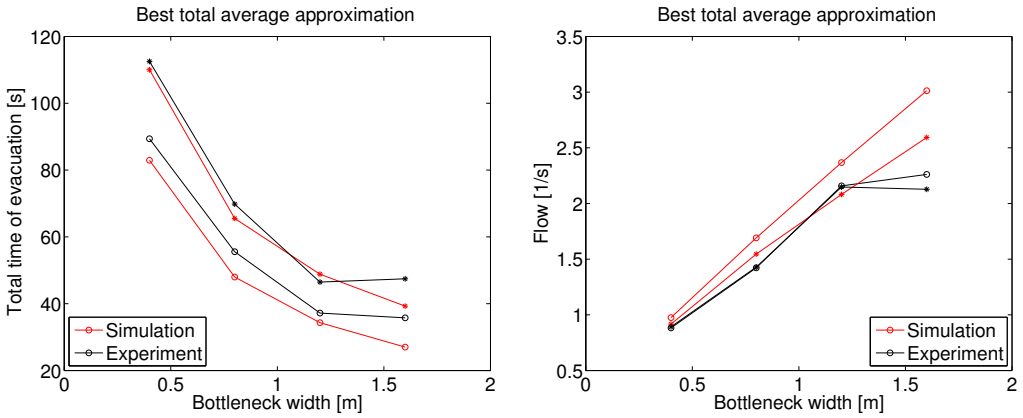

(a) Total time of evacuation against the bottleneck width

(b) Mean flow against the bottleneck width

Figure 4.30: Approximation of the second experiment using the average best combination of the two experiments

In these first two sections we studied all the effects of the movement parameters on the simulation of different quantities in two different experiments. The aim of the next section is to validate the model, i.e. to apply the model on different experiments with different settings, in order to prove that it is able to reproduce even different experimental data from the ones used in the calibration.

4.1.3 Validation

In order to validate the model with the fixed parameters found in the calibration, the model has to be able to reproduce different experimental data compared to the one used previously.

The first experiment considered [35], had as its goal to study the dependence of the density on the velocity of the pedestrians in a plane corridor without bottlenecks. The settings of the corridor are shown in Fig.4.31. The width of the passageway in the measurement section is $0.8m$, while on the

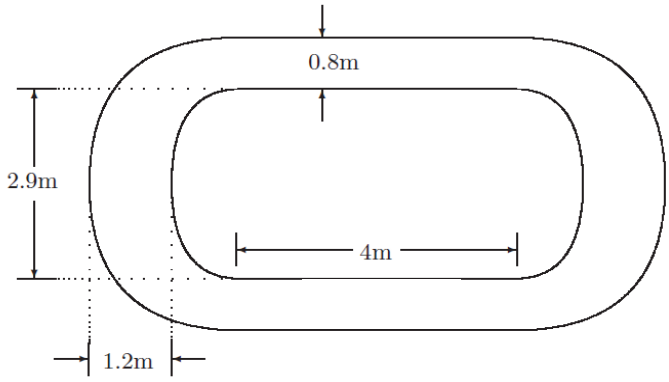

Figure 4.31: Schematic illustration of the first experiment (validation)

curve it is equal to $1.2m$. Using the combination of parameters found in the last section we want to try to reproduce the results found in the experiment. Fig.4.32 shows the comparison between the experimental and simulated results. It is possible to see how the model overestimates a bit the velocity for densities between $1\frac{1}{m^2}$ and $4.5\frac{1}{m^2}$, however is able to replicate the decrease of the velocity with the increase of the density. The overestimation can be caused by the fact that in the experiment the pedestrians were not allowed to surpass, while in the simulation they were, since the passageway has a width of $0.8m$. Although the simulated velocity does not have the exact same shape of the experimental one, we can consider the result satisfactory for the reasons just explained.

The second experiment taken into account is the flow through a narrow bottleneck of width $1m$ and length $5m$ described in [33]. The walking area in the experiment has a length of $10m$ and a width of $4m$ (Fig.4.33).

The quantities studied are the average spatial distributions of the densities and velocities in the room in different periods of the experiment. In the first period ($t \in [0s, 120s]$) they observed low densities and relatively high velocities. During this period pedestrians used only a small portion of the walking area. In the second period $[120s, 240s]$, the densities were still relatively low, but the velocities started to decrease, because pedestrians could not walk at their desired speed. Even in this case the walking area was not fully used. They observed higher speeds at the edges of the useful area compared to the ones in the middle due to pedestrians that walked around the low-speed region near the center. The last period $t \in [360s, 480s]$ was characterized by the congestion next to the bottleneck and a larger portion of the walking area used. The average density rose up to $2.5\frac{1}{m^2}$, while the average speed in the bottleneck and upstream of the bottleneck was $1\frac{m}{s}$ and

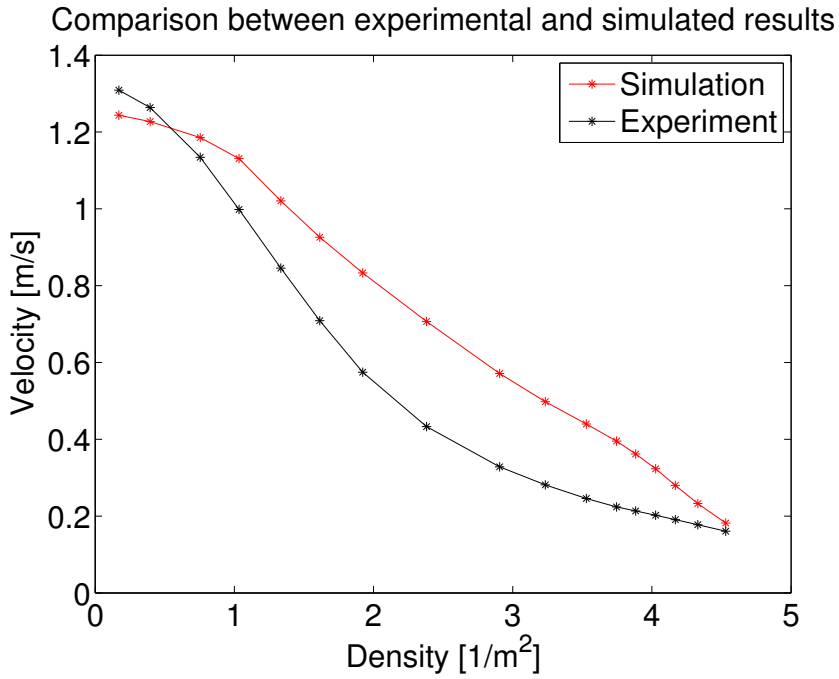

Figure 4.32: Horizontal velocity against density of pedestrians in the corridor (validation)

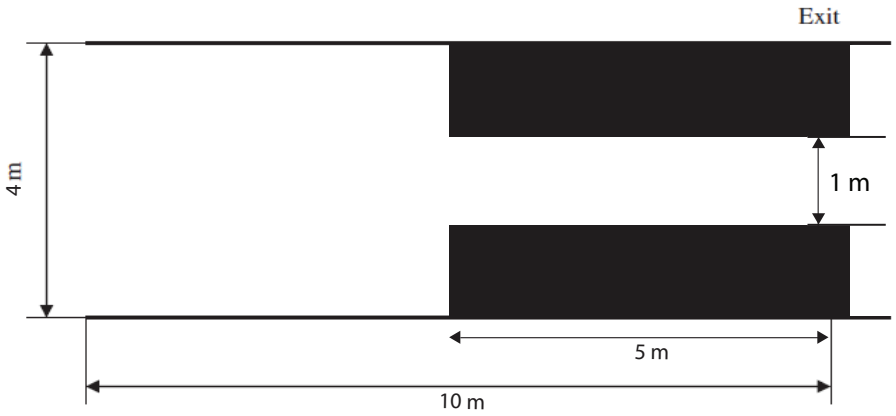

Figure 4.33: Schematic illustration of the second experiment (validation)

$0.3\frac{m}{s}$ respectively. In summary the three periods were characterized by free flow, minor congestion and major congestion respectively.

The quantities studied in the experiment describe the precise movements of the pedestrians, therefore we do not expect that the model is able to reproduce them in a perfect way. However we expect that the general results can be replicated. Moreover it is not so clear in the description of the experiment how the pedestrians re-enter in the room after passing the bottleneck. In the simulation we consider closed boundary conditions and this causes an acceleration in the congestion of the room, however this is not so important, because the aim of this particular study is to see if the model is able to replicate the three different periods characterized by free flow, minor congestion and major congestion respectively.

Fig.4.34 shows the results of the simulations in the three different periods. In the first period ($t \in [0s, 30s]$) we can observe low densities and that the particles use only a small portion of the walking area like in the experiment. The velocities observed are lower than the ones in the experiment, while the densities are higher. Normally pedestrians try to keep a certain distance from other pedestrians, while this does not happen to the simulated particles causing a higher increase of the densities. In the second period ($t \in [30s, 60s]$) it is possible to notice how the densities around the bottleneck begin to increase, although the walking area is still not completely used by the particles. The velocities start to decrease in this period due to the clogging next to the bottleneck. The last period ($t \in [90s, 120s]$) is characterized by a high congestion. It is possible to see how the densities upstream the bottleneck are really high and consequently the velocities in the same area really low.

Although the simulated results are not perfectly related to the ones in the experiment, we can consider them really satisfactory, because the model is able to reproduce almost perfectly the behaviour of the pedestrians next to the bottleneck. Indeed even in the simulation we obtain the three different periods that characterized also the experiment previously described.

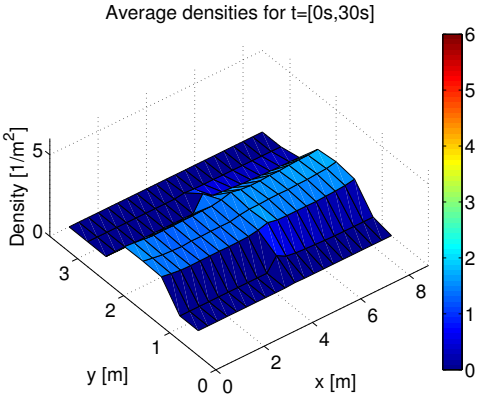

(a) Average densities for t=(0s,30s)

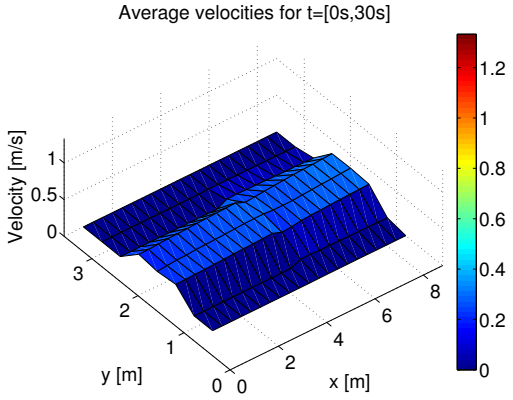

(b) Average velocities for t=(0s,30s)

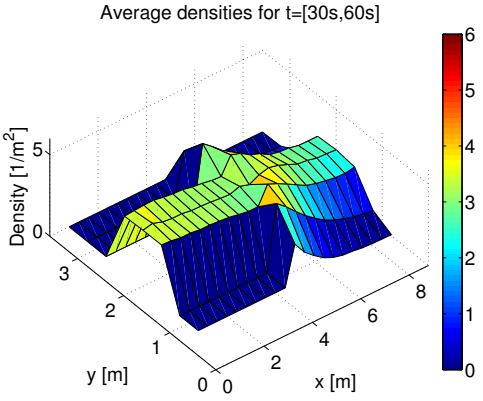

(c) Average densities for t=(30s,60s)

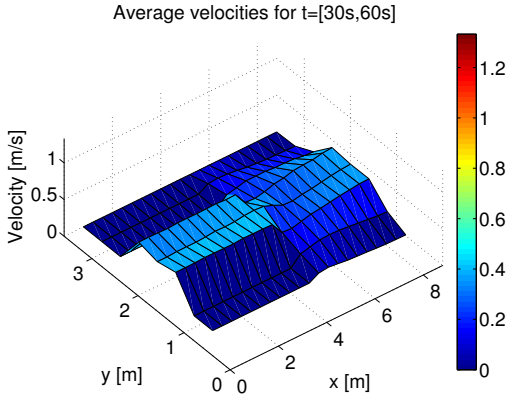

(d) Average velocities for t=(30s,60s)

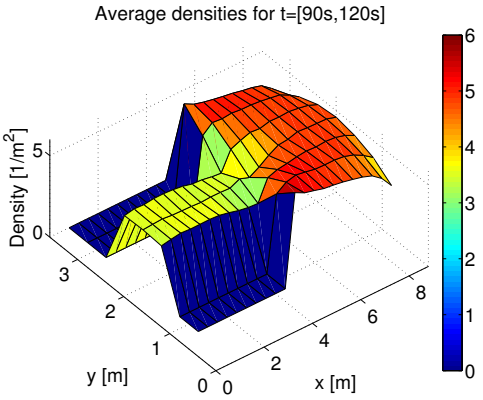

(e) Average densities for t=(90s,120s)

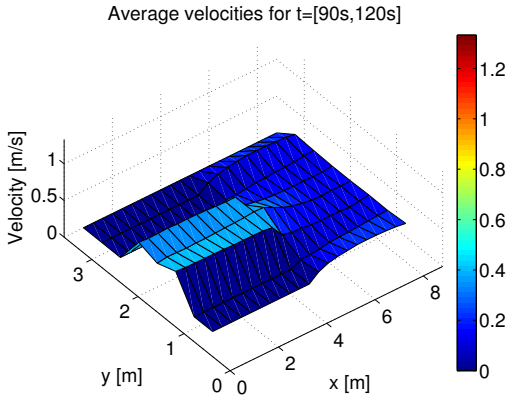

(f) Average velocities for t=(90s,120s)

Figure 4.34: Surface plots showing the average spatial distributions of the densities and speeds in the walking area (validation)

Chapter 5

Conclusions and future works

In this work we have addressed the understanding and simulation of pedestrian dynamics. The first part has focused on the description of the empirical observations, fundamental for a deep understanding of the subject and for the development of mathematical models, which are able to reproduce these dynamics. The model used for the simulations is the Cellular Automata model, that has been chosen for its simplicity and its ability to reproduce even complex situations.

The mathematical framework for the simulations has been implemented through shared libraries using an object-oriented programming language (C++).

In the first simulations we have encountered some overflow problems to excessively high values of the $staticfloorfields$. For this reason we decided to normalize this field with the average value of the dynamic floor field for a fixed combination of the system parameters: 1) size of the room, 2) initial density of pedestrians in the room, 3) the destruction parameter and 4) the diffusion parameter. This study did not only solve the overflow problems, but also gave an important contribution on the calibration of the model. For each fixed combination of parameters of the system we equalized the intensities of the two fields, so that the right proportion of the two coupling strengths k_S and k_D did not depend on the system considered.

The last part has focused on the calibration of the model in normal situations. We have tested the model on different experiments reaching a very good agreement with the real dynamics of the pedestrians. Furthermore this study helped to understand in detail the influences of the movement parameters and the sensitivity parameter on the behaviour of the simulated particles.

To conclude, we wish to mention some possible directions for future activities and investigations:

1. The CA model described in Chapter 3 can be improved in different ways. It is possible to implement the model, so that the particles are able to have different velocities. This can be done by decreasing the reaction time and by stopping the slowest particles in some time-steps. Another possible extension is the addition of a finer discretisation of the space. For some applications the discretisation used in this work could not be adequate and a finer one can be necessary [30].

2. In the calibration chapter we have assumed that the 3 movement parameters and the sensitivity parameter are constant. Analysing the simulations we have seen that they depend on the time of evacuation and on the system settings. It is possible to improve the calibration removing the assumption done in Chapter 4.

Bibliography

[1] MSA. Report on Exercise Invicta. Technical report, Marine Safety Agency (1997)

[2] B.D. Hankin, R.A. Wright. *Passenger flow in subways.* Oper. Res. Quart. 9 81-88 (1958)

[3] FP Navin, RJ Wheeler. *Pedestrian flow characteristics.* Traffic Engineering 39 (1969)

[4] Dirk Helbing, Illes J. Farkas, Peter Molnar, Tamas Vicsek. *Simulation of Pedestrian Crowds in Normal and Evacuation Situations.* (2002)

[5] Andreas Schadschneider, Wolfram Klingsch, Hubert Klupfel, Tobias Kretz, Christian Rogsch, Armin Seyfried. *Evacuation Dynamics: Empricial Results, Modeling and Applications.* In Encyclopedia of Complexity and System Science, Springer (2008)

[6] Dirk Helbing, Illes J. Farkas, Peter Molnar, Tamas Vicsek *Simulation of Pedestrian Crowds in Normal and Evacuation Situations* (2002)

[7] Fruin. *Pedestrian planning and design.* (1971)

[8] Thompson, Marchant. *Simulex; developing new computer modelling techniques for evaluation.* (1994)

[9] Ulrich Weidmann. *Transporttechnik der fussgänger* (1992).

[10] V. M. Predtechenskii, A. I. MilinskiÄ. *Planning for foot traffic flow in buildings.* (1978)

[11] S. J. Older, *Movement of pedestrians on footways in shopping streets.* Traffic engineering and control (1968)

[12] D. Helbing, J. Anders , Habib Zein Al-Abideen. *Dynamics of crowd disasters: An empirical study.* Physical review E 75.4 (2007)

[13] L.F. Henderson. *The statistics of crowd fluids* Nature, 229:381-383 (1971)

[14] L.F. Henderson. *On the fluids mechanics of human crowd motion* Transportation research, 8:509-515 (1974)

[15] D. Helbing. *A fluid-dynamic model for the movement of pedestrians* Complex system, 6:391-415 (1992)

[16] D. Helbing, P. Molnar. *Social force model for pedestrian dynamics* (1998)

[17] D. Helbing, P. Molnar. *Self-Organization Phenomena in Pedestrian Crowds* (1998)

[18] M. Bando, K. Hasebe, A. Nakayama, A. Shibata, Y. Sugiyama. *Dynamical model of traffic congestion and numerical simulation* Phys. Rev. E 51 (1995)

[19] A. Nakayama, K. Hasebe, Y. Sugiyama. *Instability of pedestrian flow and phase structure in a two-dimensional optimal velocity model* (2005)

[20] Victor J. Blue, Jeffrey L. Adler. *Cellular automata microsimulation for modeling bi-directional pedestrian walkways.* Transport Research Part B 35 (2001) 293-312

[21] Victor J. Blue, Jeffrey L. Adler. *Cellular Automata Model Of Emergent Collective Bi-Directional Pedestrian Dynamics.* (2000)

[22] Minoru Fukui, Yoshihiro Ishibashi. *Self-Organized Phase Transitions in Cellular Automaton Models for Pedestrians.* Journal of the Physical Society of Japan Vol. 68 No. 8 (1999) pp.2861-2863

[23] Minoru Fukui, Yoshihiro Ishibashi. *Jamming Transition in Cellular Automaton Models for Pedestrians on Passageway.* Journal of the Physical Society of Japan Vol. 68 No. 11 (1999) pp.3738-3739

[24] C. Burstedde, K. Klauck, A. Schadschneider, J. Zittartz. *Simulation of pedestrian dynamics using a two-dimensional cellular automaton.* (2001)

[25] Ansgar Kirchner, Andreas Schadschneider. *Simulation of evacuation processes using a bionics-inspired cellular automaton model for pedestrian dynamics.* (2002)

[26] Andreas Schadschneider, Armin Seyfried. *Empirical results for pedestrian dynamics and their implications for cellular automata models.* (2008)

[27] Nuria Pelechano, Ali Malkawi. *Evacuation simulation models: Challenges in modelling high rise building evacuation with cellular automata approaches.* (2007)

[28] Ansgar Kirchner, Katsuhiro Nishinari, Andreas Schadschneider. *Friction effects and clogging in a cellular automaton model for pedestrian dynamics.* (2008)

[29] Katsuhiro Nishinar, Ansgar Kirchner, Alireza Namazi, Andreas Schadschneider. *Extended floor field CA model for evacuation dynamics.* (2008)

[30] Ansgar Kirchner, Hubert Klupfel, Katsuhiro Nishinari, Andreas Schadschneider, Michael Schreckenberg. *Discretisation effects and the influence of walking speed in cellular automata models for pedestrian dynamics.* (2004)

[31] Debashish Chowdhury, Vishwesha Guttal, Katsuhiro Nishinari, Andreas Schadschneider. *A cellular-automata model of flow in ant-trails: non-monotonic variation of speed with density.* (2002)

[32] Motonari Isobe, Dirk Helbing, Takashi Nagatani. *Many-particle simulation of the evacuation process from a room without visibility.* (2003)

[33] Serge P. Hoogendoorn, W. Daamen. *Pedestrian Behavior at Bottlenecks.* (2005)

[34] Tobias Kretz, Anna Grünebohm, Michael Schreckenberg. *Experimental study of pedestrian flow through a bottleneck.* (2006)

[35] Armin Seyfried, Bernhard Steffen, Wolfram Klingsch, Maik Boltes. *The Fundamental Diagram of Pedestrian Movement Revisited* (2005)

[36] Ryoichi Nagai, Masahiro Fukamachi, Takashi Nagatani. *Evacuation of crawlers and walkers from corridor through an exit* (2005)

[37] Dirk Helbing, Lubos Buzna, Anders Johansson, Torsten Werner. *Self-Organized Pedestrian Crowd Dynamics: Experiments, Simulations, and Design Solutions.* Institute for Operations Research and the Management Sciences (2005)

[38] Yordphol Tanaboriboon, Sim Siang Hwa, Chin Hoong Chor. *Pedestrian characteristics study in Singapore.* J. Transp. Eng. 112:229-235 (1986)

[39] Dirk Helbing, Anders Johansson, Habib Zein Al-Abideen. *The Dynamics of Crowd Disasters: An Empirical Study.* (2007)

[40] B. Ashe, T. J. Shields. *Analysis and Modelling of the Unannounced Evacuation of a Large Retail Store.* Fire Mater. 23, 333-336 (1999)

[41] Caesar Saloma, Gay Jane Perez, Giovanni Tapang, May Lim, Cynthia Palmes-Saloma. *Self-organized queuing and scale-free behavior in real escape panic.* (2003)

[42] Dirk Helbing, Peter Molnar, Illes J Farkas, Kai Bolay. *Self-organizing pedestrian movement.* Environment and Planning B: Planning and Design, volume 28, pages 361-383 (2001)

[43] Dirk Helbing, Illes Farkas, Tamas Vicsek. *Simulating dynamical features of escape panic.* Nature, Vol.40 (2000)

[44] Dirk Helbing. *A mathematical model for the behavior of pedestrians.* Behavioral Sci. 36 298-310 (1991)

[45] Dirk Helbing. *Verkehrsdynamik [Traffic Dynamics].* Springer (1997)

[46] D. Helbing, P. Molnar, F. Schweitzer. *Self-Organization of Complex Structures: From Individual to Collective Dynamics.* Gordon and Breach 569-577 (1997)

[47] D. Helbing, M. Isobe, T. Nagatani, K. Takimoto. *Lattice gas simulation of experimentally studied evacuation dynamics.* Physical Rev. E 67 (2003)

[48] M. Isobe, D. Helbing, T. Nagatani. *Many-particle simulation of the evacuation process from a room without visibility.* Physical Rev. E 69 (2004)

[49] S. Gwynne, E.R. Galea, M. Owen, P.J. Lawrence, L. Filippidis. *A systematic comparison of buildingEXODUS predictions with experimental data from the Stapelfeldt trials and the Milburn House evacuation.* Applied Mathematical Modelling 29 818-851 (2005)

[50] Kardi Teknomo. *Microscopic Pedestrian Flow Characteristics: Development of an Image Processing Data Collection and Simulation Model.* (2002)